

# Liquid-Liquid Phase Separation of a Bacterial Protein Family

**Leon Babl**

Complete reprint of the dissertation approved by the TUM School of Natural Sciences of the  
Technical University of Munich for the award of the  
Doktor der Naturwissenschaften (Dr. rer. nat.).

Chair: Prof. Dr. Johannes Buchner

Examiners:

1. Prof. Dr. Petra Schwille
2. Prof. Dr. Job Boekhoven

The dissertation was submitted to the Technical University of Munich on 03.05.2023 and  
accepted by the TUM School of Natural Sciences on 03.07.2023.

---

# Liquid-Liquid Phase Separation of a Bacterial Protein Family

Leon Babl

---

2023

---

# Liquid-Liquid Phase Separation of a Bacterial Protein Family

Leon Babl

---

Dissertation  
an der Fakultät für Chemie  
der technischen Universität  
München

vorgelegt von  
Leon Babl  
aus Regensburg, Germany

München, den 26<sup>th</sup> April 2023

Erstgutachter: Prof. Dr. Petra Schwille

Zweitgutachter: Prof. Dr. Job Boekhoven

---

*To all the bright minds and huge smiles that surround me day and night.*



# Eidesstattliche Erklärung

Hiermit versichere ich an Eides statt, dass die vorliegende Dissertation von mir selbstständig und ohne unerlaubte Hilfe angefertigt wurde. Des Weiteren erkläre ich, dass ich nicht anderweitig ohne Erfolg versucht habe, eine Dissertation einzureichen oder mich der Doktorprüfung zu unterziehen. Die Dissertation liegt weder ganz, noch in wesentlichen Teilen einer anderen Prüfungskommission vor.

München, 6. März 2023

Leon Babl





# Table of contents

<b>Eidesstattliche Erklärung</b>	<b>VII</b>
<b>List of Figures</b>	<b>XI</b>
<b>Abstract</b>	<b>XIII</b>
<b>Kurzfassung</b>	<b>XV</b>
<b>1 Introduction</b>	<b>1</b>
1.1 Phase transitions in biology . . . . .	1
1.1.1 Lipid phase separation . . . . .	3
1.2 Molecular mechanisms and theory of liquid-liquid phase separation . . . . .	5
1.3 Out-of-equilibrium phase separation . . . . .	8
1.4 Liquid-liquid phase separation on surfaces . . . . .	11
1.5 Biological examples of phase separating structures and functions . . . . .	14
1.5.1 The Nucleolus . . . . .	14
1.5.2 The Nuclear Pore Complex . . . . .	16
1.6 Phase separation from an evolutionary viewpoint . . . . .	17
1.7 Liquid-liquid phase separation in bacteria . . . . .	19
1.8 The ParB protein family . . . . .	19
1.8.1 The ParABS-System and ParB . . . . .	20
1.8.2 Nucleoid Occlusion and Noc . . . . .	22
1.9 Main methods . . . . .	23
1.9.1 Phase diagrams and turbidity measurements . . . . .	23
1.9.2 Fluorescence microscopy . . . . .	23
1.9.3 Model membrane systems . . . . .	24
1.9.4 Fluorescence correlation spectroscopy in biomolecular condensates . . . . .	24
<b>2 Objectives</b>	<b>27</b>
	<b>IX</b>

<b>3</b>	<b>List of publications</b>	<b>29</b>
<b>4</b>	<b>Additional publications</b>	<b>31</b>
<b>5</b>	<b>Publications</b>	<b>33</b>
5.1	Publication P1. Self-organized protein patterns: the MinCDE and ParABS systems . . . . .	33
5.2	Publication P2. CTP-controlled liquid-liquid phase separation of ParB . . . . .	45
5.3	Publication P3. Membrane mediated phase separation of the bacterial nucleoid occlusion protein Noc . . . . .	67
<b>6</b>	<b>Discussion and perspectives</b>	<b>83</b>
<b>7</b>	<b>Bibliography</b>	<b>87</b>
	<b>List of abbreviations</b>	<b>99</b>
	<b>Acknowledgements</b>	<b>101</b>

# List of Figures

1.1	Phase transitions are ubiquitous in biologically relevant systems. . . . .	2
1.2	Lipid phase separation as an example of a biological phase transition. . . .	3
1.3	Theory and molecular grammar of liquid-liquid phase separation. . . . .	7
1.4	Out-of-equilibrium liquid-liquid phase separation exhibits novel properties.	9
1.5	Wetting transition of a biomolecular condensate on a lipid bilayer. . . . .	11
1.6	Biomolecular condensates wet and deform lipid membranes. . . . .	13
1.7	The Nucleolus as a biomolecular condensate . . . . .	15
1.8	The Nuclear Pore Complex . . . . .	16
1.9	The ParABS system is responsible for genome and plasmid segregation. . .	20
1.10	Noc regulates the Z-Ring assembly above the nucleoid in <i>B. subtilis</i> . . . .	22



# Abstract

Phase transitions are ubiquitous in physical and biological systems, occurring when a system undergoes a sudden change in its physical or functional properties as a result of a small change in external conditions or internal interactions. In biology, phase transitions play a critical role in various processes, from protein folding and assembly to membrane organization and cell division. In this thesis, I will explore the mechanisms and implications of phase transitions in biological systems, focusing on the interplay between biochemistry, biophysics, and evolution. The goal is to gain a deeper understanding of how phase transitions regulate biological function, and how these fundamental principles can be applied to design new strategies for controlling biological processes. Herein, I will focus on the members of a protein family, the ParB proteins which fulfil a variety of functions within bacteria such as genome segregation and nucleoid occlusion. For several of these proteins, a phase separating mechanism has been suggested to underlie the formation of higher order structures observed in *in vivo* imaging experiments. Using the powerful approach of *in vitro* reconstitution, I will study the potential liquid-liquid phase separation of the ParB protein family.



# Kurzfassung

Phasenübergänge sind in physikalischen und biologischen Systemen allgegenwärtig. Sie treten auf, wenn sich die physikalischen oder funktionellen Eigenschaften eines Systems infolge einer kleinen Änderung der äußeren Bedingungen oder der internen Wechselwirkungen plötzlich ändern. In der Biologie spielen Phasenübergänge eine entscheidende Rolle bei diversen Prozessen, von der Proteinfaltung und -assemblierung bis zur Membranorganisation und Zellteilung. In dieser Arbeit werde ich die Mechanismen und Auswirkungen von Phasenübergängen in biologischen Systemen untersuchen und uns dabei auf das Zusammenspiel von Biochemie, Biophysik und Evolution konzentrieren. Das Ziel ist es, ein tieferes Verständnis dafür zu erlangen, wie Phasenübergänge biologische Funktionen regulieren und wie diese grundlegenden Prinzipien angewandt werden können, um neue Strategien zur Steuerung biologischer Prozesse zu entwickeln. In dieser Arbeit konzentriere ich mich auf die Mitglieder einer Proteinfamilie, die ParB-Proteine, die eine Vielzahl von Funktionen in Bakterien erfüllen. Für mehrere dieser Proteine wurde ein Phasentrennungsmechanismus vorgeschlagen, der der Bildung von Strukturen höherer Ordnung zugrunde liegt, die in *In-vivo*-Bildgebungsexperimenten beobachtet werden. Durch *in vitro* Rekonstitution werde ich die Flüssig-Flüssigphasentrennung dieser Proteine untersuchen.





# Introduction

## 1.1 Phase transitions in biology

Phase transitions have been recognized as fundamental processes in early states of biological research. In 1938, Oparin made use of the recently discovered coacervation process -a first-order phase transition- to build his model of the origin of life [1]. By now, phase transitions have been used to describe an immense variety of biological systems, ranging from the reordering of lipid-bilayers [2, 3] to the synchronization of neural firing [4], drastic changes in the environment [5], the flocking of bird or ant swarms [6, 7] and the formation of subcellular structures [8, 9, 10]. While the individual biological phenomena described by phase transition theories are highly diverse and complex, the underlying physics are relatively simple.

Phase transitions in biology are often first order reactions which are characterized through a discontinuous parameter change under certain environmental conditions. More precisely, a phase transition is a physical, chemical or biological change that occurs when an entity transitions from one phase or state of matter to another. Phase transitions are characterized by changes in the macroscopic properties of the system, such as density, fluidity, or volume, while the molecular structure typically remains unchanged. Examples of such parameter changes leading to phase transitions can be the melting of ice upon a temperature increase, the emergence of superconductivity as temperature is lowered [11] or a sudden difference of density in a flock of birds upon changing the flying velocity [12]. While these are rather macroscopic changes, phase transitions have also been discovered in cell biology, and were demonstrated to play a fundamental role in cellular organization.

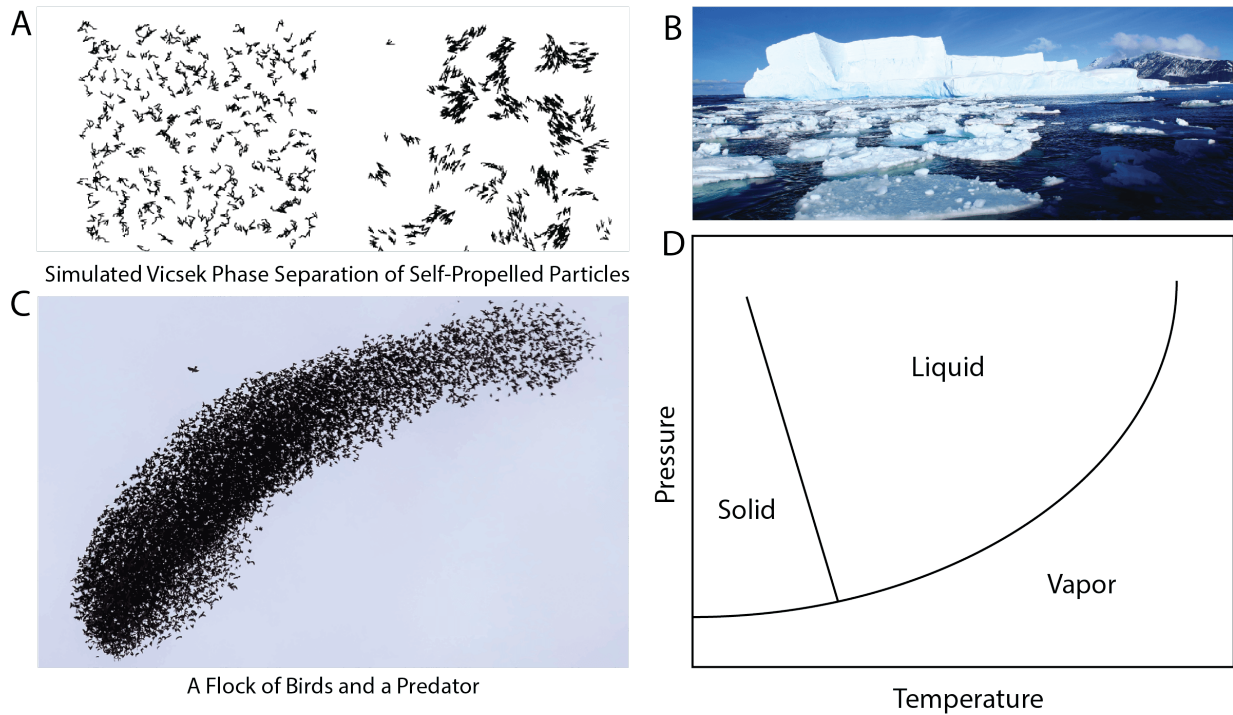


**Figure 1.1: Phase transitions are ubiquitous in biologically relevant systems.** A) shows a so-called Vicsek phase transition of self-propelled particles. Upon a change of velocity, the particles flock together in denser structures. Reprinted from [12] with permission. B) shows the co-existing of two phases of water, solid and liquid. Image reprinted with permission from 'upsplash.com'. C) A flock of birds escaping from a predator can also be described as a phase transition. Image taken from Wikipedia under CC4 license. D) Schematic of a phase diagram showing the different transitions from a liquid to a solid or vapor state.

### 1.1.1 Lipid phase separation

The most prominent example of a molecular phase transition phenomena used to explain fundamental cell biology is likely the re-ordering of lipid bilayers into distinct lipid rafts, altering in lipid and protein composition and other biophysical parameters. Already in 1972, Singer and Nicholson formulated the fluid mosaic model to describe the cellular plasma membrane [13]. This model pictures the cell membrane as a two-dimensional fluid, mainly composed of lipids with proteins embedded into the bilayer. Additionally, diffusion within the membrane can be restricted by protein-protein, protein-lipid and lipid-lipid interactions. Building on this model, further investigations of the composition of the cellular membrane led to the identification of different rafts, variable in size and composition [14, 15, 16, 17, 3]. These rafts are often enriched in sphingolipids and cholesterol and exhibit altered diffusional dynamics [18].

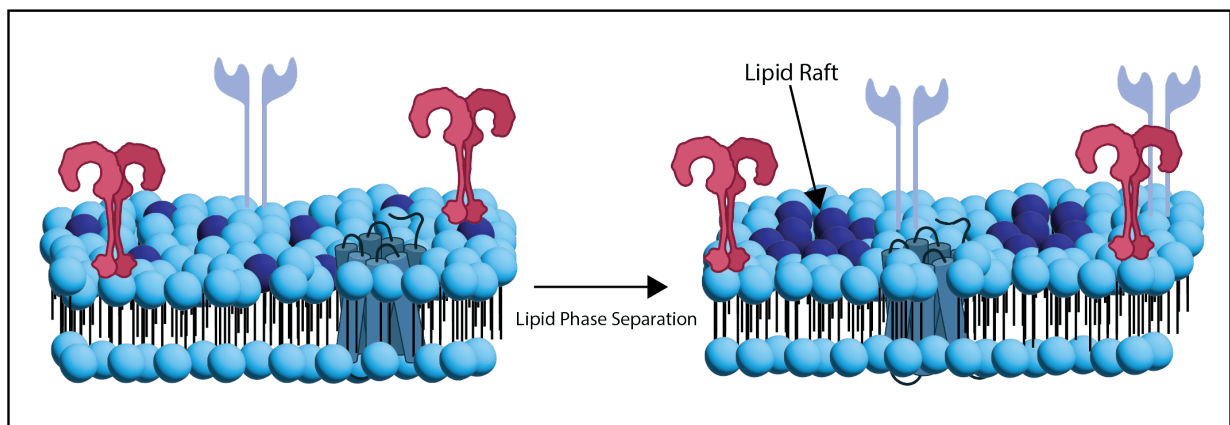


**Figure 1.2: A schematic representation of a lipid bilayer phase separation as an example of a biological phase transition.** The different components of a lipid-bilayer can demix into distinct phases. The lipid composition and protein within the rafts can differ from the surrounding membrane and therefore allow different biochemical reactions to happen.

Subsequently, the mechanism of lipid raft formation was uncovered. It is now widely accepted that lipid bilayers, depending on their composition, can undergo a liquid-liquid phase separation forming different membrane domains. Through the demixing into a liquid disordered ( $L_D$ ) and a liquid ordered ( $L_O$ ) phase, the membrane is thought to minimize its free energy [19]. The different membrane components preferentially partition into different phases. For example, cholesterol is enriched in the  $L_O$ -phase, whereas many proteins are up-concentrated in  $L_D$ -phases [20]. Intriguingly, these findings were soon linked to actual biochemical events such as signal transduction [21, 22, 23], vesicle trafficking [24, 25], cell adhesion and motility [26], and entry of pathogenic viruses and bacteria [27, 28]. An interesting example of lipid raft driven biochemical process is the endocytosis of the SV40 virus, which has been demonstrated to utilize  $L_D$ -phase lipid domains to enter its host cells

[29]. Also, the clustering of signaling complexes such as the epidermal growth factor EGF has been suggested to happen via membrane phase separation [30, 20].

Taken together, lipid rafts differ in lipid and protein composition and have been linked to a variety of biological processes such as cell signaling or viral entry. While explicit evidence of these lipid rafts *in vivo* is still debated, the discovery of lipid domain formation has brought phase separation to the spotlight. But how does a molecular phase separation occur? Intriguingly, the underlying concepts applicable to lipid phase separation have been shown to also apply to other biomolecules such as proteins or nucleic acids.

## 1.2 Molecular mechanisms and theory of liquid-liquid phase separation

Liquid-liquid phase separation (LLPS) is a phenomenon that occurs when certain biomolecules, such as proteins, lipids or nucleic acids demix from the bulk solution to form two distinct phases upon reaching a specific concentration, the saturation concentration. The two formed phases differ in composition, viscosity and many other biophysically relevant parameters [8], but the liquid-like nature of the condensates allows for constant exchange of molecules with the environment. Usually, this process is enthalpically favorable as the interactions of the biomolecules make up for the loss of entropy upon the demixing. The phase boundary is used to describe the concentration necessary for phase separation, and can differ depending on the cellular environment, post-translational modifications of the phase separating protein or the temperature [31, 32]. Interestingly, the underlying theory often used to describe LLPS has been formulated by Flory and Huggins to explain the behavior of polymer blends [33, 34]. While it likely does not account for the complexity of all biomolecular condensates, it has successfully been applied to a variety of phase separating proteins [31, 35].

Some protein condensates do not behave like simple polymer blends [36, 37], but often change their property over time or upon protein mutations [38]. Such aberrant phase transitions have been linked to a variety of neurodegenerative diseases like Huntington or ALS, and often the material properties of the formed liquid-like condensate has been identified as a potential source of these diseases [39]. Especially aging of condensates, so the transformation of a liquid-like state to a hardened gel-like state, has been the focus for novel drug targeting strategies [40, 41]. Often caused by protein mutations, the biomolecular condensate dynamics drastically change and toxic aggregation is taking place in the protein-dense environment. Complementing the *in vitro* work on these disease causing processes, novel theory has been developed to accommodate the highly complex phenomena observed [36].

As we gain more understanding of the underlying interactions that drive biomolecular condensation, the theoretical framework to describe the formation and regulation of these liquid-like structures is advancing. The molecular grammar of many phase separating proteins has been identified as multivalent, but rather weak interactions evenly distributed over the protein sequence [31, 42, 43, 44]. These findings were summarized in the widely accepted sticker-and-spacer model of phase separation [45]. Herein, the sum of multivalent interactions and their spacing across the protein sequence dictates the phase boundary and the material properties of the formed phases [46]. The sticker-and-spacer model has initially been demonstrated for the polymer-like structure of many eukaryotic phase sep-

arating proteins. These proteins have been shown to be highly enriched in unstructured regions, so called intrinsically disordered domains. While these unstructured protein domains are not abundant in prokaryotes [47], the model can also be applied to multivalent interactions of folded proteins.

While LLPS has been the most prominent mechanism of biomolecular condensate formation, other underlying processes have been identified. Namely, bridging-induced phase separation (BIPS) has been suggested to drive the collapse of chromatin into a globular liquid-like phase almost indistinguishable from droplets formed by LLPS. Yet, BIPS is not mediated by multivalent protein-protein interactions, but rather by the bridging of a long polymer (such as DNA) through proteins [48, 49]. Taken together, the advances in understanding the underlying grammar of protein and nucleic acid phase separation allow a more rigorous theoretical description, also of disease relevant aberrant phase separations.

However, many biological systems are not sufficiently described by equilibrium processes. Biomolecular condensates, similar to many other macromolecular cellular structures, are most likely maintained in an 'out of equilibrium'-state to allow for more precise control over their composition, size and localization.

## 1.2 Molecular mechanisms and theory of liquid-liquid phase separation

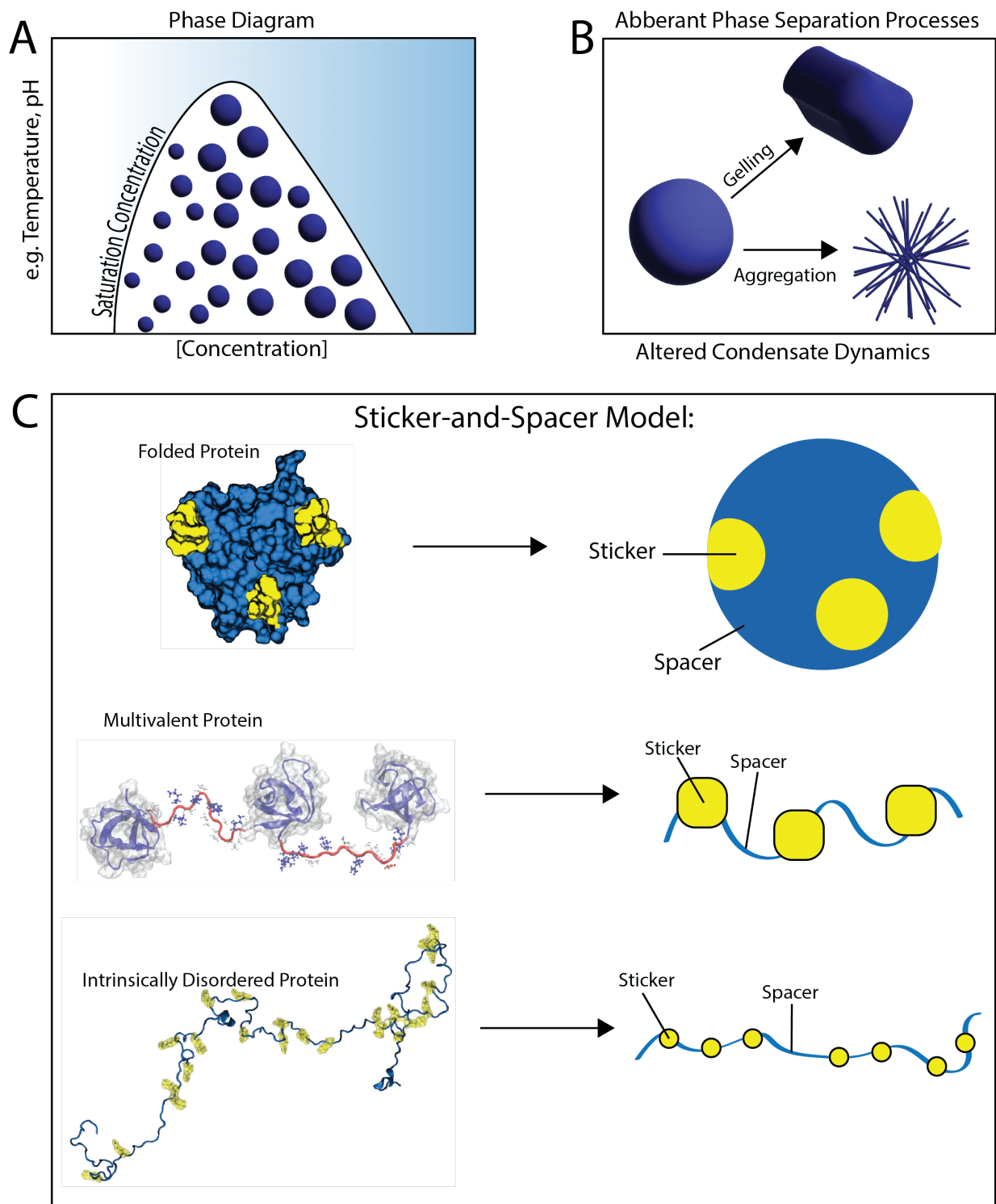


**Figure 1.3: Theory and molecular grammar of liquid-liquid phase separation.** A) shows a schematic phase diagram. Upon reaching the saturation concentration of the phase separating molecule, the solution demixes into two distinct phases differing in composition, viscosity and other parameters. B) illustrates aberrant phase separation processes such as gelling or aggregation. Such processes have been linked to various neurodegenerative diseases. C) shows the sticker-and-spacer framework describing the interactions driving liquid-liquid phase separation of forms of proteins. Images reprinted with permission from [45].

### 1.3 Out-of-equilibrium phase separation

Life happens away from equilibrium. As highly organized and complex organisms all current life forms present, they cannot afford to give in to entropy. Therefore, all living systems have developed metabolism to ensure a constant supply of energy, keeping their interior organized and functional. Some of the most exciting molecular machines, such as the ATP-Synthase, have evolved to use out-of-equilibrium conditions to generate energy [50]. This energy is then used to maintain functional structures such as the cytoskeleton, reaction networks or protein gradients. While many known biological systems operate out-of-equilibrium, biomolecular condensates have mostly been studied under equilibrium conditions. However, an intriguing body of theoretical work has shown that condensate properties can differ between equilibrium and out-of-equilibrium conditions.

As biomolecular condensates have been suggested to serve as reaction hubs orchestrating a variety of biochemical processes, theoretical work has started to unravel the novel properties that such active droplets can exhibit. After nucleation, in-equilibrium condensates will undergo a process called Ostwald ripening [51]. Herein, smaller condensates lose material to larger ones, as the surface tension is higher for smaller droplets and therefore pushes molecules to partition into the larger condensates. This leads to a single, large droplet after enough time for condensate ripening and equilibration. However, in out-of-equilibrium condensates, Ostwald ripening can be suppressed and therefore allows the cell to simultaneously maintain multiple functional condensates within its cytoplasm. This process would not be possible without energy dissipation and likely plays an important role in condensate regulation [52]. Also, shape instabilities of biochemically active condensates have been predicted, dividing individual condensates into two daughter droplets [53]. This process has been suggested to allow for early life-like properties of active condensates, but still awaits experimental verification.

The rate of chemical reactions happening within a biomolecular condensate can control other parameters, such as condensate size. Depending on the turnover of phase separating material through chemical reactions, the overall volume and number of droplets is scaling with the reaction rate. These mechanisms allow for precise structuring of the cytoplasm with differently sized biomolecular condensates [54, 55].

Similarly, the formation of condensates can be highly dependent on protein gradients. For *C. elegans* P-granules, the first membraneless organelles to be described as liquid-like condensate, dissolution of P-granules is mediated by a gradient forming protein (Mex-5). Mex-5 can compete for the RNA-binding of important P-granule constituents *in vitro* and *in vivo* and therefore dissolve the formed condensates. As Mex-5 is non-homogeneously distributed within the cytoplasm, P-granules only form in the regions of



### 1.3 Out-of-equilibrium phase separation

low Mex-5 abundance [9, 56, 57]. Therefore, the P-granule is an intriguing example of a protein gradient translating to an out-of-equilibrium positioning of biomolecular condensates.

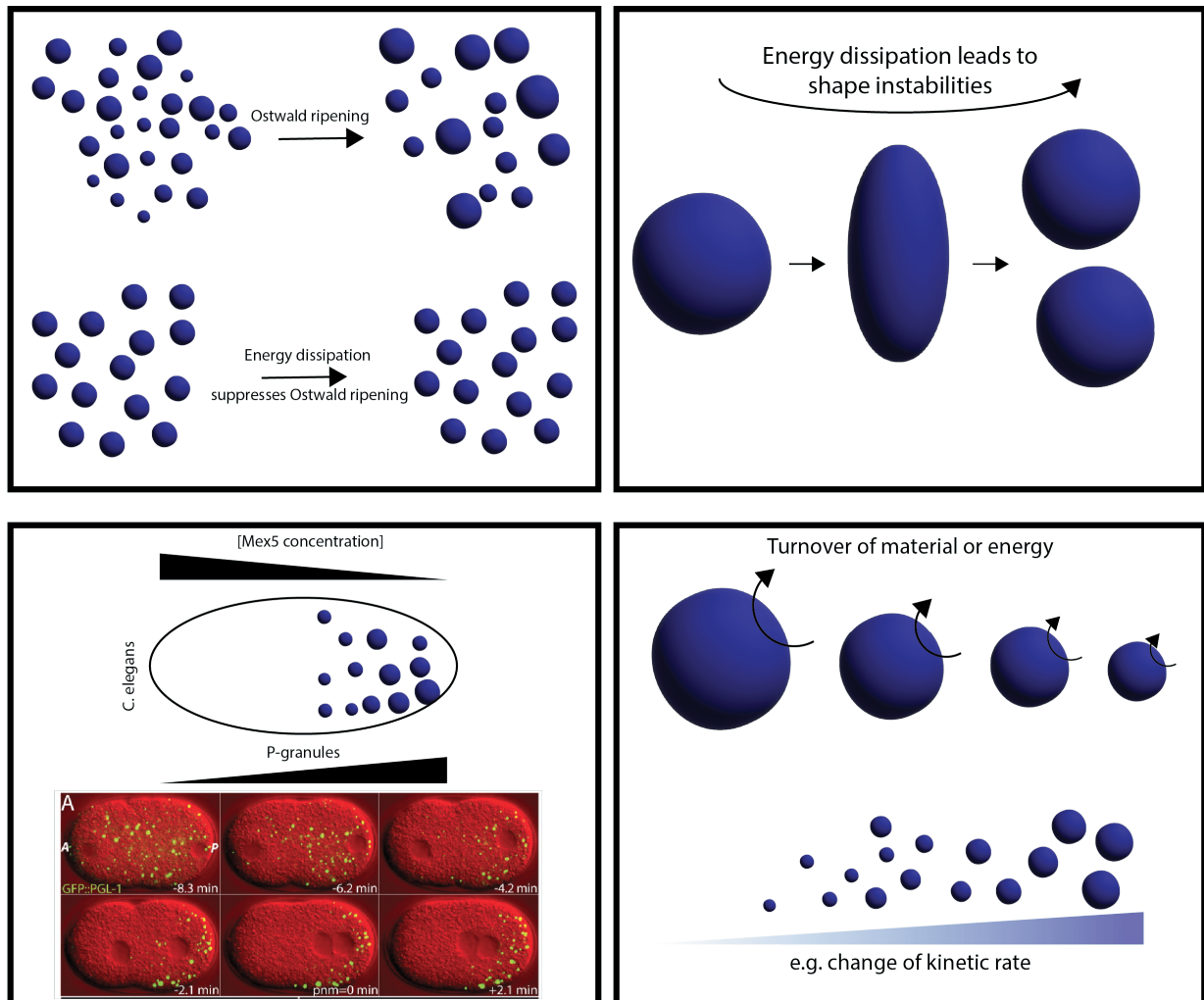


**Figure 1.4: Out-of-equilibrium liquid-liquid phase separation exhibits novel properties.** A) Equilibrium condensates undergo Ostwald ripening, so larger droplets acquire material from smaller droplets due to an increased Laplace pressure. In out-of-equilibrium conditions, condensates can maintain their initial size by energy dissipation [52]. B) schematically shows suggested shape instabilities of condensates induced by energy dissipation [53]. C) demonstrates how a protein gradient can translate to out-of-equilibrium positioning of *C. elegans* P-Granules. Image reprinted with permission from [9]. D) schematically shows how material turnover by energy dissipation can regulate condensate size as demonstrated in [55].

Surprisingly, it is still largely unexplored how the partitioning of active biochemical processes into condensates influences enzymatic reactivity and signaling cascades. Initial studies have demonstrated a concentration-dependent or independent enhancement of re-

action rates through substrate and enzyme sequestration [58]. However, these examples were rather artificial condensate systems and *in vivo* evidence is still scarce.

Taken together, active processes have a tremendous potential to shape biomolecular condensates. While many theoretical studies have explored the implications of energy dissipation for condensates, less experimental evidence is available [59]. However, the known examples of active condensates have demonstrated that out-of-equilibrium phase separation is likely to play a key role in condensate regulation and utilization.

## 1.4 Liquid-liquid phase separation on surfaces

As we learn more about phase separation and biomolecular condensates, we come to the conclusion that these cellular substructures do not exist isolated from other cellular features such as lipid bilayers or DNA strands [60]. More precisely, many of the characterized biomolecular condensates are known to interact with a variety of macromolecular structures. Interestingly, the interaction of a condensate with a surface offers an extended theoretical framework known as wetting [61, 62]. While the process of wetting has long been known and extensively studied in material or physical sciences, it is a relatively unexplored area of cell biology. Different phenotypes of surface wetting condensates have been observed *in vivo* and *in vitro*. These range from a thick film on a DNA-strand, condensates on cytoskeletal fibers to clear three-dimensional structures on membrane vesicles [63, 64, 65].

Theoretically, the preferential interaction with a surface allows proteins to form films or condensates at lower concentrations than in bulk. As saturation concentrations for *in vitro* phase separation of some proteins are significantly higher than their *in vivo* concentration, this process has been suggested to enable the phase separation of many DNA- and membrane-binding proteins *in vivo* [63]. Also, the specific interaction with DNA or membranes, mediated e.g. by sequence-specific DNA binding or preferential interaction with lipid raft components, have been demonstrated to enable precise positioning of nucleation points for the formation of biomolecular condensates [66]. Wetting therefore permits fine spatial control over the otherwise stochastic process of condensate nucleation.

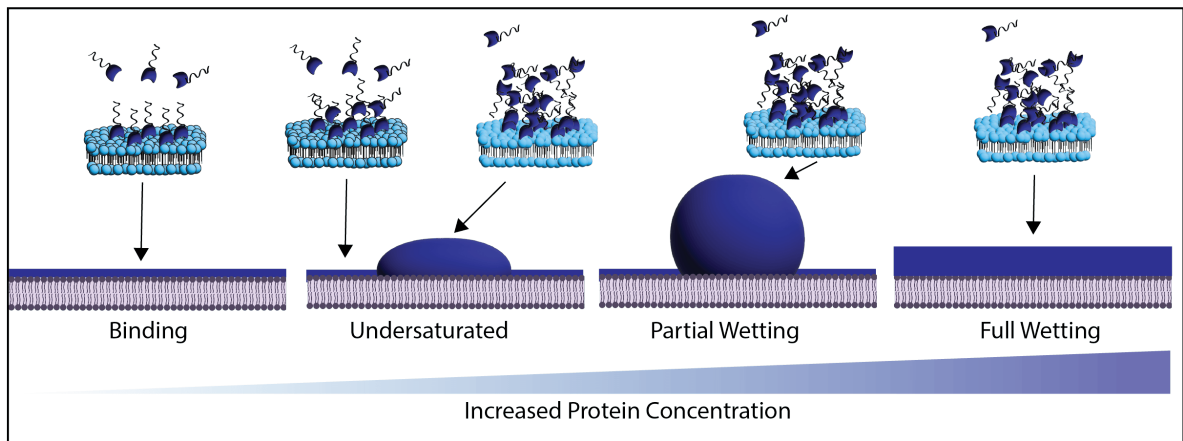


**Figure 1.5: Wetting transition of a biomolecular condensate on a lipid bilayer.** Membrane binding of phase separating proteins allows them to transition from bulk to a pre-wetting and wetting state as explored in [61]. Different morphologies of wetting can be achieved through differences in protein concentrations.

Interestingly, phase separated organelles are not only nucleated on the surface but can also exhibit forces on said surface. Protein condensates have been shown to exert forces on single or double stranded DNA strands, collapsing them into a spherical shape [63, 67]. This collapse is mediated by interactions of proteins on the DNA strand and can be seen as a first order phase separation. This process is highly reversible and force dependent, allowing for precise regulation of the formation of a DNA-protein condensate. Such compaction of DNA upon protein phase separation could also play a role in chromatin organization [48].

Similarly, biomolecular condensates have been shown to transform lipid membranes upon phase separation. Prominent examples of such membrane-interacting biomolecular condensates are found at the so-called post-synaptic densities, in cellular signaling systems or tight junctions connecting different cells [68, 69, 70]. Early work using simple aqueous-two phase systems constituted of artificial polymers (ATPS) has demonstrated that membranes can be strongly deformed by phase separating systems [71, 72, 73, 74]. These studies have identified a variety of wetting-mediated phenomena on model membrane systems including membrane tubulation, deformations and even complete budding induced by bulk phase separation. More recent work has shown that phase separating proteins rather than artificial polymers can cause similar deformations or membrane tubulations *in vitro* and *in vivo* [75, 64, 76, 77].

It is therefore obvious, that surface condensation offers a great variety of novel biological mechanisms to spatially control condensate nucleation, but also exert forces on other macroscopic cellular features. An intriguing example is the possibility of exo- or endocytosis of condensates driven by membrane interactions. The plausibility of this process was demonstrated by the endocytosis of membrane binding and phase separating molecules but could also be applicable to clathrin mediated endocytosis [80, 79].

While the field of surface-mediated phase separation of biomolecules is still in its infancy, it is certain that interesting biological and biophysical questions may be answered with further model systems. We have now explored how biomolecular condensates can be controlled and maintained, but what biochemical functions do these cellular structures actually fulfill?

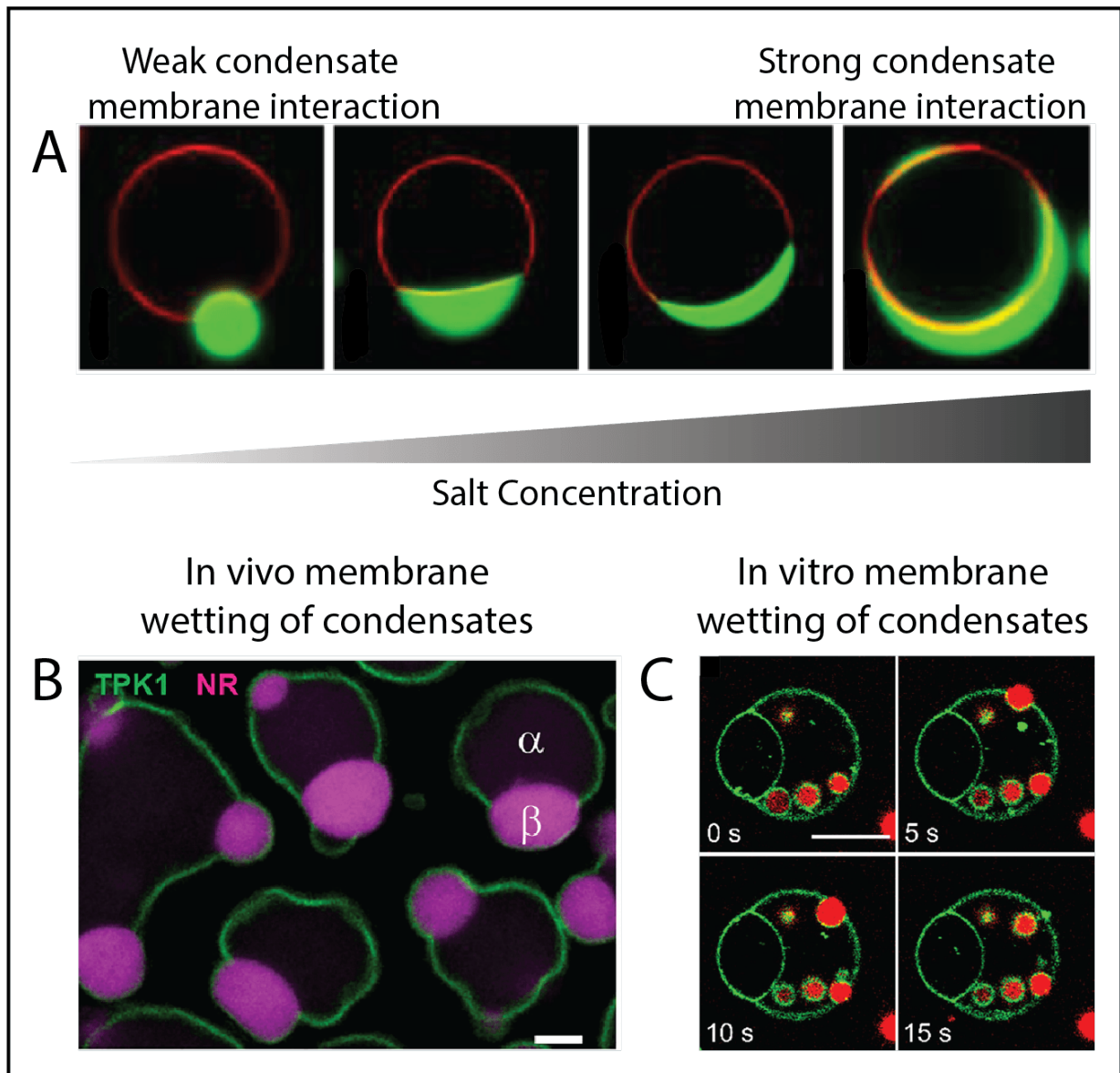


**Figure 1.6: Biomolecular condensates wet and deform lipid membranes.** A) shows the differential wetting of a biomolecular condensate on a lipid bilayer (GUV) in dependence on the environmental salt concentration *in vitro*. Image taken with permission from [78]. B) shows *in vivo* condensates wetting the vacuolar membrane and deforming said vesicles. Image taken from [77] and reprinted with permission. C) shows the wetting-mediated endocytosis of biomolecular condensates into GUVs. The image was taken with permission from [79].

## 1.5 Biological examples of phase separating structures and functions

More than a decade after the discovery of liquid-liquid phase separation as the underlying principle of *C. elegans* P-granule formation, an impressive variety of biomolecular condensates have been identified across the tree of life. The discovery of these phase separated cellular compartments was accompanied by assigning biological functions to the novel condensates. These range from transcription, mRNA, buffering of cellular noise and protein storage to the nucleation of microtubule formation [81, 8, 82, 83]. While many of these claims are still awaiting their *in vivo* verification, there are some intriguing examples of complex biomolecular condensates fulfilling biochemical functions.

### 1.5.1 The Nucleolus

The Nucleolus is probably the most prominent membraneless organelle, likely due to its clear visibility and interesting function. As it is detectable by rather simple brightfield microscopy, it was first described as early as 1830. However, it took another 130 years to assign a potential function to this obvious nuclear compartment and the mechanism of its assembly was not resolved until very recently [84, 85].

The nucleolus is now widely accepted as the ribosome biogenesis site within the cell nucleus. It forms around repetitive rDNA sequences and builds multiple layers to accommodate the complex ribosome assembly. In particular, the nucleolus consists of three distinguishable, non-membrane bound layers. The most inner layer is the so-called fibrillar center, following the dense fibrillar component and the granular component. All three layers are thought to have different biological functionalities and differ in composition. The fibrillar center is responsible for rRNA transcription, which is then shuttled to the dense fibrillar component for processing. Finally, ribosome biogenesis is taking place in the granular component [85, 86].

While this hierarchical layering is highly relevant to the function of the nucleolus, it was not understood how such complex topography is achieved. Initial experiments on the dynamics of the nucleolus suggest a viscous but liquid-like behavior, with components constantly exchanging with the environment [88]. These findings lead to the hypothesis that the nucleolus is a multilayered biomolecular condensate [89].

Upon *in vitro* reconstitution, it was found that each of the main components of the three phases can undergo liquid-liquid phase separation. Intriguingly, the biophysical properties differed between the distinct protein droplets, suggesting potential separate environments for their specialized tasks within the nucleolus. Upon full *in vitro* recon-

## 1.5 Biological examples of phase separating structures and functions

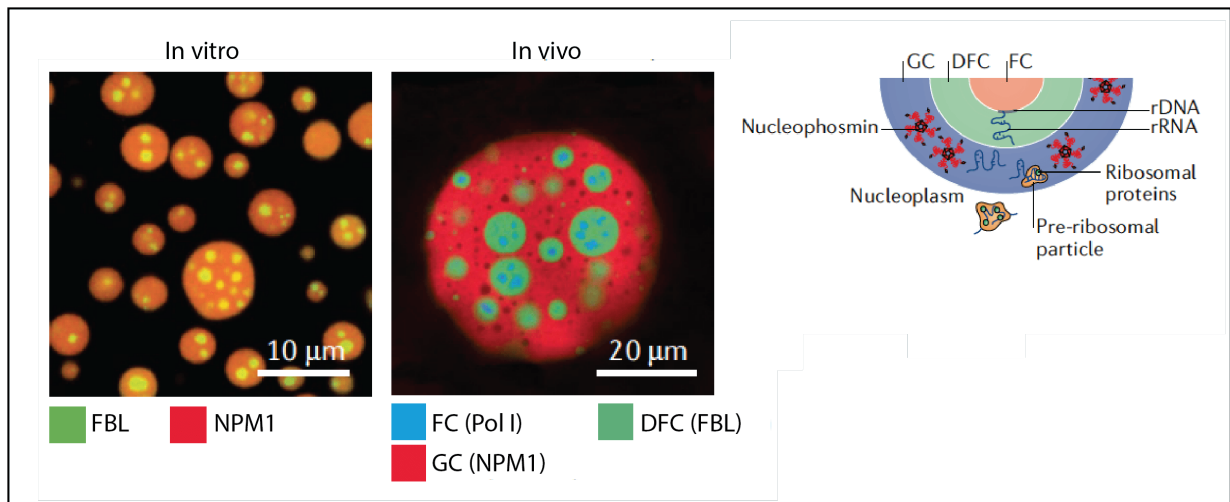


**Figure 1.7: The Nucleolus as a biomolecular condensate.** *In vitro* reconstitution of the nucleolus components unraveled a multilayered structure of liquid-like condensates. The multilayering is regulated by differences in the surface tension of the individual condensates and intriguingly recapitulates the *in vivo* structure of the nucleolus. Each layer is thought to fulfil a different biological function. Images reprinted with permission from [85, 87].

stitution, the three proteins formed liquid-like droplets which showed immiscibility, but perfectly reconstituted the *in vivo* layering of the nucleolus. Interestingly, the immiscibility of the three distinct protein phases is governed by the different biophysical properties of the formed dense phase, such as viscosity and surface tension [85].

These findings demonstrate the unique capability of phase separating systems to build highly complex and functional structures through fine tuning of biophysical parameters. Moreover, *in vitro* reconstitution is a suitable method to unravel these complex mechanisms.

## 1.5.2 The Nuclear Pore Complex

Nuclear pores are large protein complexes that act as gatekeepers for the transport of molecules in and out of the cell nucleus [90]. They play a crucial role in regulating the exchange of genetic information, macromolecules, and signaling pathways between the nucleus and cytoplasm [91]. Nuclear pore complexes are composed of tens of different proteins, arranged in a precise but dynamic manner, forming a selective filter that controls the traffic of molecules based on their size, shape, and charge.

In this way, nuclear pores play a key role in maintaining the integrity of the genome, as well as in modulating the expression of genes and the response of cells to their environment. Understanding the structure and function of nuclear pores is essential for uncovering the fundamental mechanisms of cell biology. While the composition of these highly complex structures is largely known, the mechanism of selective transport was, until recently, not well understood. Nuclear pores contain a permeability barrier which prevents uncontrolled transfer of larger molecules and only allows passage of cargo-nuclear transport receptor complexes larger than 30-40 kD. This permeability barrier is composed of multiple nucleoporins, which form the scaffold and contain phenylalanine-glycine (FG)-repeat domains that allow nuclear target receptors to cross the permeability barrier efficiently [90]. The binding of nuclear target receptors to the hydrophobic clusters in FG-repeats is essential for facilitated nuclear pore complex passage [92].

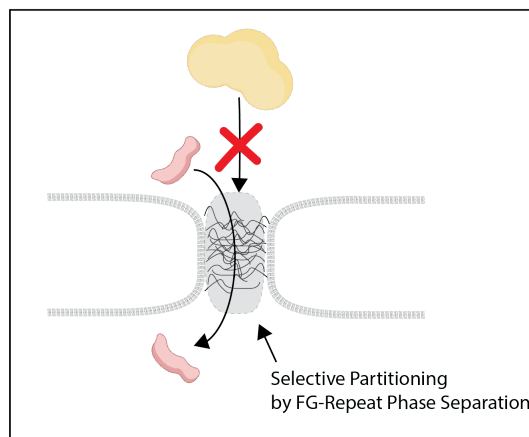


**Figure 1.8: The Nuclear Pore Complex exhibits properties of a biomolecular condensate.** Through the phase separation of so-called FG-repeat domains, core functionalities of the nuclear pore complex such as selective transport of molecules were *in vitro* reconstituted [93, 94].

It is therefore clear that the FG-repeats are fundamental to the functioning of the nuclear pore complex. However, the mechanism of assembly and regulation of molecular diffusion through these structures has not yet been explored. Upon *in vitro* purification of the FG repeats of several nucleoporins, a phase transition (gelling) process was observed



[93, 94]. This gelling takes place under physiological conditions and is reversible, suggesting non-covalent interactions as building blocks of the structure. Intriguingly, the formed gel was able to recapitulate the selective permeability of nuclear pore complexes [94]. Upon exposure of the gel phase with differently sized molecules, it was found that small molecules were able to penetrate the gel. However, large molecules were excluded from the gel unless a specific transportation signal, such as importin beta was bound to the large cargo. Therefore, the phase separation from FG-repeats of nucleoporins can explain key properties of the nuclear import mechanism. Depending on the saturation of the interactions within the formed gel, a highly selective phase is formed, allowing for tight control over nuclear import.

These two examples, out of many possible, clearly demonstrate the molecular diversity of phase separation processes. Also, for both presented biomolecular condensates, the material properties of the formed phases are inherently intertwined with the biological function fulfilled by these cellular substructures.

## 1.6 Phase separation from an evolutionary viewpoint

Proteins have evolved over time to perform a wide variety of functions in the cell, such as catalyzing metabolic reactions, replicating DNA, responding to stimuli, or transporting molecules across the plasma membrane. As these processes are fundamental to an organisms' survival, they are strongly shaped by evolutionary pressure. Malfunctioning proteins lead to less efficient reproduction of an individual and will therefore be driven out of the genetic pool of a species and ecosystem. Clearly, this evolutionary pressure does not only act on a single protein level, but also shapes macromolecular structures which fulfil cellular tasks.

A variety of macroscopic cellular features have evolved to maintain the structural and functional properties of cells. Examples include the organization of proteins and other biomolecules into subcellular compartments, such as the nucleus, or the formation of cytoskeletal structures, such as microtubules and microfilaments, that provide mechanical support and shape to the cell or orchestrate the biochemistry of the cytosol.

An intriguing example of evolutionary forces on a macroscopic cellular structure is the adaption of the bacterial flagellum to different environmental constraints. The more viscous the surrounding media of a bacterial genus, the higher the torque the flagellum must create to allow movement. On a molecular level, this can be observed as a larger diameter of the flagellum and therefore a direct change of a macroscopic protein structure through evolutionary pressure [95].

While biomolecular condensate assembly and regulation has been of great interest in

the last decade, only few studies focus on evolutionary conservation of phase behavior and properties [96, 97, 98, 99, 100, 101]. As claims for the fundamental nature of biomolecular condensates are surging, this is rather surprising. If condensates really fulfil many of the functions attributed to them, one expects high conservation of properties and functionalities across species. Intriguingly, recent work has started to shed light on the evolutionary conservation of phase separation and their subtle changes driven by evolutionary pressure, also providing more rigid proof of the functional relevance of these cellular substructures.

An interesting example is the heat stress response of the fungal Ded1p protein: Upon a change of the environmental temperature, this protein undergoes a phase separation which has been suggested to adapt important translational processes to the change of growth conditions. Obviously, this temperature-driven process is highly dependent on the natural environmental conditions of any given organism. Therefore, the phase transition temperature of Ded1p should correlate with the natural optimal growth temperature of the organism. Indeed, this correlation was found and could be attributed to selection towards higher or lower tryptophan content in the phase separating proteins, finely adjusting the transition temperature of the protein. This study therefore shows that biophysical parameters such as the transition temperature of a phase separating protein can be subject to evolutionary pressure and selection on an amino acid level [98].

Similarly, another study identified a protein family, the so-called DEAD-box helicases as global regulators of biomolecular condensates in eukaryotes and prokaryotes. These proteins are thought to orchestrate the formation of a variety of liquid-like condensates within cells through their unstructured tails. Importantly, many of the members of this protein family have recently been shown to phase separate [96].

However, an evolutionary view on the underlying biophysics and regulation thereof has been missing. Hondele et al. first compared the sequence features allowing LLPS of DEAD-box helicases and found that only the protein family members with intrinsically disordered regions formed droplets *in vitro* and *in vivo*. Remarkably, the sequence conservation of these intrinsically disordered regions within the family is low, showing that standard bioinformatic tools to study protein evolution such as multiple sequence alignments would perform poorly on these features. Following, the authors linked the regulation of forming condensates to the ATPase and RNA binding activity of these proteins, showing a loss of dynamics or dissolution condensates upon mutating the enzymatic activity [96].

This exceptional work demonstrates that not only the propensity of a protein family to form liquid-like condensates can be conserved, but also that regulative mechanisms are subject to evolutionary pressure and selection. Also, our usual bioinformatic tools to study the similarities of proteins should be taken with caution when applied to proteins containing intrinsically disordered domains.

## 1.7 Liquid-liquid phase separation in bacteria

While liquid-like compartments have attracted significant interest in eukaryotic organisms, fewer examples of membraneless organelles are known in prokaryotes. This is likely linked to the limiting dimensions of most bacteria, making *in vivo* observations of membraneless organelles rather challenging. Traditionally, bacteria and other prokaryotes were long described as ‘bags of enzymes’, lacking the complex internal organization of many eukaryotes.

However, it has become apparent that the bacterial cytoplasm is highly organized in space and time [102]. An intriguing variety of cellular organelles has been found in bacteria: These include lipid bilayer encapsulated cellular substructures such as Magnetosomes or the protein-shelled microcompartments like the bacterial carboxysomes [103, 104]. With the emergence of biomolecular condensates in eukaryotes, researchers begin to look for similar structures in prokaryotes [105]. Excitingly, recent studies have identified several liquid-like compartments in a variety of bacteria, such as cyanobacteria [106], *C. crescentus* [107] or *E. coli* [108, 109]. In similarity to eukaryotes, the membraneless organelles identified in bacteria are thought to fulfill a surprising variety of cellular tasks, such as regulation of transcription [108], compartmentalization of carbon dioxide fixation [106] or partition complex formation [109]. Most of these studies used a combination of *in vitro* reconstitution and *in vivo* single molecule tracking or super resolution microscopy to link the observed *in vitro* phase separation to biological functions.

These examples of biomolecular condensates prove that prokaryotes, just like eukaryotes, utilize phase separation processes to structure their cytoplasm and regulate biochemical reactions in time and space.

## 1.8 The ParB protein family

The ParB protein family is a group of bacterial proteins that play a crucial role in chromosome segregation and nucleoid occlusion during cell division. While the precise mechanistic details of chromosome segregation differ between species, the overall structure of these ParB proteins is highly similar. They have a charged N-terminal region, allowing them to interact with ParB’s binding partner ParA. Also, all ParB protein family members have a Helix-turn-Helix DNA-binding motif, which allows binding to the chromosomal DNA. Lastly, the C-terminus of ParB proteins is responsible for homodimer formation. While much of this structure is conserved for the Noc subfamily, slight adaptations to the differing biological function are obvious. Instead of the charged N-terminal region for ParA interaction, Noc has a membrane binding helix allowing it to recruit the nucleoid to the

plasma membrane. The helix-turn-helix and dimerization domains however are conserved. It was even demonstrated that the sequence specific DNA-binding of Noc and ParB can be switched by a handful of amino acid substitutions [110]. It is therefore clear that the ParB protein family fulfills different biological functions, but remains structurally similar.

### 1.8.1 The ParABS-System and ParB

The tripartite ParABS system consists of two proteins, ParA and ParB, and a DNA-sequence, parS. First discovered in *E. coli* as the responsible protein machinery for plasmid partitioning, it is now known to occur in many different bacterial species [110]. Also, the ParABS system is not only capable of low-copy plasmid segregation but has been shown to segregate whole bacterial chromosomes in different species [111]. While the exact mechanism of action is not yet clear, several hypotheses have been suggested. ParA is a Walker-type ATPase and a non-specific DNA binding protein. Upon ATP binding, ParA dimerizes which increases the affinity to DNA, therefore relocating ParA to the bacterial nucleoid. ParB stimulates the ParA-ATPase activity, which leads to ParA monomerization and detachment from the DNA. As ParB forms higher order structures on parS sites, these clusters cooperatively detach ParA from the nucleoid. This dissociating and rebinding of ParA generates a gradient which moves the ParBS complex towards the cell poles, therefore segregating the chromosome or plasmids [112, 113, 114].

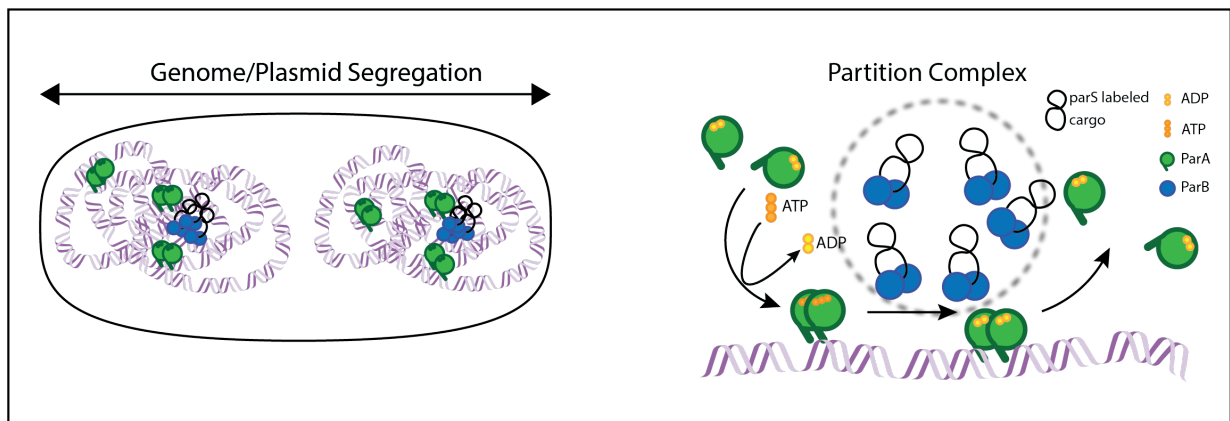


**Figure 1.9: The ParABS system is responsible for genome and plasmid segregation.** The partition complex as central element of the ParABS system displaces ParA from the nucleoid, therefore forming a gradient along which it moves to the cell poles. Figure partially adapted from [115].

However, several questions regarding the ParABS system remain open. Most importantly, the formation of the higher order complex by ParB on the parS sites is not yet understood. With the emergence of phase separated condensates in bacterial cell biology, it was hypothesized that this so-called partition complex is a liquid-like structure [116].

Through a combination of *in vivo* and *in silico* experiments, an initial model for partition complex based on the combination of DNA binding and ParB-ParB interactions revealed the potential of condensate formation [117, 116]. Further *in vivo* analysis through super resolution microscopy and single particle tracking revealed a round shape, fusion and fission events of the *E. coli* partition complex [109]. This further supported the hypothesis of a liquid-like nature of the partition complex. An *in vitro* reconstitution of the partition complex therefore represents the missing link for a coherent picture of its assembly and regulation.

Moreover, it was recently established that ParB is an enzyme, concretely a CTPase [118, 119, 120, 121]. This CTPase activity has been linked to the ability of ParB to bind to parS sites and spread from there to the surrounding, non-specific DNA. Linking the CTPase activity of ParB to the formation of higher order structures could explain partition complex regulation. *In vivo* studies have linked the CTPase activity to the size of the partition complex [119]. While it is not yet clear if a phase separation process is needed to explain the three-dimensional structure of the partition complex, it is certainly an intriguing possibility and a worthy motivation for further studies.

## 1.8.2 Nucleoid Occlusion and Noc

Nucleoid occlusion is a regulative process for positioning the bacterial divisome in midcell and avoiding the guillotining of the nucleoid by the constricting cell division machinery [122, 123, 124]. It was first identified in *E. coli* but the molecular factors involved remained mysterious. A decade after the initial discovery, SlmA was identified as the protein responsible for nucleoid occlusion in *E. coli* and shortly after, Noc was found in *B. subtilis* [122, 123]. While the phenotypes of Noc and SlmA knock-outs are relatively similar, the molecular mechanisms seem to differ between the two species. SlmA has been shown to enhance the disassembly of the filamentous protein FtsZ which is thought to drive divisome constriction, therefore making an assembly close to SlmA unstable [125]. As SlmA binds the nucleoid at specific sites, the divisome is less likely to assemble above the nucleoid. Together with other divisome positioning mechanisms, such as the MinCDE system, this prevents aberrant division sites and ensures faithful chromosome segregation. Interestingly, it was recently demonstrated that SlmA can form liquid-like condensates upon interaction with FtsZ monomers [126]. Once FtsZ starts polymerizing, the SlmA-FtsZ droplets dissolve due to a lack of FtsZ monomers, but reversibly reform when GTP is depleted. It is, however, not yet clear if this regulative process of buffering FtsZ monomers plays an *in vivo* role.

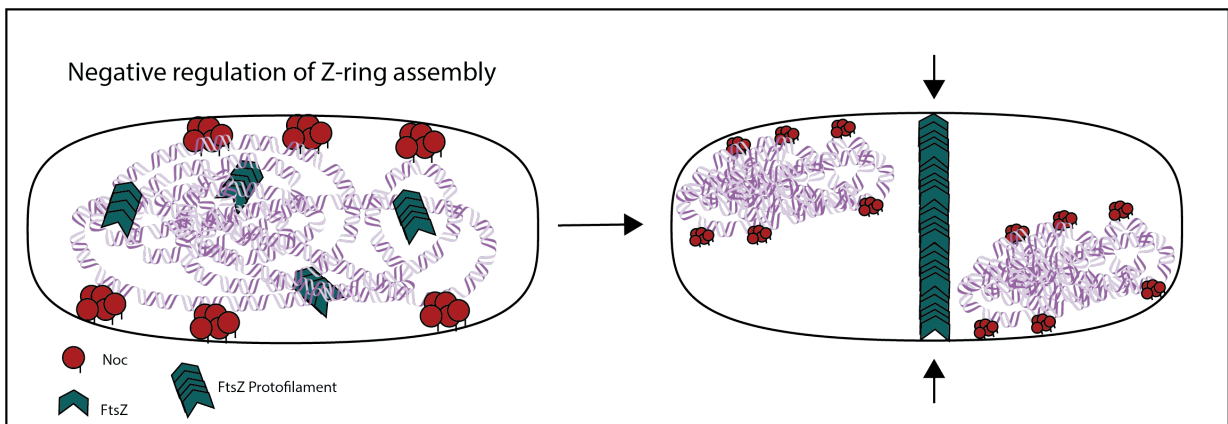


**Figure 1.10: Noc regulates the Z-Ring assembly above the nucleoid in *B. subtilis*.** Most likely through corraling FtsZ protofilaments, Noc foci restrict Z-Ring assembly to nucleoid-free space. This prevents the guillotining of the bacterial chromosome through the constricting Z-ring.

The *B. subtilis* nucleoid occlusion protein Noc however has not been shown to destabilize these filaments through direct interactions. More likely, Noc forms large complexes on the nucleoid which corral the FtsZ protofilaments diffusion towards midcell [127]. These foci have been studied *in vivo* and were found to be highly responsive to environmental changes [124]. Dynamic disassembly of Noc foci upon depletion of the membrane potential was observed. Also, Noc is known to recruit the nucleoid to the membrane and was hy-

pothesized to sterically hinder FtsZ ring formation in proximity to the membrane bound nucleoid. Like other ParB protein family members, Noc has recently been identified as a CTPase. However, CTP binding and hydrolysis is thought to regulate Noc's membrane binding and spreading, rather than its affinity to DNA. Mutants lacking the CTP-binding and hydrolysis ability show no or impaired foci formation on the membrane, indicating a regulative role of CTP-binding in nucleoid occlusion complex formation.

While the exact mechanism of action of Noc nucleoid occlusion is not yet unraveled, it is obvious that the formation of large foci on the membrane is fundamental for the process of FtsZ ring regulation. Also, the *E. coli* counterpart of Noc, SlmA, has been shown to undergo a liquid-liquid phase separation capable of regulating FtsZ-ring assembly *in vitro*. A potential liquid-liquid phase separation by Noc is therefore a plausible hypothesis and an exciting endeavor for *in vitro* reconstitution efforts.

## 1.9 Main methods

### 1.9.1 Phase diagrams and turbidity measurements

Phase diagrams are fundamental to all research on phase transitions, may it be the classic liquid-solid transition of water, or the formation of an Einstein-Bose condensate. These basic processes are best characterized by phase diagrams [38]. In this thesis, I use a simple but robust protocol to measure the protein concentration of the dilute phase in a variety of conditions. The protocol allows to introduce changes in environmental conditions, such as ionic strength or pH, but also accommodates the addition of small molecules. Similarly, measuring the overall amount of phase separated material is a simple, but conclusive way to back phase diagrams up with a different protocol. I used a simple turbidity measurement as a proxy for the overall amount of phase separated material. Through the formation of phase separated droplets, the sample turns turbid and scatters light. An increase in phase separated material increases light scattering, allowing a rough estimate of the effect of environmental conditions or small molecules on the phase separation process.

### 1.9.2 Fluorescence microscopy

Fluorescence microscopy is a powerful imaging technique used in cell biology and other related fields to visualize cellular structures and processes. It works by using a combination of fluorescent dyes and specialized light sources to produce highly detailed images of cells and their components. The fluorescence dyes emit light of specific wavelengths when excited by the light source, allowing for selective labeling and visualization of cellular structures. This technique has revolutionized our understanding of cellular biology,

enabling researchers to study the dynamic interactions of various cellular components and observe cellular processes in real-time. In this thesis, I used fluorescence microscopy to visualize biomolecular condensates and quantitatively measure partitioning of molecules into protein droplets.

### 1.9.3 Model membrane systems

To reconstitute the liquid-liquid phase separation of the membrane binding protein Noc, I used two different *in vitro* model membrane systems. While supported lipid bilayers allow quantitative imaging of binding and phase separation processes, giant unilamellar vesicles represent more physiological membrane properties, such as deformability and faster diffusion of the lipid molecules.

Supported lipid bilayers (SLBs) are thin bilayers of lipid molecules that are supported by a solid substrate, such as a glass or silicon surface. They are useful because they mimic the physical and chemical properties of biological membranes, allowing for the study of biological processes in a controlled and well-defined environment. Supported lipid bilayers can be used to study a variety of cellular processes, including membrane transport, protein-lipid interactions, and signal transduction. Additionally, they can be used to develop biosensors and other biotechnological applications. The controlled and well-defined environment provided by supported lipid bilayers allows for the precise manipulation and study of biological processes, providing valuable insights into the underlying mechanisms of these processes.

Giant Unilamellar Vesicles (GUVs) are large lipid vesicles (spherical or cylindrical) that consist of a single lipid bilayer and an inner aqueous compartment. They range in size from few to tens of microns and are used to study cellular processes *in vitro*, as they closely mimic the physical and chemical properties of biological membranes. GUVs can be used to study membrane transport, protein-lipid interactions, membrane fusion, and other biological processes. The large size and simplified structure of GUVs make them useful for imaging and biophysical studies, as well as for developing biosensors and other biotechnological applications. The ability to control the composition and physical properties of GUVs also makes them valuable tools for investigating the fundamental principles of cellular and molecular biology.

### 1.9.4 Fluorescence correlation spectroscopy in biomolecular condensates

Fluorescence Correlation Spectroscopy (FCS) is a technique used to analyze the behavior of fluorescently labeled molecules in solution at the single-molecule level. It works



by measuring the fluctuations in fluorescence intensity produced by the diffusing molecules in a diffraction-limited observation volume. The autocorrelation of these fluctuations is analyzed to determine the diffusion coefficient and concentration of the fluorescent molecules. FCS is a highly sensitive and quantitative method that provides information about the kinetics and dynamics of molecular interactions in solution. It is widely used in biophysics, chemical physics, and cell biology to study a variety of processes, such as protein-protein interactions, membrane transport, and molecular diffusion in crowded environments. While FCS has been used in biomolecular condensates to study molecular diffusion and concentrations [68, 128, 129], there are several experimental pitfalls. In publication 4, we optimized FCS measurements to account for the unique properties of the condensate environment. A particular problem is the refractive index mismatch created by the phase separation and slow molecular diffusion. Refractive index mismatch can cause a distortion of the confocal volume and therefore lead to misinterpretation of the data. Also, the high viscosity and therefore low diffusion rates of molecules in condensates can cause excessive bleaching, making various data analysis adjustments necessary. We developed approaches to check for these pitfalls and potential experimental strategies for circumventing them.



# Objectives

The process of protein self-assembly has been extensively studied for its critical role in cellular function and regulation. Self-assembly refers to the spontaneous formation of higher order structures from individual protein molecules without the need for external assistance. The ability of proteins to self-assemble into a wide range of structures, such as filaments, shells, and droplets, has been essential for the evolution of complex life forms. Thus, the study of protein self-assembly has gained significant attention in recent years due to its wide-ranging implications in biotechnology, origin of life, and the molecular basis of cellular function. This thesis explores the self-assembly of a large bacterial protein family, focusing on the molecular and regulative aspects of the process, and how they are conserved across different species and protein family members.

Liquid-liquid phase separation (LLPS) is a biophysical process in which proteins self-assemble into liquid-like droplets within a cellular environment, and is distinct from other organizational processes in several ways. Unlike other protein self-assembly mechanisms, LLPS is highly dynamic allowing for the rapid exchange of proteins between the liquid droplet and surrounding cellular environment in response to changes in the environment or the cellular homeostasis. This flexibility enables the regulation of cellular processes through the modulation of protein or client concentrations within the liquid droplet or droplet material properties such as viscosity. As a result, LLPS is a versatile mechanism for the formation of complex protein structures in cells. An increasing variety of biological functions have been assigned to these biomolecular condensates and first therapeutic approaches drugging these cellular substructures are being developed. While our knowledge on the regulation, formation and maintenance of these condensates is advancing, we only have few examples of the evolutionary adaption and conservation of phase separation processes within protein families. Therefore, studying a bacterial protein family for the evolutionary conservation of liquid-liquid phase separation offers insights into the functional importance and broad occurrence of this self-assembly process in various organisms and distinct cellular processes. There are four main reasons why I choose to study the bacterial ParB protein family in this thesis:

1) ParB proteins are highly abundant in prokaryotes and essential for faithful segregation of genetic material. This allowed me to test several homologues of ParB for their propensity to phase separate and even more excitingly, characterize the phase behavior of a orthologue with a distinct biological function. This comparison across distinct biological functions offers the opportunity to find similarities, but also differences between the orthologues.

2) While *in vivo* studies have shown higher order structures of ParB proteins and theoretical and *in vivo* studies suggest a liquid-like behavior of the partition complex, no *in vitro* reconstitution has been carried out so far. By this reconstitution, I am able to explore the specific biochemical and environmental parameters influencing ParB phase behavior, unraveling details hardly accessible by *in vivo* studies.

3) The recently discovered enzymatic activity of ParB proteins has been linked to the control of the partition complex assembly and ParB spreading on DNA. Theoretical studies have suggested that active processes can be highly efficient in controlling the nucleation, growth and distribution of biomolecular condensates. ParB's CTPase activity is therefore a perfect model system to study the potential influence of enzymatic processes on condensates.

4) ParB phase separation is inherently intertwined with its interaction with DNA, and similarly Noc's formation of higher order structures is related to its membrane binding activity. Therefore, both proteins interact with different biological surfaces or large molecules. I will explore the impact of phase separation on these large cellular structures and aim to understand the specificity of droplet formation on biological surfaces such as lipid membranes.

These four topics are not only relevant to the biochemistry of the ParB protein family, but rather represent areas of general interest for the field of biomolecular condensates. By exploring the diverse properties of the ParB protein family, I will be able to explore out-of-equilibrium regulation of condensates, surface wetting and the evolutionary conservation of the formed liquid-like condensates.

# List of publications

- P1 Merino-Salomón, A.\*, **Babl, L.\*** and Schwille, P. (2021). Self-organized protein patterns: The MinCDE and ParABS systems. *Current Opinion in Cell Biology*, 2021. DOI: 10.1016/j.ceb.2021.07.001 (*Review*) \* shared first-author
- P2 **Babl, L.**, Giacomelli, G., Ramm, B., Gelmroth, A. K., Bramkamp, M., & Schwille, P. CTP-controlled liquid–liquid phase separation of ParB. *Journal of Molecular Biology*, 2022, 167401. <https://doi.org/10.1016/j.jmb.2021.167401>
- P3 **Babl, L.**, Merino-Salomón, A., Kanwa, N. et al. Membrane mediated phase separation of the bacterial nucleoid occlusion protein Noc. *Sci Rep* 12, 2022. <https://doi.org/10.1038/s41598-022-22680-5>



## Additional publications

- P4 In vitro Measurements of Partition Coefficients in Biomolecular Condensates using Fluorescence Correlation Spectroscopy, Jan-Hagen Krohn, **Leon Babl**, Lise Isnel, Yusuf Qutbuddin and Petra Schwille, in preparation for submission to *Methods in Mol Biol*, 2023.
- P5 Repulsive electrostatic interactions modulate dense and dilute phase properties of biomolecular condensates. Michael D. Crabtree, Jack Holland, Purnima Kompella, **Leon Babl**, Noah Turner, Andrew J. Baldwin, Timothy J. Nott, *BioRxiv* 2020; doi: <https://doi.org/10.1101/2020.10.29.357863>; *under review in Molecular Cell*.
- P6 A highly specific and sensitive serological assay detects SARS-CoV-2 antibody levels in COVID-19 patients that correlate with neutralization. Peterhoff, D., Glück, V., Vogel, M. **et al.**. *Infection* 2021; <https://doi.org/10.1007/s15010-020-01503-7>
- P7 Regulating DNA-Hybridization Using a Chemically Fueled Reaction Cycle. Michele Stasi, Alba Monferrer, **Leon Babl**, Sreekar Wunnava, Christina Felicitas Dirscherl, Dieter Braun, Petra Schwille, Hendrik Dietz, and Job Boekhoven. *Journal of the American Chemical Society* 2022; DOI: 10.1021/jacs.2c08463.
- P8 Crosslinking by ZapD drives the assembly of short, discontinuous FtsZ filaments into ring-like structures in solution. Adrián Merino-Salomón, Jonathan Schneider, **Leon Babl**, Jan-Hagen Krohn, Marta Sobrinos-Sanguino, Tillman Schäfer, Juan R. Luque-Ortega, Carlos Alfonso, Mercedes Jiménez, Marion Jasnin, German Rivas, Petra Schwille. *BioRxiv* 2023; doi: <https://doi.org/10.1101/2023.01.12.523557>; *under review in PLOS Biology*.
- P9 Designing a protein with emergent function by combined in silico, in vitro and in vivo screening. Shunshi Kohyama(\*), Béla P. Frohn(\*), **Leon Babl**, Petra Schwille. *BioRxiv* 2023; doi: <https://doi.org/10.1101/2023.02.16.528840>.

P10 Membrane-induced 2D phase separation of focal adhesion proteins. Thomas Litschel(\*), Charlotte F Kelley(\*), Xiaohang Cheng, **Leon Babl**, Naoko Mizuno, Lindsay B. Case, Petra Schwille. BioRxiv 2023; <https://doi.org/10.1101/2023.03.31.535113>.

(\* shared first-author.



# Publications

## 5.1 Publication P1

### Self-organized protein patterns: The MinCDE and ParABS systems

Summary:

The review article explores recent advances in the understanding of two prokaryotic pattern-forming systems, the MinCDE system and the ParABS system, that play important roles in biological decision-making processes such as cell division and DNA segregation. Both systems have similar molecular components, mechanisms, and strategies to achieve biological robustness despite functional differences [115].

Reprinted with permission from Elsevier.

Merino-Salomón, A.\*, **Babl, L.\*** and Schwille, P. (2021). Self-organized protein patterns: The MinCDE and ParABS systems. *Current Opinion in Cell Biology*, (*Review*); *shared first author*.





## Self-organized protein patterns: The MinCDE and ParABS systems

Adrián Merino-Salomón<sup>a</sup>, Leon Babi<sup>a</sup> and Petra Schwille

### Abstract

Self-organized protein patterns are of tremendous importance for biological decision-making processes. Protein patterns have been shown to identify the site of future cell division, establish cell polarity, and organize faithful DNA segregation. Intriguingly, several key concepts of pattern formation and regulation apply to a variety of different protein systems. Herein, we explore recent advances in the understanding of two prokaryotic pattern-forming systems: the MinCDE system, positioning the FtsZ ring precisely at the midcell, and the ParABS system, distributing newly synthesized DNA along with the cell. Despite differences in biological functionality, these two systems have remarkably similar molecular components, mechanisms, and strategies to achieve biological robustness.

### Addresses

Dept. Cellular and Molecular Biophysics, Max Planck Institute of Biochemistry, Am Klopferspitz 18, Martinsried, 82152, Germany

Corresponding author: Schwille, Petra ([schwille@biochem.mpg.de](mailto:schwille@biochem.mpg.de))

<sup>a</sup> These authors contributed equally to this work.

Current Opinion in Cell Biology 2021, 72:106–115

This review comes from a themed issue on Cell Dynamics

Edited by Danijela Vignjevic and Robert Insall

For a complete overview see the Issue and the Editorial

<https://doi.org/10.1016/j.ceb.2021.07.001>

0955-0674/© 2021 Elsevier Ltd. All rights reserved.

### Introduction

Living entities depend on the continuous formation and maintenance of structures and gradients. The spatiotemporal symmetry breaks that these can be achieved based on various levels, ranging from the formation of concentration gradients in single cells up to multicellular or organismic organization [1,2]. Protein gradients, in particular, show interesting properties, pointing to essential requirements for life-like systems. Several well-studied examples of pattern-forming protein systems can be found in various model organisms. In yeast, the Rho family GTPase Cdc42 plays a key role in polarity induction and cytoskeletal organization [3], while the organization and division of *C. elegans* are driven by the PAR proteins [4]. Cell division, in particular, is often

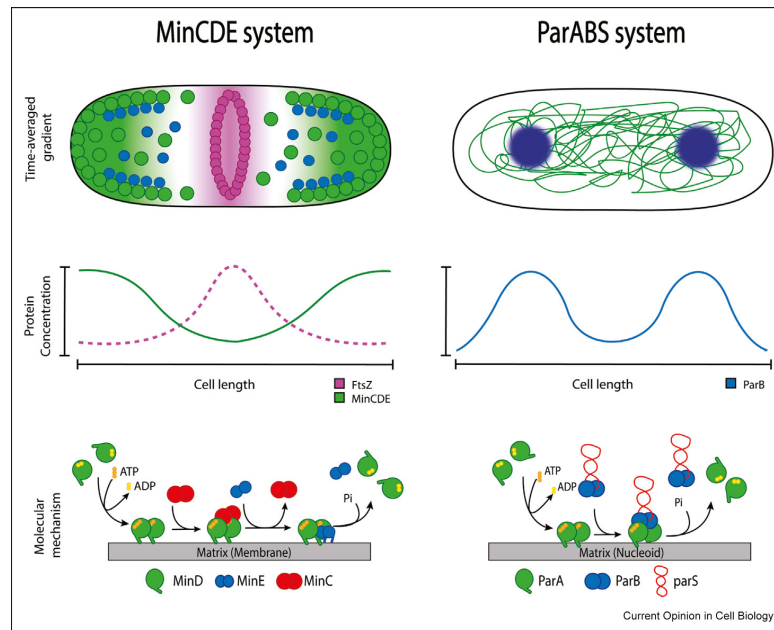
guided by specifically oriented morphogenetic cues that are, in fact, concentration gradients of proteins reflecting on the cell's spatial features. Similarly, prokaryotes use protein patterns and gradients to achieve the positioning of large-scale structures. Extensive research on the *Escherichia coli* Min system has shown a dynamic gradient on the cell membrane which achieves the precise positioning of the division machinery to midcell [5,6]. In a similar manner, the ParABS system forms patterns on the nucleoid and thereby achieves faithful segregation of genetic material [7]. A large number of quantitative biology and theoretical biological physics approaches have been accompanying the experimental investigations of pattern and gradient formation throughout the history of modern cell biology, with increasing success and predictive power [1,8–12]. However, elucidating the fundamental molecular features supporting the emergence of self-organized patterns generated by protein reaction-diffusion, actively regulated by the cell through energy dissipation to maintain its out-of-equilibrium state is still a formidable goal in biology.

The prokaryotic Min system has been extensively studied, and the mechanisms of pattern formation and regulation are thought to be well understood [5]. However, recent advances have revealed not only new surprising discoveries on pattern formation, linking the biochemical reaction-diffusion mechanisms to biophysical phenomena, such as active directional transport on membranes induced by MinCDE, but also the role of charge-dependent effects, such as liquid condensate formation, in the ParABS system. Intriguingly, these new insights point toward important differences in the molecular mechanisms of pattern formation, despite several conceptual and molecular similarities of the Min and Par systems. Thus, in this study, we focus particularly on a comparison between pattern-forming mechanisms of these prokaryotic systems, highlighting the general importance of the Min and the Par system as models for understanding biological self-organization mechanistically from first principles (see Figure 1).

### The MinCDE system

The Min protein system constitutes a spatiotemporal regulatory mechanism for positioning the division machinery in *E. coli* [13]. Min proteins self-organize after a reaction-diffusion mechanism forming a protein concentration gradient that allows the assembly of the divisome only at midcell (Figure 2A and B).

Figure 1



Comparison of the cellular organization of the two pattern-forming protein systems MinCDE and ParABS. The MinCDE system positions the FtsZ ring (purple) through negative feedback, while the ParABS system localizes cargo DNA through a positive feedback mechanism. The time-averaged gradients of the systems display the differences of negative versus positive feedback. However, the molecular mechanisms of both systems are intriguingly similar.

Briefly, the P-Loop ATPase MinD dimerizes in an ATP-dependent fashion, enhancing its membrane affinity and binding to the plasma membrane in a cooperative manner [14–16]. The MinD ATPase-activating protein MinE is then recruited by a threshold concentration of membrane-bound MinD, forming an asymmetric MinDE complex. MinE stimulates the ATPase activity of MinD, which in turn results in MinD's monomerization and detachment from the membrane (Figure 2A) [14,17–20]. Thereby, MinDE proteins appear to move along the bacterial membrane through a reaction-diffusion mechanism of membrane attachment-detachment that generates pole-to-pole oscillations.

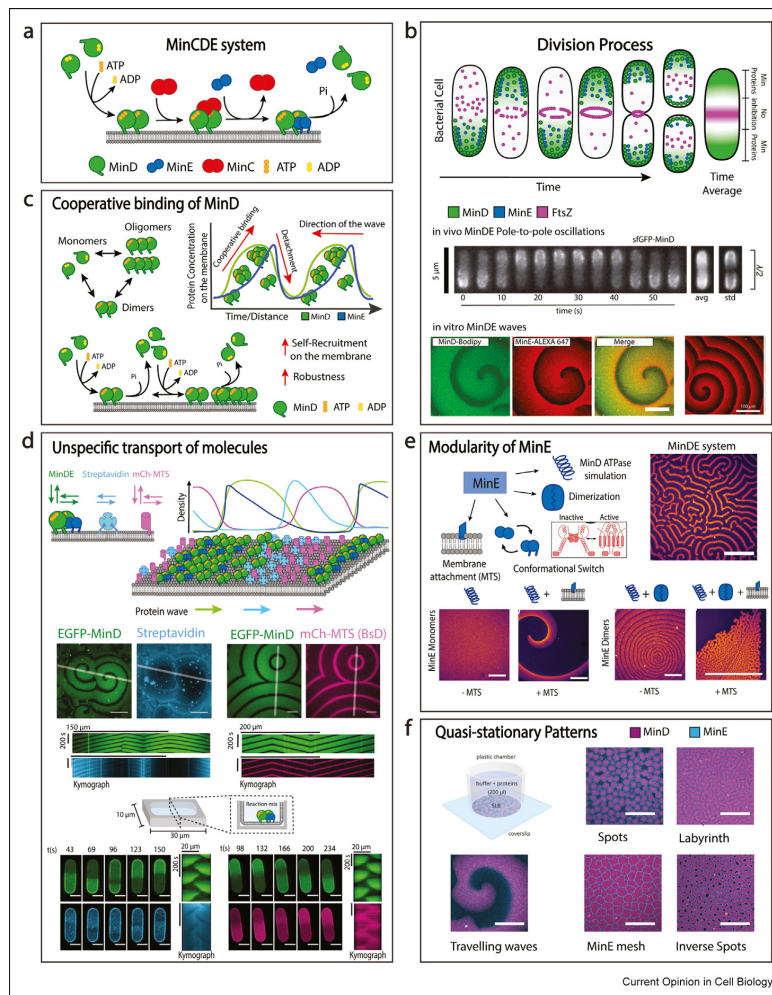
The third component of the Min system is MinC, which is also recruited by membrane-bound MinD and inhibits the assembly of the early division machinery on the membrane [14,17]. MinC does not participate in the reaction-diffusion mechanism, although it is displaced by MinE during the MinDE oscillatory process. As a result, MinC travels with the MinDE movement generating a time-averaged MinC gradient that prevents the assembly of the divisome at the cell poles, driving its formation at the geometric cell center.

Despite its compositional simplicity, the actual interaction mechanisms of MinDE self-organization on the

structural level are still far from being comprehensively understood. However, a key feature underlying the Min dynamics is the dimerization and cooperative self-enhancement of MinD on the membrane after ATP complexation (Figure 2C) [21,22]. Previous studies suggested that membrane-bound MinD dimers recruit further proteins from solution, although the mechanism has long been unknown [21,23]. However, a recent study has determined the presence of MinD–MinD interaction interfaces distinct from the canonical dimerization site, allowing the formation of higher-order oligomers [16]. The presence of multiple transient low-affinity interactions gives rise to a dynamic oligomeric equilibrium that leads to higher robustness needed for the MinDE wave formation and propagation on the membrane [16]. Thus, the classical model of MinD monomeric/dimeric state is now expanded to a dynamic scenario in which MinD exists in a range of oligomeric states.

Interestingly, it has recently been found that Min proteins can also regulate the localization of other peripheral membrane proteins without any specific molecular interactions (Figure 2D) [24]. Cooperative self-recruitment of MinD generates a mobile diffusion barrier able to locally affect the membrane attachment and detachment of proteins by binding site competition

Figure 2



**MinCDE system.** (a) Scheme of the MinCDE reaction mechanism. (b) Min proteins drive the localization of the division machinery. Pole-to-pole oscillations generate a time average protein gradient that inhibits the formation of the FtsZ ring at cellular poles. Min proteins form pole-to-pole oscillations *in vivo* and dynamic waves (among other patterns) *in vitro*. Scale bar is 50  $\mu\text{m}$  (Images adapted by permission from the study by Loose et al. [15], Wu et al. [37]). (c) MinD shows a cooperative membrane binding forming oligomeric species on the membrane that favor its self-recruitment from the cytoplasm. (d) MinDE proteins can regulate the localization of other membrane proteins without any specific molecular interaction by binding site competition and repulsion. *In vitro* reconstitution of the MinDE system in supported lipid bilayers (SLBs) adding Membrane-bound streptavidin (restricted detachment from the membrane, only lateral movement) and mCherry-mts (Lateral movement, exchange with cytoplasm). (Top) Scheme of the unspecific binding and fluorescence intensity profiles. (middle) Representative time-lapse images and kymographs of MinDE oscillations, streptavidin and mCherry-mts counter-oscillations. Scale bars 50  $\mu\text{m}$ . (below) Reconstitution of those systems in cell-sized PDMS microcompartments, scheme of the experimental setup and representative images of the time-lapse images. Scale bar 10  $\mu\text{m}$ . Images and schemes adapted by permission from the study by Ramm et al. [24]. (e) MinE can be dissected into four functional modules: ATPase stimulation, dimerization, conformational switch and membrane attachment. Representative images of the MinDE system reconstituted in SLBs using minimal MinE modules. Scale bars 300  $\mu\text{m}$ . Images adapted with permission from the study by Glock et al. [29]. (f) Quasi-stationary patterns formed using MinDE proteins reconstituted in SLBs. Representative confocal images of patterns were observed under different MinD-MinE protein ratios. Adapted with permission from the study by Glock et al. [44]. Scale bar 50  $\mu\text{m}$ .

[24,25]. Even more intriguingly, diffusible membrane proteins unable to dissociate will be directionally pushed by the traveling MinDE by repulsive and frictional forces into large-scale gradients, described as diffusiophoresis [26]. This mechanism may function as an unspecific active transport system in bacteria and might disclose new insights of possible additional roles of the Min system inside the cell [27]. In particular, the Min system may play a role in the chromosomal segregation process by directly or indirectly driving the localization of components involved in the process [28]. Even though more research has to be conducted on this phenomenon, the unspecific transport of molecules is an interesting feature that might be found in other self-organizing systems able to generate protein gradients.

The second key molecule of the dynamic Min system, MinE, has been the primary target of bottom-up functionality engineering because of its small size. MinE's structure can be principally dissected into four functional modules: ATPase stimulation of MinD, dimerization, membrane binding and conformational switch between a catalytically active and inactive form [29] (Figure 2E). MinE ATPase stimulation of MinD is mediated by a short peptide [15,30] and its dimerization has been found to be important to generate patterns *in vitro* [31]. While the MinE membrane attachment regulates the Min wave shape and dynamics *in vitro* [32–34], its conformational switch enhances the robustness of the pattern formation over different protein concentrations [35,36]. Curiously, Glock *et al.* have reduced MinE to the minimum function of each module, revealing the structure-function relationship and the minimal requirements to form Min patterns *in vitro* (Figure 2E) [29]. The minimal peptide of MinE required to stimulate MinD ATPase activity is not able to generate patterns, although its combination to either of the two protein motifs for membrane attachment or dimerization results in MinDE patterns with different dynamics [29]. Importantly, these modular features may be replaced by artificial units of similar function. This has recently been demonstrated by fusing the catalytic MinE peptide to minimal dimerizing motifs, such as short complementary nucleic acid strands, the DNA-peptide hybrids resulting in clear pattern formation [31]. The combination of different functional modules enriches the capacity of MinE to modulate the MinDE dynamics, affecting the outcome of the reaction-diffusion system, and highlighting the structural plasticity of MinE.

New insights about the Min system have been possible thanks to a remarkable improvement of its *in vitro* reconstitution in recent years, which have revealed a rich variety of different dynamics [5,8]. Besides traveling waves, several patterns can be found mostly driven by differential protein densities [32]. Interestingly, other factors such as geometry or bulk-to-surface ratio of

the chambers are found critical for the MinDE oscillatory features [37–39]. Min proteins adapt their behavior and pattern formation under different geometries, highlighting the high plasticity of the system [40]. At the same time, 3D confinement into lipid vesicles and other transformable membrane structures revealed the Min proteins' capacity to affect the physical properties of the membrane and actually induce mechanical forces [41–43]. Furthermore, a recent study has observed the formation of quasi-stationary patterns that assemble into a variety of shapes reminiscent of 'Turing patterns' depending on the protein concentration and MinD/MinE ratio [10–12,44] (Figure 2F). In those patterns, Min proteins are in constant exchange with the membrane, although the patterns appear to be arrested in space once they are established [44]. To our knowledge, they represent the first reconstitution of dynamic Turing-like patterns by a biological reaction-diffusion system, an interesting discovery for the self-organized systems [1,9,12].

To sum up, improvements in the understanding of the cooperative membrane binding of MinD and detailed MinE structure-function relationships have shed light on the dynamics of the Min system. Formation of quasi-stationary patterns and new and unexpected Min features and functionalities, such as non-specific active transport of membrane proteins or mechanical membrane transformations, suggest interesting secondary roles of the system in the cellular context that may have been lost or masked in the progress of evolution.

### The ParABS system

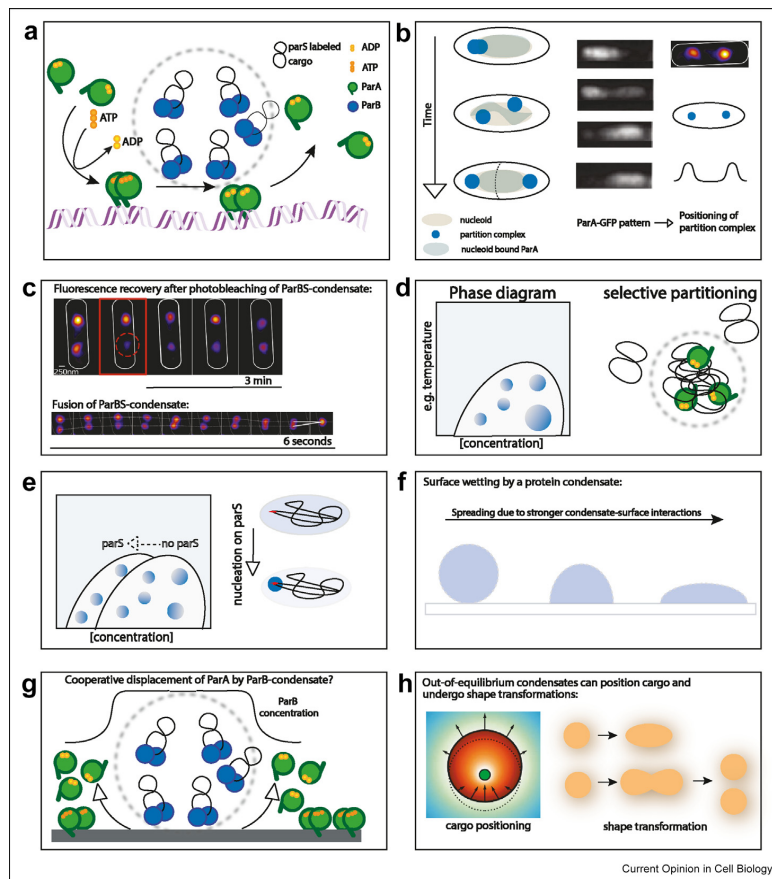
Similar to the positioning of the division site, faithful segregation of genetic material is a fundamental requirement for functional cell division. Many bacteria achieve this complex task using the so-called ParABS system. Like for the Min protein system, the active, that is, energy-dissipating core of the ParABS system is a P-Loop ATPase, ParA. However, unlike the Min system that operates *via* variable membrane affinity, the Par system attaches to DNA as a template, achieving cargo positioning by a DNA-binding protein (ParB) and a DNA sequence (*parS*). But still, the proposed mechanism of DNA segregation shows many parallels to the MinCDE system: The P-Loop ATPase ParA dimerizes in an ATP-dependent manner which increases non-specific template — in this case, DNA-binding affinity, recruiting the ParA dimers to the nucleoid. ParB dimers, bound to *parS* marked cargo, interact with nucleoid-bound ParA and stimulate the ParA-ATP hydrolysis rate. ATP hydrolysis subsequently leads to ParA-DNA dissociation, which generates a ParA-gradient on the nucleoid. This ParA-gradient is thought to cause the ParBS complex to travel along with the formed patterns through a still debated mechanism, separating the newly synthesized DNA or plasmid cargo [45–47] (Figure 3A and B).

The mechanisms of formation and regulation of the ParBS complex are not yet fully understood, and different models have been discussed. These models can be categorized by their different modes of ParB–ParB and ParB–DNA interactions. A one-dimensional (1D) ParB binding to *parS* and either recruiting more ParB through ParB–ParB interactions [48] or sliding along the DNA until a conformational switch modulates ParB–DNA affinity [49] was used to explain the spreading from *parS* sites found in ChIP-Seq data. Other models assume a higher-order structure of the ParBS complex. Herein, ParB initially binds *parS* and then bridges DNA through interactions with non-specific

DNA and other ParB dimers bound to non-specific DNA [50–52]. However, a more detailed structure of the partition complex remains elusive.

An intriguing possible explanation on how the ParBS complex is formed and regulated has been theoretically proposed in the study by Broedersz et al. [50] and was recently experimentally supported *in vivo* by Guilhas et al. [60]. It involves the possibility of liquid condensate formation, at present, very widely discussed phenomenon in the cell biological context [53]. Single-molecule imaging revealed that the ParBS complex is a spherical and ParB-rich structure with lowered

Figure 3



ParABS liquid-liquid phase separation. (a) Mechanism of ParB mediated ParA displacement. (b) *In vivo* pattern of ParA (images adapted from the study by Ringgaard et al. [71]) and ParB positioning (Image adapted from the study by Guilhas et al. [60]). (c) FRAP and fusion of ParBS condensate adapted from the study by Guilhas et al. [60]. (d) Phase diagram describes parameter space for demixing of homogenous solution into two distinct liquids. These demixed liquids can have different biochemical and biophysical properties. (e) Potential lowering of ParB phase boundary and dependence of condensate formation on *parS*. (f) Condensate wetting surfaces. (g) Potential cooperative displacement of ParA by a ParB condensate; (h) Properties of active condensates (adapted from the study by Zwicker et al. [57], Zwicker et al. [64]).

molecular mobility. Fluorescently tagged ParB was able to diffuse between different ParBS clusters, and these clusters were observed to fuse upon contact (Figure 3C). Also, fluorescence recovery after photobleaching indicates a mobile phase rather than a solid-like structure. Taken together, these experiments point toward a formation of the partition complex through liquid–liquid phase separation (LLPS).

LLPS has been shown to organize a wealth of biochemical processes in eukaryotes, from pattern-forming P-granules in *C. elegans* embryos to complex stress responses [54,55]. More recently, a variety of bacterial proteins involved in different biological functions have been shown to undergo LLPS *in vitro* and *in vivo* [56].

LLPS is a highly cooperative molecular process. Upon reaching a saturation concentration, a homogenous solution is separated into two distinct phases. These liquid phases usually differ in composition, dielectric constant, and viscosity and are, therefore, thought to provide a distinct chemical environment for certain biological processes [53] (Figure 3D). They have even been discussed in the context of constituting the first potential compartmentation strategies in the evolution of cells before the emergence of membranes from amphipathic building blocks as defined boundaries [57].

Intriguingly, key properties of the ParBS complex could be explained by liquid–liquid phase separation. Nucleic acids have been shown to organize many LLPS driven processes and alter the biophysical properties of condensates [58,59]. ParB condensate formation depends on the presence of at least one *parS* site [51,60], and biophysical properties of ParB condensates could be altered by *parS* as has been observed for other phase separating systems [59]. ParB specifically binds to *parS* sites, and therefore, local protein concentration at *parS* sites is significantly enriched when compared to cytoplasmic concentrations. Thus, this would be a plausible mechanism to spatially control the nucleation of ParBS condensates (Figure 3E).

Recently, it was found that different ParB orthologs have enzymatic CTPase activity, which is stimulated upon *parS* binding [49,61,62]. The ParB CTPase activity was shown to facilitate the reopening of closed ParB dimers to unload ParB from non-specific DNA. Intriguingly, mutations of the CTP binding pocket lead to a more uniform distribution of ParB in cells, pointing toward a regulatory mechanism of the energy dissipation in the potential liquid–liquid phase separation of the ParBS complex [61].

ParB clusters are known to spread to non-*parS* sites *in vivo*, but until recently *in vitro* reconstitution of this spreading behavior was not possible. In the study by Soh *et al.* [49], 1D spreading *in vitro* is achieved by addition

of CTP, which was shown to facilitate the formation of a ring-like structure of ParB. However, ChIP-Seq data points to more complex behavior *in vivo* with 3-dimensional interactions within the ParBS cluster [52,72]. LLPS of ParB offers an exciting mechanistic explanation for these observations. Interactions of condensates with large surface structures can lead to a wetting behavior, where the liquid phase spreads around the original nucleation point, like a drop of water wets a glass surface. Therefore, a ParB condensate could bridge and condense surrounding non-specific DNA as observed *in vivo* (Figure 3F).

Also, ParB–CTPase activity and its dependence on *parS* presence could be another physiologically relevant representation of the theoretically predicted ‘out-of-equilibrium’ condensates [64]. The positioning of *parS* sites within ParB condensates could, in this case, be explained by the theoretical framework of active particle behavior within condensates. Herein, the particle is positioned precisely in the middle of a condensate because of chemical fluxes originating at the particle surface [64]. This theory was successfully applied to eukaryotic centrosome formation through liquid–liquid phase separation [65] and could potentially be transferred to the bacterial ParBS complex, where *parS* stimulates ParB–CTPase activity. It was recently argued that ParB foci sizes do not scale with cell length, as expected by equilibrium LLPS [66]. However, energy-dissipating condensates can regulate size, shape, and localization through kinetic rates of chemical reactions [67] (Figure 3H).

Interactions of ParBS condensates with ParA could answer some outstanding questions with regard to the ParABS mechanism. All currently discussed diffusion ratchet models assume a lag time after ParA displacement where no rebinding is occurring [45–47]. This could be achieved by partitioning of ParB-displaced ParA monomer into the viscous ParBS condensate (Figure 3D). Also, the ParBS condensate interface constitutes a strong chemical gradient, and its interaction with nucleoid-bound ParA dimers could lead to the highly cooperative displacement of ParA, reminiscent of the traveling wavefront of the MinCDE system as discussed previously, generating higher chemical gradients and larger molecular forces to act on the ParBS condensate (Figure 3G).

Taken together, the recently hypothesized concept of the partition complex as a bacterial condensate offers interesting insights and may help to explain pertinent questions regarding the mechanisms of complex formation, function, and interaction with ParA. The formation of dynamic patterns through liquid–liquid phase separation has been shown for eukaryotic systems, where protein gradients achieve the spatial positioning of phase-separated P granules [54].



		MinCDE		ParABS	
Components		<b>MinD</b>	P-Loop ATPase Protein Dimerization (ATP-dependent) Membrane Attachment (ATP-dependent) Cooperative Binding Interaction with MinE and MinC	<b>ParA</b>	P-Loop ATPase Protein Dimerization (ATP-dependent) DNA Attachment (ATP-dependent) Interaction with ParB
		<b>MinE</b>	Dimeric Protein Membrane attachment Conformational switch MinD ATPase activating protein Unclear mechanism of traveling on the membrane	<b>ParB</b>	Dimeric Protein CTPase activity DNA attachment Conformational switch ParA ATPase-activating protein Unclear mechanism of traveling through the Nucleoid Cooperative LLPS
		<b>MinC</b>	Dimeric Protein Cargo of the system Interaction with MinD Inhibitor of Z-ring	<b>parS</b>	DNA sequence Cargo-tether of the system Interaction with ParB
Matrix			Plasma membrane		DNA from Nucleoid
Cooperativity			Oligomerization		potential LLPS
Function			Positioning of divisome by negative feedback		Chromosomal Segregation by positive feedback
Pattern	<i>In vivo</i>		Pole-to-pole Oscillations		Oscillations on the Nucleoid
Formation	<i>In vitro</i>		High Variety		(?)

### Summary and perspectives

MinCDE and ParABS represent two pattern-forming protein systems in bacteria that show remarkable similarities at first glance (Table 1). The purpose of both protein patterns is to provide a spatiotemporal cue for cell division by the generation of a protein gradient on a matrix. Their modular composition and mechanistic details of the pattern-forming systems are remarkably similar. The two systems use ATP-dependent dimerization and subsequent binding to a matrix, that is, dramatic reduction of their diffusional mobility, to generate a uniform layer of protein-covered matrix. The molecular antagonist of the matrix binding protein then stimulates ATP hydrolysis and causes detachment of the matrix-bound protein. Intriguingly, this ATP-operated and thus, energy-dissipating switch of molecular mobility and consequently, diffusional range of an ‘activator’ molecule, additionally classified by cooperative binding to its matrix, is a biologically very straightforward variant of the local self-amplification and long-range inhibition, as originally proposed by Gierer and Meinhard [68]. Herein, the long-range inhibition is simply implemented by dramatically slowing down the activator molecule — with respect to its inhibitor — upon matrix binding. For the MinCDE system, it has already been demonstrated that MinD binding to the membrane reduces the diffusion coefficient by at least two orders of magnitude [15,19]. Similar to the change of diffusion by MinD membrane binding, ParA mobility is drastically reduced by three orders of magnitude upon DNA binding [69]. To drive the speculations further,

also the transition of molecules into liquid condensates, with their presumably increased viscosity and thereby reduced diffusion, could be one way of fulfilling the condition early formulated for pattern-forming systems of symmetry breaking in diffusional mobility.

However, despite these conceptual similarities, the detailed modes of assembly and the mechanisms of transport in the two discussed bacterial systems appear to be different. Moreover, while the MinCDE system positions the divisome through negative feedback, the ParABS system achieves positioning through positive feedback. On a molecular scale, this difference is obvious by the inhibition of FtsZ polymerization through MinC on one hand and the direct interaction of ParB with parS on the other hand. Both systems use cooperativity to enhance the stability of the positioning, however, different players show cooperative behavior. MinD forms higher-order oligomers to ensure the robustness of the MinCDE pattern [16], and the ParB liquid–liquid phase separation offers a mechanism to buffer cellular noise through a cooperative process [56,70].

To conclude, even though there seem to be some shared conceptual motifs in the design of the two discussed bacterial pattern-forming protein systems, a remarkably similar composition, and conserved crucial details of the molecular mechanism, their variations are remarkable and intriguing. Both patterns forming systems make use of different strategies to achieve cargo positioning and to

confer robustness. In better understanding these differences, we hope to be able to significantly enrich our conceptual toolkit for the bottom-up design of biological structure and function. With respect to the physiological understanding of the principles that govern self-organized systems, their reconstitution *in vitro* in recent studies has not only helped to shed light on the common mechanisms of protein gradient formation but also revealed functionalities that have neither been observed nor hypothesized in the cellular context so far, such as the ability of the MinDE system to directionally transport membrane-attached molecules of mechanically transform membranes. It seems, therefore, obvious that *in vitro* reconstitution should ideally accompany any mechanistic study in cell biology to enlarge our still far too limited assortment of mechanistic hypotheses for the fundamental functions of life.

### Conflict of interest statement

Nothing declared.

### Acknowledgements

The authors would like to thank Tamara Heermann for helpful discussions. This work has been supported by the Transregional Collaborative Research Center "Spatiotemporal dynamics of bacterial cells" (TRR 174) and the Max Planck-Bristol Centre for Minimal Biology. A.M is part of IMPRS-LS. L.B. is funded by the Max Planck School "Matter to Life".

### References

Papers of particular interest, published within the period of review, have been highlighted as:

- \* of special interest
- \*\* of outstanding interest

1. Schweisguth F, Corson F: **Self-organization in pattern formation.** *Dev Cell* 2019, <https://doi.org/10.1016/j.devcel.2019.05.019>.
2. McCusker D: **Cellular self-organization: generating order from the abyss.** *Mol Biol Cell* 2020, <https://doi.org/10.1091/mbc.E19-04-0207>.
3. Khalili B, Lovelace HD, Rutkowski DM, Holz D, Vavylonis D: **Fission yeast polarization: modeling Cdc42 oscillations, symmetry breaking, and zones of activation and inhibition.** *Cells* 2020, <https://doi.org/10.3390/cells9081769>.
4. Lang CF, Munro E: **The PAR proteins: from molecular circuits to dynamic self-stabilizing cell polarity.** *Development* 2017, <https://doi.org/10.1242/dev.139063>.
5. Ramm B, Heermann T, Schwille P: **The E. coli MinCDE system in the regulation of protein patterns and gradients.** *Cell Mol Life Sci* 2019, <https://doi.org/10.1007/s00018-019-03218-x>.  
Excellent review summarizing all previous studies using the MinCDE system.
6. Raskin DM, de Boer PAJ: **MinDE-dependent Pole-to-Pole oscillation of division inhibitor MinC in Escherichia coli.** *J Bacteriol* 1999, <https://doi.org/10.1128/jb.181.20.6419-6424.1999>.
7. Jindal L, Emberly E: **DNA segregation under Par protein control.** *PLoS One* 2019, <https://doi.org/10.1371/journal.pone.0218520>.
8. Vendel KJA, Tschirpke S, Shamsi F, Dogterom M, Laan L: **Minimal in vitro systems shed light on cell polarity.** *J Cell Sci* 2019, <https://doi.org/10.1242/jcs.217554>.
9. Landge AN, Jordan BM, Diego X, Müller P: **Pattern formation mechanisms of self-organizing reaction-diffusion**

**systems.** *Dev Biol* 2020, <https://doi.org/10.1016/j.ydbio.2019.10.031>.

10. Halatek J, Frey E: **Rethinking pattern formation in reaction-diffusion systems.** *Nat Phys* 2018, <https://doi.org/10.1038/s41567-017-0040-5>.  
Highly recommended theoretical study to better understand the role of protein gradients and how they drive the formation of functional patterns.
11. Frey E, Halatek J, Kretschmer S, Schwille P: **Protein pattern formation.** In *Physics of biological membranes*; 2018.
12. Kondo S, Miura T: **Reaction-diffusion model as a framework for understanding biological pattern formation.** *Science* 2010, <https://doi.org/10.1126/science.1179047> (80-).
13. De Boer PAJ, Crossley RE, Hand AR, Rothfield LI: **The MinD protein is a membrane ATPase required for the correct placement of the Escherichia coli division site.** *EMBO J* 1991, <https://doi.org/10.1002/j.1460-2075.1991.tb05015.x>.
14. Lackner LL, Raskin DM, De Boer PAJ: **ATP-dependent interactions between Escherichia coli Min proteins and the phospholipid membrane in vitro.** *J Bacteriol* 2003, <https://doi.org/10.1128/JB.185.3.735-749.2003>.
15. Loose M, Fischer-Friedrich E, Ries J, Kruse K, Schwille P: **Spatial regulators for bacterial cell division self-organize into surface waves in vitro.** *Science* 2008, <https://doi.org/10.1126/science.1154413> (80-).
16. Heermann T, Ramm B, Glaser S, Schwille P: **Local self-enhancement of MinD membrane binding in min protein pattern formation.** *J Mol Biol* 2020, <https://doi.org/10.1016/j.jmb.2020.03.012>.  
This study aims to elucidate the molecular origin of cooperative membrane binding, supposed to be of key importance for pattern formation in the MinDE system. MinD mutants arrested in monomeric or dimeric state revealed self-interaction apart from the canonical dimerization site to efficiently form oligomers on the membrane.
17. Hu Z, Saez C, Lutkenhaus J: **Recruitment of MinC, an inhibitor of Z-ring formation, to the membrane in Escherichia coli: role of minD and minE.** *J Bacteriol* 2003, <https://doi.org/10.1128/JB.185.1.196-203.2003>.
18. Park KT, Wu W, Lovell S, Lutkenhaus J: **Mechanism of the asymmetric activation of the MinD ATPase by MinE.** *Mol Microbiol* 2012, <https://doi.org/10.1111/j.1365-2958.2012.08110.x>.
19. Loose M, Fischer-Friedrich E, Herold C, Kruse K, Schwille P: **Min protein patterns emerge from rapid rebinding and membrane interaction of MinE.** *Nat Struct Mol Biol* 2011, <https://doi.org/10.1038/nsmb.2037>.
20. Ayed SH, Cloutier AD, McLeod LJ, Foo ACY, Damry AM, Goto NK: **Dissecting the role of conformational change and membrane binding by the bacterial cell division regulator MinE in the stimulation of MinD ATPase activity.** *J Biol Chem* 2017, <https://doi.org/10.1074/jbc.M117.805945>.
21. Miyagi A, Ramm B, Schwille P, Scheuring S: **High-speed atomic force microscopy reveals the inner workings of the MinDE protein oscillator.** *Nano Lett* 2018, <https://doi.org/10.1021/acs.nanolett.7b04128>.
22. Mileykovskaya E, Fishov I, Fu X, Corbin BD, Margolin W, Dowhan W: **Effects of phospholipid composition on MinD-membrane interactions in vitro and in vivo.** *J Biol Chem* 2003, <https://doi.org/10.1074/jbc.M302603200>.
23. Wettmann L, Kruse K: **The min-protein oscillations in Escherichia coli: an example of self-organized cellular protein waves.** *Philos Trans R Soc B Biol Sci* 2018, <https://doi.org/10.1098/rstb.2017.0111>.
24. Ramm B, Glock P, Mücksch J, Blumhardt P, García-Soriano DA, Heymann M, Schwille P: **The MinDE system is a generic spatial cue for membrane protein distribution in vitro.** *Nat Commun* 2018, <https://doi.org/10.1038/s41467-018-06310-1>.  
First report of a new unexpected feature of the Min system by which membrane-attached molecules of no functional connection can be directionally transported through MinDE self-organization and made to form large-scale gradients on the membrane.

25. Shih YL, Huang LT, Tu YM, Lee BF, Bau YC, Hong CY, Lee H lin, Shih YP, Hsu MF, Lu ZX, *et al.*: **Active transport of membrane components by self-organization of the min proteins.** *Biophys J* 2019, <https://doi.org/10.1016/j.bpj.2019.03.011>.
26. Ramm B, Goychuk A, Khmelinskaia A, Blumhardt P, Eto H, Ganzinger KA, Frey E, Schwille P: **A diffusio-phoretic mechanism for ATP-driven transport without motor proteins.** *Nat Phys* 2021, 17:850–858, <https://doi.org/10.1038/s41567-021-01213-3>.
27. Taviti AC, Beuria TK: **Bacterial Min proteins beyond the cell division.** *Crit Rev Microbiol* 2019, <https://doi.org/10.1080/1040841X.2018.1538932>.
28. Shen JP, Chang YR, Chou CF: **Frequency modulation of the Min-protein oscillator by nucleoid-associated factors in *Escherichia coli*.** *Biochem Biophys Res Commun* 2020, <https://doi.org/10.1016/j.bbrc.2020.02.161>.
29. Glock P, Brauns F, Halatek J, Frey E, Schwille P: **Design of biochemical pattern forming systems from minimal motifs.** *Elife* 2019, <https://doi.org/10.7554/eLife.48646>.  
This paper describes a modular deconstruction approach of a pattern-forming protein in the true spirit of bottom-up synthetic biology. Herein, MinE of the Min system is dissected into four structural modules associated with different functions. It could be shown that the core functional unit responsible for ATPase stimulation may be complemented by a single additional function (dimerization or membrane binding) to become effective for self-organization.
30. Glock P, Broichhagen J, Kretschmer S, Blumhardt P, Mücksch J, Trauner D, Schwille P: **Optical control of a biological reaction–diffusion system.** *Angew Chem Int Ed* 2018, <https://doi.org/10.1002/anie.201712002>.
31. Heermann T, Franquelim HG, Glock P, Harrington L, Schwille P: **Probing biomolecular interactions by a pattern-forming peptide–conjugate sensor.** *Bioconjug Chem* 2020, <https://doi.org/10.1021/acs.bioconjugchem.0c00596>.
32. Vecchiarelli AG, Li M, Mizuuchi M, Hwang LC, Seol Y, Neuman KC, Mizuuchi K: **Membrane-bound MinDE complex acts as a toggle switch that drives Min oscillation coupled to cytoplasmic depletion of MinD.** *Proc Natl Acad Sci U S A* 2016, <https://doi.org/10.1073/pnas.1600644113>.
33. Kretschmer S, Zieske K, Schwille P: **Large-scale modulation of reconstituted Min protein patterns and gradients by defined mutations in MinE's membrane targeting sequence.** *PLoS One* 2017, <https://doi.org/10.1371/journal.pone.0179582>.
34. Kretschmer S, Harrington L, Schwille P: **Reverse and forward engineering of protein pattern formation.** *Philos Trans R Soc B Biol Sci* 2018, <https://doi.org/10.1098/rstb.2017.0104>.
35. Denk J, Kretschmer S, Halatek J, Hartl C, Schwille P, Frey E: **MinE conformational switching confers robustness on self-organized Min protein patterns.** *Proc Natl Acad Sci U S A* 2018, <https://doi.org/10.1073/pnas.1719801115>.
36. Kohyama S, Fujiwara K, Yoshinaga N, Doi N: **Conformational equilibrium of MinE regulates the allowable concentration ranges of a protein wave for cell division.** *Nanoscale* 2020, <https://doi.org/10.1039/d0nr00242a>.
37. Wu F, Van Schie BGC, Keymer JE, Dekker C: **Symmetry and scale orient Min protein patterns in shaped bacterial sculptures.** *Nat Nanotechnol* 2015, <https://doi.org/10.1038/nnano.2015.126>.
38. Zieske K, Schwille P: **Reconstituting geometry-modulated protein patterns in membrane compartments.** *Methods Cell Biol* 2015, <https://doi.org/10.1016/bs.mcb.2015.02.006>.
39. Brauns F, Pawlik G, Halatek J, Kerssemakers J, Frey E, Dekker C: **Bulk-surface coupling reconciles Min-protein pattern formation in vitro and in vivo.** *bioRxiv* 2020, <https://doi.org/10.1101/2020.03.01.971952>.
40. Schweizer J, Loose M, Bonny M, Kruse K, Morich I, Schwille P: **Geometry sensing by self-organized protein patterns.** *Proc Natl Acad Sci U S A* 2012, <https://doi.org/10.1073/pnas.1206953109>.
41. Godino E, López JN, Foschepoth D, Cleij C, Doerr A, Castellà CF, Danelon C: **De novo synthesized Min proteins drive oscillatory liposome deformation and regulate FtsA-FtsZ cytoskeletal patterns.** *Nat Commun* 2019, <https://doi.org/10.1038/s41467-019-12932-w>.  
First comprehensive demonstration of cell-free produced MinDE proteins that self-organize in SLBs and inside liposomes. Global shape transformations and local membrane undulations can result from dynamic redistribution of the in synthesized Min proteins inside vesicles.
42. Litschel T, Ramm B, Maas R, Heymann M, Schwille P: **Beating vesicles: encapsulated protein oscillations cause dynamic membrane deformations.** *Angew Chem Int Ed* 2018, <https://doi.org/10.1002/anie.201808750>.
43. Mazor S, Regev T, Mileykovskaya E, Margolin W, Dowhan W, Fishov I: **Mutual effects of MinD-membrane interaction: I. Changes in the membrane properties induced by MinD binding.** *Biochim Biophys Acta Biomembr* 2008, <https://doi.org/10.1016/j.bbamem.2008.08.003>.
44. Glock P, Ramm B, Heermann T, Kretschmer S, Schweizer J, Mücksch J, Alagöz G, Schwille P: **Stationary patterns in a two-protein reaction-diffusion system.** *ACS Synth Biol* 2019, <https://doi.org/10.1021/acssynbio.8b00415>.
45. Lim HC, Surovtsev IV, Beltran BG, Huang F, Bewersdorf J, Jacobs-Wagner C: **Evidence for a DNA-relay mechanism in ParABS-mediated chromosome segregation.** *Elife* 2014, <https://doi.org/10.7554/eLife.02758>.
46. Vecchiarelli AG, Neuman KC, Mizuuchi K: **A propagating ATPase gradient drives transport of surface-confined cellular cargo.** *Proc Natl Acad Sci U S A* 2014, <https://doi.org/10.1073/pnas.1401025111>.
47. Le Gall A, Cattoni DI, Guilhas B, Mathieu-Demazière C, Oudjedi L, Fiche JB, Rech J, Abrahamsson S, Murray H, Bouet JY, *et al.*: **Bacterial partition complexes segregate within the volume of the nucleoid.** *Nat Commun* 2016, <https://doi.org/10.1038/ncomms12107>.
48. Rodionov O, ŁObocka M, Yarmolinsky M: **Silencing of genes flanking the P1 plasmid centromere.** *Science* 1999, <https://doi.org/10.1126/science.283.5401.546> (80-).
49. Soh YM, Davidson IF, Zamuner S, Basquin J, Bock FP, Taschner M, Veening JW, de Los Rios P, Peters JM, Gruber S: **Self-organization of parS centromeres by the ParB CTP hydrolase.** *Science* 2019, <https://doi.org/10.1126/science.aay3965> (80-).  
Biochemical and structural description of ParB CTPase activity showing N-engagement. The authors use crosslinking studies beside other biochemical methods to identify changes in ParB structure upon CTP binding. Together with (Osorio *et al.*, 2019), this work is the first demonstration of CTPase activity.
50. Broedersz CP, Wang X, Meir Y, Loparo JJ, Rudner DZ, Wingreen NS: **Condensation and localization of the partitioning protein ParB on the bacterial chromosome.** *Proc Natl Acad Sci U S A* 2014, <https://doi.org/10.1073/pnas.1402529111>.
51. Graham TGW, Wang X, Song D, Etson CM, van Oijen AM, Rudner DZ, Loparo JJ: **ParB spreading requires DNA bridging.** *Genes Dev* 2014, <https://doi.org/10.1101/gad.242206.114>.
52. Debaugny RE, Sanchez A, Rech J, Labourdette D, Dorignac J, Geniet F, Palmeri J, Parmeggiani A, Boudsoq F, Anton Leberre V, *et al.*: **A conserved mechanism drives partition complex assembly on bacterial chromosomes and plasmids.** *Mol Syst Biol* 2018, <https://doi.org/10.15252/msb.20188516>.
53. Hyman AA, Weber CA, Jülicher F: **Liquid-liquid phase separation in biology.** *Annu Rev Cell Dev Biol* 2014, <https://doi.org/10.1146/annurev-cellbio-100913-013325>.
54. Brangwynne CP, Eckmann CR, Courson DS, Rybarska A, Hoeghe C, Gharakhani J, Jülicher F, Hyman AA: **Germline P granules are liquid droplets that localize by controlled dissolution/condensation.** *Science* 2009, <https://doi.org/10.1126/science.1172046> (80-).
55. Protter DSW, Parker R: **Principles and properties of stress granules.** *Trends Cell Biol* 2016, <https://doi.org/10.1016/j.tcb.2016.05.004>.

56. Azaldegui CA, Vecchiarelli AG, Biteen JS: **The emergence of phase separation as an organizing principle in bacteria.** *Biophys J* 2020, <https://doi.org/10.1016/j.bpj.2020.09.023>.  
A detailed review of currently known bacterial condensates and methods that can be used to study these *in vivo*.
57. Zwicker D, Seyboldt R, Weber CA, Hyman AA, Jülicher F: **Growth and division of active droplets provides a model for protocells.** *Nat Phys* 2017, <https://doi.org/10.1038/nphys3984>.  
A landmark theoretical framework discussing physical properties of energy-dissipating condensates. First predictions of shape transformations in active condensates suggesting a potential role of coacervates as protocells.
58. Langdon EM, Qiu Y, Niaki AG, McLaughlin GA, Weidmann CA, Gerbich TM, Smith JA, Crutchley JM, Termini CM, Weeks KM, *et al.*: **mRNA structure determines specificity of a polyQ-driven phase separation.** *Science* 2018, <https://doi.org/10.1126/science.aar7432> (80-).
59. Elbaum-Garfinkle S, Kim Y, Szczepaniak K, Chen CCH, Eckmann CR, Myong S, Brangwynne CP: **The disordered P granule protein LAF-1 drives phase separation into droplets with tunable viscosity and dynamics.** *Proc Natl Acad Sci U S A* 2015, <https://doi.org/10.1073/pnas.1504822112>.
60. Guilhas B, Walter JC, Rech J, David G, Walliser NO, Palmeri J, Mathieu-Demaziere C, Parmeggiani A, Bouet JY, Le Gall A, *et al.*: **ATP-driven separation of liquid phase condensates in bacteria.** *Mol Cell* 2020, <https://doi.org/10.1016/j.molcel.2020.06.034>.  
Super resolution microscopy and single molecule tracking showing liquid condensate like structure and material properties for *E. coli* partition complex. The authors show that there are two ParB populations with highly different diffusion dynamics.
61. Osorio-Valeriano M, Altegoer F, Steinchen W, Urban S, Liu Y, Bange G, Thanbichler M: **ParB-type DNA segregation proteins are CTP-dependent molecular switches.** *Cell* 2019, <https://doi.org/10.1016/j.cell.2019.11.015>.  
*In vitro* and *in vivo* study identifying ParB's CTPase activity and demonstrating necessity of ParB-CTP interaction in DNA segregation and partition complex assembly.
62. Jalal AS, Tran NT, Le TB: **ParB spreading on DNA requires cytidine triphosphate *in vitro*.** *Elife* 2020, <https://doi.org/10.7554/eLife.53515>.
- The authors characterize ParB spreading on open and closed DNA substrates, characterizing ParB-parS interactions in presence and absence of CTP for a variety of ParBs.
64. Zwicker D, Baumgart J, Redemann S, Müller-Reichert T, Hyman AA, Jülicher F: **Positioning of particles in active droplets.** *Phys Rev Lett* 2018, <https://doi.org/10.1103/PhysRevLett.121.158102>.
65. Zwicker D, Decker M, Jaensch S, Hyman AA, Jülicher F: **Centrosomes are autocatalytic droplets of pericentriolar material organized by centrioles.** *Proc Natl Acad Sci U S A* 2014, <https://doi.org/10.1073/pnas.1404855111>.
66. Biedzinski S, Parmar B, Weber SC: **Beyond equilibrium phase diagrams: enzymatic activity shakes up bacterial condensates.** *Mol Cell* 2020, <https://doi.org/10.1016/j.molcel.2020.06.035>.
67. Söding J, Zwicker D, Sohrabi-Jahromi S, Boehning M, Kirschbaum J: **Mechanisms for active regulation of biomolecular condensates.** *Trends Cell Biol* 2020, <https://doi.org/10.1016/j.tcb.2019.10.006>.
68. Gierer A, Meinhardt H: **A theory of biological pattern formation.** *Kybernetik* 1972, <https://doi.org/10.1007/BF00289234>.
69. Surovtsev IV, Lim HC, Jacobs-Wagner C: **The slow mobility of the ParA partitioning protein underlies its steady-state patterning in *Caulobacter*.** *Biophys J* 2016, <https://doi.org/10.1016/j.bpj.2016.05.014>.
70. Klosin A, Oltsch F, Harmon T, Honigmann A, Jülicher F, Hyman AA, Zechner C: **Phase separation provides a mechanism to reduce noise in cells.** *Science* 2020, <https://doi.org/10.1126/science.aav6691> (80-).
71. Ringgaard S, Van Zon J, Howard M, Gerdes K: **Movement and epositioning of plasmids by ParA filament disassembly.** *Proc Natl Acad Sci U S A* 2009, <https://doi.org/10.1073/pnas.0908347106>.
72. Walter J-C, Rech J, Walliser N-O, Dorignac J, Geniet F, Palmeri J, Parmeggiani A, Bouet J-Y: **Physical modeling of a sliding clamp mechanism for the spreading of ParB at short genomic distance from bacterial centromere sites.** *Iscience* 2020, **23**: 101861, <https://doi.org/10.1016/j.isci.2020.101861>.

## 5.2 Publication P2

### CTP-controlled liquid-liquid phase separation of ParB

Summary:

In this manuscript, I establish the *in vitro* phase separation of ParB. Together with collaboration partners, we use a combination of *in vitro* reconstitution and *in vivo* super resolution microscopy to identify CTP and parS binding as regulative mechanisms of ParB phase separation. Also, I purify and test ParB homologues and find that the propensity to phase separate and the control thereof is evolutionary conserved [130].

Reprinted with permission from Elsevier.

**Leon Babl**, Giacomo Giacomelli, Beatrice Ramm, Ann-Kathrin Gelmroth, Marc Bramkamp, Petra Schwille, CTP-controlled liquid–liquid phase separation of ParB, *Journal of Molecular Biology*, 2022.





# CTP-controlled liquid–liquid phase separation of ParB

Leon Babl<sup>1</sup>, Giacomo Giacomelli<sup>2</sup>, Beatrice Ramm<sup>1</sup>, Ann-Kathrin Gelmroth<sup>2</sup>, Marc Bramkamp<sup>2</sup> and Petra Schwille<sup>1\*</sup>

<sup>1</sup> - Max Planck Institute for Biochemistry, Am Klopferspitz 18, 82152 Planegg, Germany

<sup>2</sup> - Christian-Albrechts-Universität zu Kiel, Am Botanischen Garten 1-9, 24118 Kiel, Germany

Correspondence to Petra Schwille: [schwille@biochem.mpg.de](mailto:schwille@biochem.mpg.de) (P. Schwille)

<https://doi.org/10.1016/j.jmb.2021.167401>

Edited by Monika Fuxreiter

## Abstract

The ParABS system is supposed to be responsible for plasmid partitioning and chromosome segregation in bacteria. ParABS ensures a high degree of fidelity in inheritance by dividing the genetic material equally between daughter cells during cell division. However, the molecular mechanisms underlying the assembly of the partition complex, representing the core of the ParABS system, are still far from being understood. Here we demonstrate that the partition complex is formed via liquid–liquid phase separation. Assembly of the partition complex is initiated by the formation of oligomeric ParB species, which in turn are regulated by CTP-binding. Phase diagrams and *in vivo* analysis show how the partition complex can further be spatially regulated by *parS*. By investigating the phylogenetic variation in phase separation and its regulation by CTP, we find a high degree of evolutionary conservation among distantly related prokaryotes. These results advance the understanding of partition complex formation and regulation in general, by confirming and extending recently proposed models.

© 2021 The Authors. Published by Elsevier Ltd. This is an open access article under the CC BY-NC-ND license (<http://creativecommons.org/licenses/by-nc-nd/4.0/>).

## Introduction

Faithful segregation of genetic material during cell division is a key requirement for living systems and fundamental to evolutionary processes. While the molecular mechanisms governing chromosome segregation in eukaryotes are relatively well understood, our understanding of these processes in bacteria is still insufficient.

Bacterial chromosome and plasmid segregation is often achieved through a tripartite system, ParABS, consisting of two protein components (ParA and ParB) and a DNA-site (*parS*).<sup>1–7</sup> The interplay of specific ParB-*parS* interactions and energy-dissipation of ParA is thought to drive a diffusion-ratchet or DNA-relay mechanism.<sup>8–10</sup> ParA non-specifically binds to the nucleoid in an ATP-

dependent manner, while ParB specifically binds to *parS* sites forming a partition complex. Upon interaction of ParB with ParA, ParA-ATPase activity is stimulated which leads to a detachment from the nucleoid. The partition complex is then thought to translocate into the ParA-freed space and thereby move directionally.<sup>9–12</sup> Despite its fundamental role in prokaryotic cell biology, no molecular mechanism of partition complex assembly is fully accepted, with different models currently being discussed.<sup>13</sup>

Early findings in partition complex formation were interpreted as a 1D-filamentation process, with ParB filaments nucleating on *parS* sites and then growing to non-specific DNA sites.<sup>14,15</sup> While this mechanism is in principle feasible, the ParB concentration is likely too low to form long filament networks that could explain the spreading *in vivo*. This led to models of a higher-order partition complex

that is governed by low-affinity and long-range interactions between ParB-dimers themselves and non-specific DNA.<sup>16–18</sup> However, the underlying molecular nature of these interactions remains elusive.

A recent *in vivo* study used single molecule tracking and super resolution microscopy to investigate dynamics of the the *E. coli* F-plasmid partitioning. Intriguingly, this study suggests a liquid-like nature of the partition complex with multiple hallmark criteria for liquid–liquid phase separation (LLPS) being fulfilled.<sup>19</sup>

LLPS is an intriguingly simple physicochemical process by which a homogenous solution of two or more molecules de-mixes into two distinct phases, often driven by favorable homotypic interactions between biological polymers. These phases inherently differ in chemical and physical properties, e.g., density or dielectric constant.<sup>20</sup> The unique properties of the dense phase can influence reaction parameters and alter biomolecular structures.<sup>21,22</sup> Due to the dynamic nature of the interactions driving LLPS and its dependence on environmental parameters, the formed phases can rapidly form or dissolve, depending on changes in environment (e.g. cellular stress), protein concentration, protein modifications or ligand binding.<sup>23–25</sup> In the last decade, LLPS has emerged as an important generic organizational principle in eukaryotic cell biology.<sup>23,26–29</sup> The principle of de-mixing liquids has been shown to nucleate the formation of complex eukaryotic subcellular structures, such as the multi-layered nucleolus p,<sup>30</sup> stress-granules<sup>25</sup> or p-bodies.<sup>31</sup> Even though the formation of such ‘membraneless organelles’ would also be an attractive paradigm for certain aspects of spatiotemporal organization in the small bacteria that largely lack classical (i.e., membranous) organelles and the complex multi-protein machinery of eukaryotic cells, comparatively few examples of LLPS have been reported in prokaryotes.<sup>32</sup> It is, however, exactly the size of many bacterial structures below the diffraction limit, which makes it challenging to demonstrate and probe assembling structures and thus, also LLPS, *in vivo*. Hence, we set out to probe whether the partition complex is indeed a phase-

separated structure by reconstituting the complex *in vitro*.

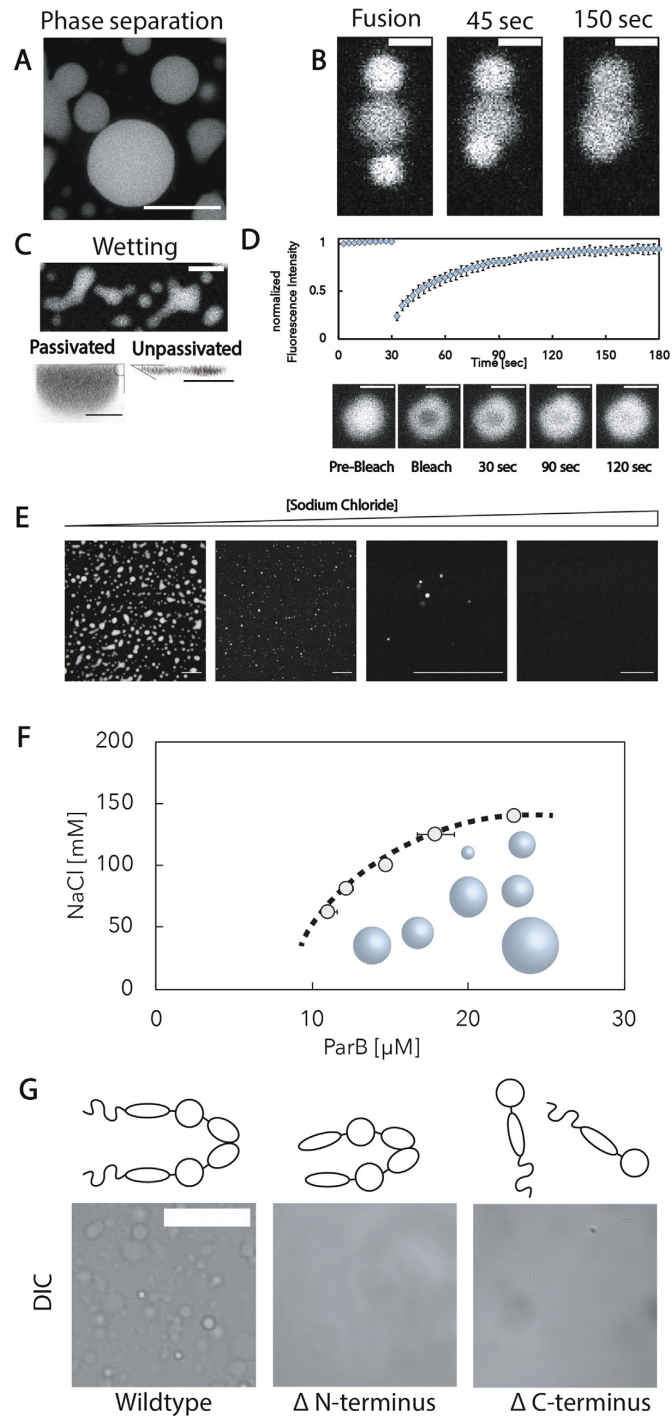
Here we show that ParB is indeed able to form liquid-like assemblies via LLPS *in vitro*. We demonstrate that ParB condensates are highly susceptible to changes in the environment and specifically interact with *parS*. Furthermore, we study the effect of CTP on ParB LLPS and find that the ParB-CTP interaction offers a regulating mechanism of ParB LLPS.

### C. glutamicum ParB undergoes liquid–liquid phase separation in vitro

As liquid–liquid phase separation has been proposed to organize partition complex assembly *in vivo*, we thought to scrutinize this hypothesis *in vitro*.<sup>19</sup> A reasonably well established model system for ParAB driven origin segregation is the system from the actinobacterium *Corynebacterium glutamicum*.<sup>33–35</sup> We therefore exposed purified *C. glutamicum* ParB to 5% 8 kDa PEG, mimicking the crowded nature of the cytoplasm,<sup>36</sup> and observed the formation of micrometer large spherical assemblies (Figure 1(A)). This phase behavior was not specific to the crowder, as we observed the same effect for other synthetic crowders (Figure S1). The spherical assemblies showed common properties of liquids: (1) Upon establishing contact, they fused into larger condensates and slowly relaxed back into a spherical shape (Figure 1(B)). (2) Larger condensates spread out and differentially wetted glass surfaces, a behavior unique to liquid-like assemblies (Figure 1(C)). (3) Fluorescence recovery after photobleaching on a minute timescale ( $t_{1/2} = \sim 30$  s) suggested a dynamic exchange of proteins with similar diffusion rates to other protein condensates (Figure 1(D)).<sup>29,37</sup> Liquid–liquid phase separation of many eukaryotic proteins has been shown to be highly dependent on electrostatic interactions and changes in environmental conditions drastically alter phase behavior.<sup>38,39</sup> Accordingly, ParB liquid–liquid phase separation was susceptible to alterations of the ionic strength, as an increase of sodium chloride concentration

**Figure 1.** ParB undergoes liquid–liquid phase separation in vitro. (A) ParB forms large spherical assemblies upon exposure to a crowded environment. Scale bar 20  $\mu\text{m}$ . (B) ParB condensates fuse upon establishing contact. (C) ParB condensates wet surfaces. Surfaces were treated by plasma cleaning and either passivated with PLL-PEG or left non-passivated. Scale bar (upper image) = 20  $\mu\text{m}$ . Lower image scale bars = 5  $\mu\text{m}$ . (D) Photobleached ParB molecules recover on a minute timescale. (E) ParB LLPS is susceptible to changes in the environment. An increase in sodium chloride concentration from 62.5 mM (left) to 350 mM (right) leads to a decrease in phase separation. Sodium chloride concentration from left to right: 62.5 mM, 140 mM, 250 mM and 350 mM. Scale bar = 20  $\mu\text{m}$ . Conditions: 30  $\mu\text{M}$  ParB with 10% eGFP-labeled ParB and 0.5  $\mu\text{M}$  double stranded *parS*. (F) Lower phase boundary measured by centrifugation assay. Final concentration before centrifugation was 30  $\mu\text{M}$  ParB, 20 mM Tris pH 7.4 varying NaCl, 2.5 mM  $\text{MgCl}_2$  and 5% 8 k PEG. The dashed line is solely a guide for the eye. (G) From left to right: DIC images of wildtype ParB, ParB delta-N terminus and ParB delta-C terminus at the same conditions as in (A–C). For (A–C) conditions were: 30  $\mu\text{M}$  ParB in 20 mM Tris pH 7.4 140 mM NaCl, 2.5 mM  $\text{MgCl}_2$  and 5% 8 k PEG.





yielded less phase separated material (Figure 1(E)) and a shift to higher saturation concentrations (Figure 1(F)). Addition of a high ionic strength solution to preformed droplets led to a rapid dissolution of the droplets (Movie S1) and a decrease of turbidity (Figure S1), demonstrating the reversibility of ParB LLPS. Interestingly, we found a stabilization of ParB phase separation by potassium glutamate, likely through a stabilization of an oligomeric state (Figure S2(D)), in similarity to a recent publication studying LLPS of bacterial single-stranded DNA binding protein (Figure S2).<sup>40</sup>

To further understand how changes in the environments, such as the increase of ionic strength (Figure 1(E and F)), could control the LLPS of ParB on the molecular level, we investigated structural changes of ParB in increasing ionic strength buffers. Using size exclusion chromatography coupled to multi-angle-light scattering (SEC-MALS) to observe changes in molecular weight of ParB, we found that increasing ionic strength resulted in a shift from ParB-ParB dimers to a mixture of dimers and monomers (Figure S3). These findings indicate that ParB-dimerization is necessary for the LLPS. We generated a mutant lacking the C-terminal dimerization domain which was unable to undergo LLPS under any tested conditions (up to 100  $\mu$ M final concentration) (Figure 1(J)). We also identified a 110 amino acid long disordered N terminus as necessary, but not sufficient for ParB LLPS (Figure S4).

Taken together, these experiments show that *C. glutamicum* ParB can indeed undergo LLPS *in vitro*, as suggested in *in vivo* and *in silico* studies.<sup>17,19</sup> Next, we turned to investigate potential mechanisms to temporally and spatially regulate ParB LLPS.

### ParB condensates are stabilized by *parS*

*In vivo*, ParB interacts with *parS* sites and, in conjunction with ParA, distributes the newly replicated DNA along the cell.<sup>41</sup> The interaction of ParB with *parS* is crucial for chromosome segregation, and deletion of *parS* produces severe phenotypes, such as anucleate and elongated cells.<sup>41</sup> Cells lacking *parS* sites only display miniature partition complexes in *C. glutamicum* (Figure 2(A)).<sup>41</sup>

As the formation of the bacterial partition complex *in vivo* depends on the presence of *parS*, we hypothesized a stabilizing effect of *parS* on ParB phase separation. We therefore assembled a plasmid (approx. 5 kbp) with three *parS* sites evenly spaced around the sequence. The same plasmid was assembled with three sequence-randomized *parS* sites, altering the ParB-binding sequence, but not the composition of the plasmid.

Two different complementary approaches were used to study potential effects of these plasmids on the phase boundary of ParB condensation: A centrifugation-based assay, as described in 29,

and turbidity measurements. While the centrifugation-based assay can determine the precise concentration of the dilute phase after liquid-liquid phase separation and hence, the exact phase boundary, turbidity gives an estimate of the overall amount of phase separated material present in the sample. Intriguingly, *parS* plasmids shifted the phase boundary to lower ParB concentrations and increased sample turbidity when compared to randomized *parS* (Figure 2(B and C)), demonstrating a stabilization of the liquid-liquid phase separation by the ParB-*parS* complex.

Next, we wondered whether these DNA substrates would also preferentially partition into the condensates, as has been shown for eukaryotic proteins such as Whi3.<sup>42</sup> Similarly, we tested potential specificity of ParB condensate interactions with *parS* by measuring partitioning of *parS* oligo compared to a sequence-randomized *parS* oligo. *ParS* oligo partitioned into the condensates with 11 kJ/mol, compared to the sequence-randomized *parS* which partitioned with 4 kJ/mol (Figure 2(D)). Thus, partitioning into ParB condensates depends on the specific ParB binding sequence. Recently, it has been shown that protein condensates can differentiate DNA substrates based on structure and length, therefore we tested if ParB condensates distinguish between short oligo DNA and long and circular plasmids, mimicking their physiological interaction partner.<sup>22</sup> Indeed, the condensates differentiate between a non-specific DNA oligo and a labeled (non-*parS*-bearing) plasmid, where the circular plasmid is partitioned by 14 kJ/mol and the oligo only with 4 kJ/mol (Figure 2(E)). Plasmid containing three *parS* sites partitioned too strongly to be quantified.

Taken together, ParB condensates can, despite their dynamic nature, exhibit sequence- and length-specificity. This allows spatial control over partition complex assembly at *parS* sites by lowering the phase boundary of ParB specifically on *parS* sites, thus providing a compelling case for the role of LLPS in complex formation *in vivo*. Also, the formation of much smaller, ParB condensates in the absence of *parS*<sup>41</sup> reflects our *in vitro* findings.

### ParB liquid-liquid phase separation is regulated by CTP

ParB does not only specifically interact with *parS* sites, but as recently discovered also displays enzymatic activity: ParB orthologues from a variety of species hydrolyze cytidine triphosphate (CTP) which alter interactions with its DNA substrate.<sup>43-45</sup> This CTPase activity is stimulated upon *parS* binding and is thought to trigger the opening of ring-like ParB dimers, unloading ParB from the DNA and limiting spreading distance.<sup>46,47</sup> However, these models do not explain the formation of higher order structures and sphericity of partition complexes *in vivo*.<sup>48</sup> We therefore

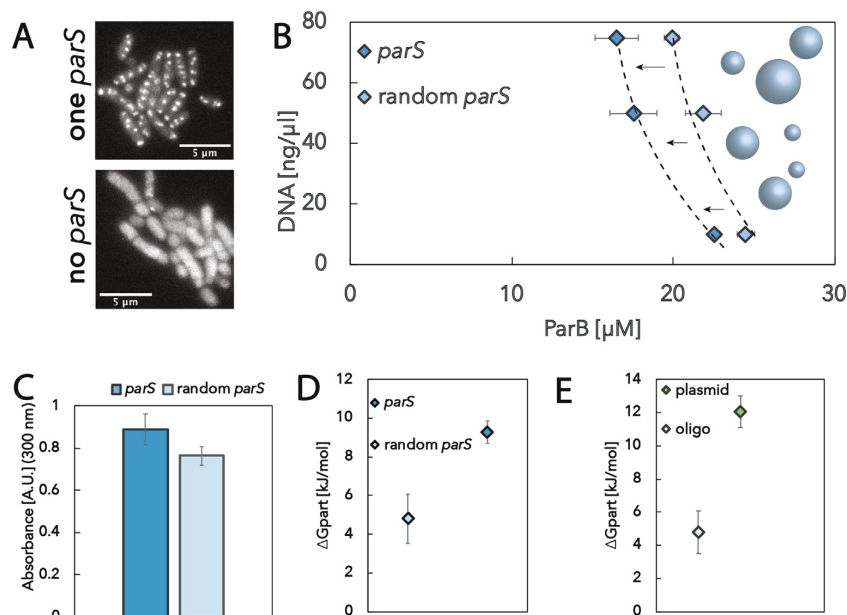


**Figure 2.** ParB condensates specifically interact with *parS*. (A) *C. glutamicum* cells harboring one (upper) or no (lower) *parS* sites per chromosome. No condensates can be observed in the no-*parS* strains. A ParB-mCherry fusion protein was used to visualize ParB in vivo distribution.<sup>41</sup> (B) *parS* shifts the phase boundary of ParB to lower concentrations compared to randomized *parS*. Three concentrations (75 ng/ul, 50 ng/ul and 10 ng/ul) of plasmids were used. Buffer conditions were 20 mM Tris pH 7.4, 140 mM NaCl, 2.5 mM MgCl<sub>2</sub> and 5% 8 k PEG. Initial protein concentration was 30 μM. Error bars represent the standard deviation of three samples. The dashed line is solely a guide for the eye. (C) *parS* increases sample turbidity compared to randomized *parS*. Sample was prepared as in (B) at 50 ng/ul of *parS* or random-*parS* plasmid and a final protein concentration of 30 μM. Error bars represent the standard deviation of three samples. (D) ParB selectively partition *parS* oligos compared to randomized *parS*. 0.5 μM of Cy-5 labeled oligo was incubated with ParB in the “hanging drop set-up” prior to imaging. Protein concentration was 30 μM with ~10% eGFP-labeled ParB. Error bars represent the standard deviation of three sample means. In each sample at least 3 different areas were analyzed. (E) Plasmids are preferentially absorbed into the dense phase compared to oligos. 0.5 μM of Cy-5 labeled oligo was incubated with ParB in the “hanging drop set-up” prior to imaging. Protein concentration was 30 μM with ~10% eGFP-labeled ParB. 0.5 μM of Cy-5 labeled plasmid was incubated with ParB in the “hanging drop set-up” prior to imaging. Protein concentration was 30 μM with 10% eGFP-labeled ParB. Error bars represent the standard deviation of three sample means.

hypothesized that ParB-CTP interactions control the LLPS of the partition complex.

Like other ParB orthologues, the ability of *C. glutamicum* ParB to hydrolyze CTP was dependent on the presence of *parS*-containing DNA (Figure 3(A)). Without *parS* in solution, the hydrolysis rate was low with ~3 molecules per hour and dimer. However, in presence of substoichiometric amounts (1/8) of double stranded *parS* oligonucleotide, hydrolysis was enhanced fivefold (Figure 3(A)). This behavior is in good agreement with recently published hydrolysis rates and stimulation thereof by *parS*.<sup>43–45</sup>

As CTP hydrolysis has been shown to alter ParB conformation and interactions with DNA,<sup>45–47,49</sup> we hypothesized that CTP interactions also regulate ParB phase separation. A large body of theoretical

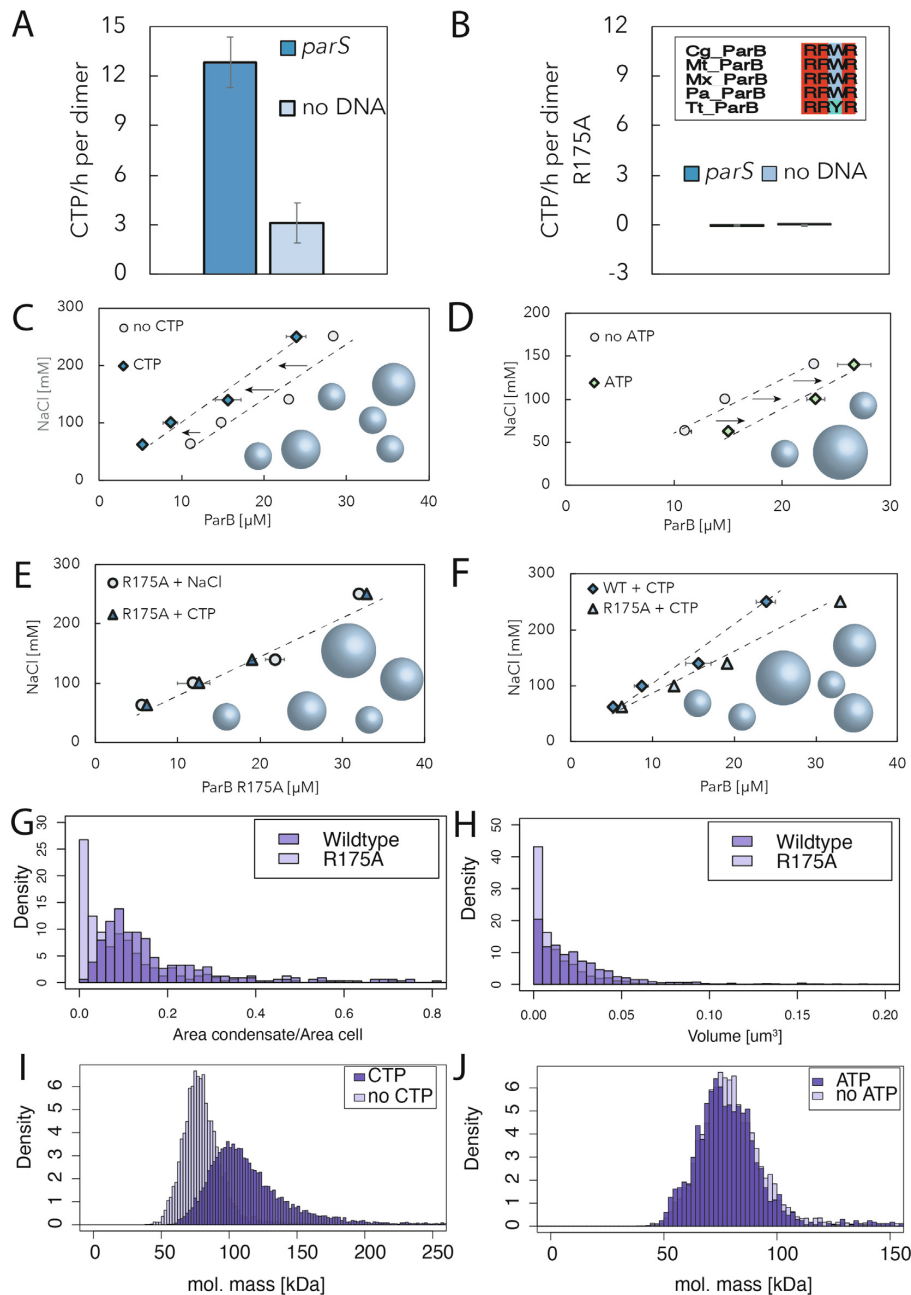
studies predicts unique properties of energy-dissipating condensates, like shape transformation or even condensate division, as described for the partition complex.<sup>50–53</sup> Hence, ParB CTPase activity might allow for dynamic control over assembly and disassembly of the partition complex.

We therefore investigated the effect of CTP on ParB phase boundary using the centrifugation-based assay and found that 0.5 mM CTP lowered ParB saturation concentration compared to an ionic strength control (NaCl). In contrast, another nucleotide that does not bind to ParB, ATP, had a destabilizing effect on the condensed phase (Figure 3(E)). Similarly, CDP, UTP and GTP destabilized the condensed ParB phase (Figure S6). Therefore, CTP specifically stabilizes the formation of a condensed phase of ParB. This stabilization can be due to a unique CTP-

condensate interaction, as recently shown for ATP and eukaryotic proteins,<sup>54</sup> or alternatively be regulated by direct ParB-CTP binding and associated structural changes in ParB.

The CTP binding pocket identified in recent studies is comprised of four well conserved arginines which have been shown to interact with

CTP (Figure 3(B)).<sup>44,45</sup> To further understand the stabilization of ParB phase behavior, we mutated arginine 175 to alanine which has been shown to abolish CTP-hydrolysis in other organisms.<sup>47</sup> Mutation of the conserved arginine residue 175 in *C. glutamicum* ParB to alanine, leads to an altered behaviour of ParB complexes *in vivo*.<sup>41</sup> We con-



firming that this mutant shows no CTPase activity *in vitro* in absence or presence of *parS* (Figure 3(B)). Furthermore, ParB<sup>R175A</sup> experienced no stabilization of the phase separation in presence of CTP (Figure 3(G)) and no change of turbidity was observed upon addition of CTP (Figure S4).

To test whether the stabilization of ParB phase separation in the presence of *parS* or CTP is caused by the same or distinct molecular mechanisms, a phase diagram and turbidity measurements in the presence of CTP and *parS* were acquired. Current models assume a differential effect of *parS* and CTP on ParB structure and dynamics which could be reflected in the phase diagram of ParB.<sup>46,47,49</sup> Indeed, the stabilization of ParB LLPS through *parS* and CTP relies on independent mechanisms, as phase boundary and turbidity show an additive shift in the presence of both molecules (Figure S4). Similarly, ParB<sup>R175A</sup>, unable to hydrolyze CTP, did not alter phase behavior in the presence of CTP (Figure 3(E)), but showed an increase of phase separation in the presence of *parS*, as measured by turbidity (Figure S4).

Recently, it was found that presence of *parS* and CTP can lead to the formation of oligomeric ParB species.<sup>45</sup> Interestingly, oligomerization is also known to effectively enhance phase separation.<sup>55–57</sup>

Accordingly, we found a change of hydrodynamic radius upon introducing 2.5 mM CTP to 30  $\mu$ M ParB from  $5.2 \pm 0.07$  nm to  $5.6 \pm 0.26$  nm in DLS measurements (Figure S2(D)). Similarly, mass photometry experiments revealed a shift to higher

molecular weights upon addition of 1 mM CTP to 200 nM ParB, which did not occur in a control sample with ATP (Figure 3(I and J)). Also, we observe the formation of higher order oligomers in the presence of CTP and *parS* (Figure S5). These experiments suggest that CTP controls ParB phase separation through the induction of oligomeric interactions which favor formation of the liquid-like phase.

In order to determine whether ParB-CTP interactions can control the *in vivo* phase separation of ParB, we quantified the amount of condensed material within wildtype and ParB<sup>R175A</sup> mutant cells using super-resolution microscopy. In accordance with the *in vitro* phase diagrams, we found that the volume of condensed ParB is significantly lower for the ParB<sup>R175A</sup> mutant compared to the wildtype (Figure 3(H)), and that wildtype ParB condensates occupy a larger area fraction of the cells (Figure 3(G)).

### ParB liquid–liquid phase separation is evolutionarily conserved

As suggested by *in vivo* experiments in the *E. coli* F-plasmid partitioning assembly by LLPS is a more wide-spread phenomenon and not only relevant in *C. glutamicum*.<sup>19</sup> To test whether other ParB orthologues have the potential to undergo LLPS, we purified *Caulobacter crescentus* and *Thermus thermophilus* ParB. Intriguingly, both orthologues showed liquid-like assemblies upon exposure to synthetic crowders (Figure 4(A and D)), and these

**Figure 3.** CTP stabilizes ParB LLPS. (A) *C. glutamicum* ParB is a CTPase which is stimulated by *parS*. 4  $\mu$ M ParB were incubated with 0.5  $\mu$ M double stranded *parS* or no DNA in a pyruvate kinase and lactate dehydrogenase coupled enzyme assay. Error bars represent the standard deviation of three samples. (B) Mutation of the conserved CTP binding pocket abolishes CTPase activity. Alignment of the conserved arginine pocket from *C. glutamicum*, *Thermus thermophilus*, *Mycobacterium tuberculosis*, *Myxococcus xanthus* and *Pseudomonas aeruginosa*.<sup>71</sup> (C) 0.5 mM CTP shifts the phase boundary to lower ParB concentrations. Initial protein concentration was 30  $\mu$ M ParB and buffer conditions were: 20 mM Tris pH 7.4 varying NaCl concentration, 2.5 mM MgCl<sub>2</sub> and 5% 8 k PEG. Error bars represent the standard deviation of three samples. (D) ATP has a destabilizing effect on ParB phase boundary. Initial protein concentration was 30  $\mu$ M ParB and buffer conditions were: 20 mM Tris pH 7.4 varying NaCl concentration, 2.5 mM MgCl<sub>2</sub> and 5% 8 k PEG. Error bars represent the standard deviation of three samples. (E) The R175A mutant shows no CTP dependent stabilization of the phase separation. Initial protein concentration was 30  $\mu$ M ParB<sup>R175A</sup> and buffer conditions were: 20 mM Tris pH 7.4 varying NaCl concentration, 2.5 mM MgCl<sub>2</sub> and 5% 8 k PEG. Error bars represent the standard deviation of three samples. (F) Wildtype ParB phase separates at lower concentrations compared to R175A ParB in the presence of 0.5 mM CTP. (Data combined from E & C). (G) Comparison of the occupancy of condensates in respect to the total cell area in wildtype and R175A cells measured by 3D-SIM followed by maximum projections. (H) Volume of condensates in wildtype and R175A cells, measured by 3D-SIM. Both volume and occupancy distributions were tested for Normality via Shapiro-Wilk normality test (*P*-value: <2.2e–16) and then compared between Wildtype and R175A via Wilcoxon rank sum test with continuity correction (Alternative H: ParB > ParB175) (*P*-value: <2.2e–16). (I) ParB shows a shift to higher molecular weights in the presence of 1 mM CTP, measured by mass photometry. Protein concentration was 200 nM ParB and buffer conditions were: 20 mM Tris pH 7.4 140 mM NaCl concentration, 5 mM MgCl<sub>2</sub> and 1 mM CTP. Three experiments were carried out and a representative histogram was chosen. (J) ATP causes no such shift in the molecular weight of ParB. Sample was measured under same conditions as (I), with 1 mM ATP instead of CTP. Three experiments were carried out and a representative histogram was chosen. All histograms are normalized to 100. Dashed lines in the phase diagrams only represent a guide to the eye.

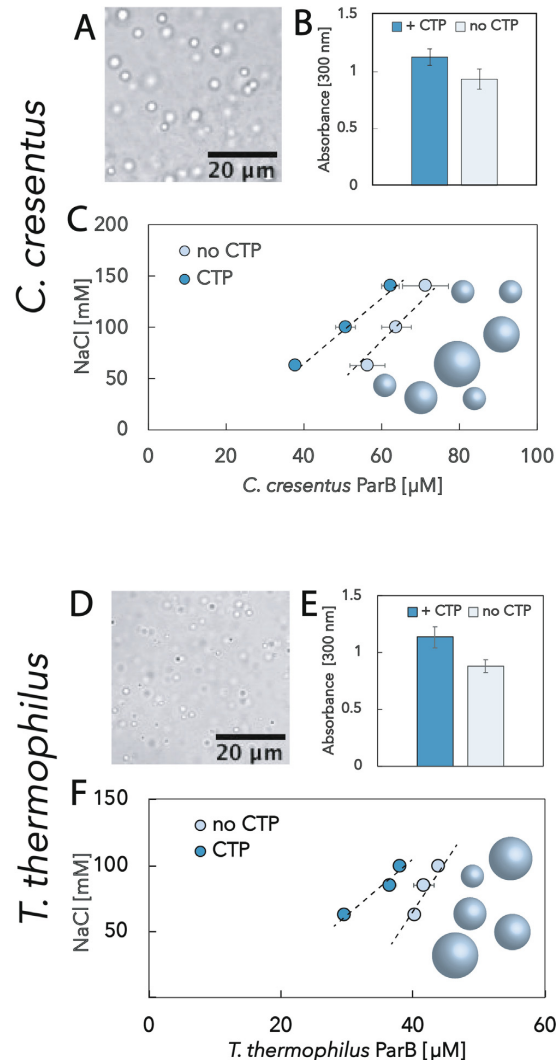


**Figure 4.** ParB phase separation is conserved in different organisms. (A) *Caulobacter crescentus* ParB forms spherical droplets in crowded environments. Conditions: 80  $\mu\text{M}$  ParB in 20 mM Tris pH 7.4, 125 mM NaCl, 2.5 mM  $\text{MgCl}_2$  and 5% 8 k PEG. (B) Turbidity of phase separated *C. crescentus* ParB increases in the presence of 0.5 mM CTP. Conditions: 80  $\mu\text{M}$  ParB in 20 mM Tris pH 7.4, 125 mM NaCl, 2.5 mM  $\text{MgCl}_2$  and 5% 8 k PEG. (C) Phase boundary shifts to lower concentrations of *C. crescentus* ParB in presence of 0.5 mM CTP. Conditions: Protein concentration before centrifugation: 80  $\mu\text{M}$  ParB in 20 mM Tris pH 7.4, varying NaCl concentration, 2.5 mM  $\text{MgCl}_2$  and 5% 8 k PEG. Error bars represent the standard deviation of three samples. The dashed line is solely a guide for the eye. (D) *Thermus thermophilus* ParB forms spherical droplets in crowded environments. Conditions: 50  $\mu\text{M}$  ParB in 20 mM Tris pH 7.4, 125 mM NaCl, 2.5 mM  $\text{MgCl}_2$  and 5% 8 k PEG. (E) Turbidity of phase separated *T. thermophilus* ParB increases in the presence of 0.5 mM CTP. Conditions: 50  $\mu\text{M}$  ParB in 20 mM Tris pH 7.4, 125 mM NaCl, 2.5 mM  $\text{MgCl}_2$  and 5% 8 k PEG. (F) Phase boundary shifts to lower concentrations of *Thermus thermophilus* ParB in presence of 0.5 mM CTP. The dashed line is solely a guide for the eye. Conditions: Protein concentration before centrifugation: 100  $\mu\text{M}$  ParB in 20 mM Tris pH 7.4, varying NaCl concentration, 2.5 mM  $\text{MgCl}_2$  and 5% 8 k PEG. Error bars represent the standard deviation of three samples.

condensates could be dissolved by increasing ionic strength (Movie S2).

It is not yet well understood whether properties of liquid–liquid phase separation are evolutionarily conserved across the tree of life. We therefore sought to test whether our hypothesis of CTP-controlled partition complex assembly is conserved across different bacterial species. Intriguingly, turbidity measurements of both protein samples show an increase in a sample containing 0.5 mM CTP (Figure 5(B and E)). Also, phase diagrams measured by the centrifugation assay show a decrease of saturation concentration for *C. crescentus* and *T. thermophilus* ParB in the presence of CTP (Figure 5(C and F)).

These results indicate that liquid–liquid phase separation of ParB is a more general mechanism of partition complex assembly, and that properties and regulation of assembly is conserved across different species.

## Discussion

In conclusion, we present *in vitro* and *in vivo* data elucidating the mechanism of assembly of the bacterial partition complex. We show that ParB dimerization and oligomerization induces liquid–liquid phase separation (LLPS), which in turn underlies multiple layers of regulation through molecular interactions with CTP and *parS* sites and can be used to spatially and temporally control partition complex formation. Finally, we demonstrate that ParB LLPS is a more widespread phenomena, as it is conserved in largely unrelated bacteria.

A recent study suggested that the bacterial partition complex forms via liquid–liquid phase separation.<sup>19</sup> While a stringent *in vivo* analysis pointed towards this mechanism of assembly, direct *in vitro* evidence was missing. Here we show that ParB alone can indeed undergo LLPS *in vitro*. The ParB condensates are highly responsive to changes in environment and can be rapidly assembled and disassembled. The condensates interact specifically with *parS*, which is preferentially partitioned into the condensates and lowers the saturation concentration necessary for ParB LLPS. These findings agree with *in vivo* experiments, showing a strong depletion of ParB foci upon deletion of *parS* and ParB's physiological function.<sup>41</sup>

The discovery of ParB's enzymatic activity has shifted paradigms of the ParABS molecular mechanism. We show that CTP not only allows loading and unloading of ParB clamps onto DNA as recently proposed,<sup>45–47,49</sup> but also alters ParB oligomeric state and therefore promotes ParB LLPS *in vitro* and *in vivo*. While the current model of partition complex assembly solely relies on a 1D-lattice diffusion, the necessity of a higher-dimensional assembly mechanism has been

raised.<sup>48,58</sup> Considering the plectoneme structure of bacterial nucleoids on a 15 kbp level of bacterial nucleoids,<sup>59</sup> a more elongated and less spherical structure of the partition complex could be expected. We therefore provide further *in vitro* evidence for the recently proposed model of 1-D short-range sliding and clamping, whereas long-range interactions observed by Chip-Seq likely emerge from a higher order structure assembled via liquid–liquid phase separation using *in vitro* reconstitution methods to probe ParB's mechanism of assembly.<sup>48</sup> Also, the formation of ParB clusters in absence of *parS* *in vivo*, as observed previously,<sup>41</sup> cannot be explained by the current models, but provides evidence for liquid–liquid phase separation as an underlying mechanism of partition complex formation. Our findings do not exclude a 1-D clamping and sliding mechanism, but rather provide *in vitro* evidence to explain long range interactions within the partition complex.<sup>48</sup> Also, condensation of DNA by the partition complex has been discussed in detail and remains an open question.<sup>13,60,61</sup> Interestingly, liquid–liquid phase separation has been shown to condense DNA.<sup>62</sup> Therefore, LLPS could be the missing link of partition complex assembly and condensation of DNA.

Interestingly, it is known that mutation of the CTPase activity, and therefore a loss of control over ParB phase separation, also impairs functional loading of SMC proteins.<sup>41</sup> Recently, yeast SMC proteins have been shown to cluster and localize via a phase separation process.<sup>63</sup> It is therefore plausible that interactions driving the SMC phase transition are similar to the interactions that drive ParB LLPS and contribute to correct loading of SMCs at the partition complex. Similarly, it will be interesting to reconstitute the interactions of ParB condensates with ParA. This reconstitution was recently achieved using ParB coated beads, strikingly reassembling phase separated condensates.<sup>9</sup>

Even though liquid–liquid phase separation has been established as a fundamental organizational principle in cell biology,<sup>64</sup> only little is known about the evolution and conservation of phase properties across species.<sup>39,65–69</sup> While it is well understood that protein and protein complex structure and function is often conserved between different species, it is not yet clear if protein liquid-phase properties are exposed to similar co-evolution. Here, we show that both, the propensity to phase separate, and the regulation mechanism are conserved between distantly related bacteria. These findings are even more intriguing, as other bacterial proteins with ParB-like functions, such as the carboxysome positioning system McdAB, have been shown to assemble via liquid–liquid phase separation.<sup>70</sup> We expect that this comparison of *in vitro* phase properties will lead to more *in vitro*, *in vivo* and especially *in silico* investigations of the conservation of phase properties across the tree of life.

Taken together, we can provide further evidence for a new model of partition complex formation governed by liquid–liquid phase separation. Condensates can be specifically nucleated by *parS* DNA sequences. We can also demonstrate that the newly discovered CTPase activity is not only altering the interactions of ParB with DNA, as recently shown, but also ParB–ParB interactions. CTP-induced oligomerization stabilizes ParB LLPS, making the partition complex an energy-dissipating bacterial condensate.

## Material and methods

### Protein purification

*C. glutamicum* ParB was purified as described elsewhere.<sup>41</sup> In brief, ParB protein production was performed in *E. coli* BL21 pLysS via the pET-16b vector-based system. Cells were grown in LB at 37 °C; gene expression was induced adding 1 mM IPTG following growth for 12 h at 18 °C. Subsequently, cells were suspended in washing buffer (50 mM Tris–HCl pH 7.4; 100 mM NaCl; 5 mM MgCl<sub>2</sub>) containing Benzonase, and lysed using a high-pressure cell homogenizer and sonication. Cell debris and membranes were removed by centrifugation at 4 °C, 18,000g for 30 min. There upon, HisTrap FF crude (GE Healthcare) purification of His-tagged protein were performed. Sample was washed using 50 mM Tris–HCl pH 7.4; 150 mM NaCl; 5 mM MgCl<sub>2</sub> and 20 mM Imidazole. Protein was eluted with buffer containing 50 mM Tris–HCl pH 7.4; 150 mM NaCl; 5 mM MgCl<sub>2</sub> and 500 mM Imidazole with a linear gradient. Protein was concentrated in Amicon concentrators (10 kDa MWCO) and loaded onto a pre-equilibrated (20 mM Tris pH 7.4 250 mM NaCl and 5 mM MgCl<sub>2</sub>) Superdex™ 200 gel filtration column (GE Healthcare Life Sciences). Protein variants (Delta C-term, Delta N-term and the disordered N terminus) were purified with the same protocol.

*T. thermophilus* and *C. crescentus* ParB were purified as described elsewhere.<sup>43</sup>

### Phase diagrams via centrifugation and Bradford assay

15 µl samples were prepared in 200 µl PCR tubes. The tubes were then centrifuged at 21,000g for 30 minutes at 25 °C. 7.5 µl of the supernatant were then carefully transferred to a fresh 200 µl PCR tube while making sure to not disturb the pellet. 5 µl of the transferred supernatant were then used to measure protein concentration by following the vendors instructions of the Biorad Bradford (Cat. No. 500–0201) assay.

### Turbidity measurements

80 µl of sample were prepared by mixing protein with the buffer containing crowding agents and

molecules of interest in 384 Greiner Black Flat Plates. After 10 minutes of incubation, turbidity was measured using a TECAN plate reader at room temperature scanning from 200–600 nm.

### Fluorescence microscopy

All images, except for SIM, were taken on a Zeiss LSM780 confocal laser scanning microscope using a Zeiss C-Apochromat × 40/1.20 water-immersion objective (Carl Zeiss). Longer time series were acquired using the built-in autofocus system. ParB-eGFP was excited using a 488 nm argon laser and Cy5-labelled oligonucleotide/plasmid using a 633 nm He–Ne laser. Images were typically recorded with a pinhole size of 2.6–4 Airy units for the eGFP and oligonucleotide/plasmid channel 512 × 512-pixel resolution and a pixel dwell time of 1.27 µs. Line-averaging was set to 2. Images were analysed in ImageJ.<sup>72</sup>

### Sample preparation for structured illumination microscopy

*C. glutamicum* cells were preinoculated in brain heart infusion medium (BHI, Oxoid™) overday, diluted in a 50–50 mix of CGXII and BHI medium overnight and finally diluted to an A<sub>600</sub> of 1 in CGXII. CGXII minimal medium was always supplemented with 120 mM acetate and the cells were always grown at 30 °C, 200 rpm. Cells were grown to exponential phase prior imaging (A<sub>600</sub> ~ 4).

### Structured illumination microscopy (lattice-SIM)

SIM imaging was performed with an Elyra 7 (Zeiss) inverted microscope equipped with two pco.edge sCMOS 4.2CL HS cameras (PCO AG) connected through a DuoLink (Zeiss). Cells were observed through an alpha Plan-Apochromat 63x/1.46 Oil Korr M27 Var2 objective in combination with an Optovar 1.6x (Zeiss) magnification changer, yielding a pixel size of 63 nm. Temperature was maintained at 30 °C for the entirety of the imaging. Ten Z-positions were taken for each Z-stack, where the measured distance between Z-planes (330 nm) is optimized for Leap mode, a novel mode of acquisition and processing developed by Zeiss. Each Z-plane was imaged in Lattice-SIM mode and comprises 13 phases.

Fluorescence was excited with a 561 nm (100 mW) diode lasers, and signals were observed through a multiple beam splitter (405/488/561/641 nm) and laser block filters (405/488/561/641 nm) followed by a DuoLink SR QUAD (Zeiss) filter module (secondary beam splitter: LP560). For each phase, cells were illuminated with the 561 nm laser at 35% intensity for 100 ms.



SIM image reconstruction was done via the ZEN 3.0 SR (black) software. Processing was performed via 3D Leap using all the Z-planes. Standard parameters were used for the reconstruction (Sharpness: standard, Fit: Fast fit). The baseline for the reconstructed intensity histograms was set as cut. The resulting distance between the reconstructed Z-plane equal to 110 nm. The lateral resolution for the SIM reconstructed images, as determined via SIMcheck<sup>73</sup> (data not shown) is approximately 110 nm.

### Image analysis

Reconstructed SIM Z-stack images were analyzed via the 3D-Roi manager from the 3D ImageJ Suite<sup>74</sup> or transformed into maximum intensity projections via Fiji is Just ImageJ (Fiji)<sup>72</sup> and further analyzed via MicrobeJ.<sup>75</sup>

Briefly, cell segmentation and cell area determination were determined via bright-field based binary masks. Construction of the binary masks was performed via the use of two semi-automated Fiji macros (<https://github.com/GiacomoGiacomelli/Bacterial-cells-segmentation-from-Bright-Field>). The identification of ParB condensates from the maximum intensity projections was performed via MicrobeJ (Z-score: 35, Tolerance: 2000, Area [ $\mu\text{m}^2$ ]  $\geq 0.001$ ).<sup>75</sup>

ParB condensate areas contained within to the same cell were summed up together and divided by the area of the cell itself, therefore determining the condensate occupancy.

3D ParB condensate were segmented via the 3D segmentation function from the 3D-Roi manager. The resulting binary stacks were used to produce three dimensional regions of interest which were then compared for volume size. Measurements characterized by NA values were removed from the analysis (NA are caused by volumes spanning for a single cube pixel).

### Statistics

Statistics were performed via R (R-studio v1.1.453, R version v3.5.0).<sup>76</sup> ParB occupancy and condensate volume distributions were tested for normality (Shapiro-Wilk normality test). As both occupancy and condensate volumes did not follow a normal distribution, differences between strains were determined via Wilcoxon rank sum test with continuity correction (Alternative Hypothesis ParB > ParB175).

### Plasmid labeling

Plasmids were labeled by Mirus "label-it" Cy5 labeling kit (Cat. No. MIR 3700) according to manufacturer's instructions to achieve a ~20 bp spacing between labels. Therefore, labeling density of oligonucleotides and plasmids is equal.

### Fluorescent recovery after photobleaching

ParB-eGFP was added in a molar ratio of 1:10 to samples containing either dsDNA or plasmids. Phase separation was induced by mixing buffer with protein and leaving samples as a hanging drop to equilibrate for 10–15 minutes. Then, the hanging drop was sandwiched between two siliconized coverslips (Hampton Research), sealed by vacuum grease. The sample was imaged on a Zeiss LSM780. Droplets of similar size were bleached in the middle and recovery was observed in 3 second time intervals.

### Circular Dichroism (CD) measurement

CD spectra of the disordered N terminus was recorded on a JASCO-715CD-spectrophotometer. Protein was dialyzed in no salt buffer (20 mM Phosphate, pH 7.4, 5 mM  $\text{MgCl}_2$ ). Data were collected at room temperature and consisted of averaging 10 individual spectra followed by buffer average subtraction. Measuring speed was set to 100 nm/min. Protein concentration was determined to be 0.275 mg/ml (measured by Bradford assay).

### CTPase assay

Nucleotide hydrolysis was measured using a coupled enzyme assay.<sup>77</sup> Reactions contained 8  $\mu\text{M}$  ParB variants, 20 U/mL pyruvate kinase (Sigma Aldrich), 20 U/mL L-lactate dehydrogenase (Sigma Aldrich), 800 mg/mL NADH and 3 mM PEP. 140  $\mu\text{l}$  of the reaction mixture were transferred into a 96-well microtiter plate and supplemented with CTP to a final concentration of 1 mM to start the reactions. The reaction was followed by measuring the decrease in NADH absorbance at 340 nm at 15 second intervals. Initial velocities were calculated by linear regression analysis of each time course and corrected for spontaneous CTP hydrolysis and NADH oxidation.

### Partitioning

Droplets were formed like described in 'FRAP'. At least three Z-stacks were taken from representative areas of three different samples. Using Fiji, the mean pixel intensity was extracted from regions of interest within and outside of droplets and compared. The free energy of partitioning was calculated using the equation:  $\Delta G = RT \ln(K)$ , where  $K$  is (Int. inside/Int. outside). Standard deviation was calculated of the three means of the replicates.

### Mass photometry

Measurements were performed on the first generation Refeyn mass photometer. Glass cover slides were sonicated in isopropanol for cleaning. A drop of 19  $\mu\text{l}$  of buffer containing either just

buffer, 1 mM ATP or 1 mM CTP was deposited on the surface and the autofocus was activated. Once stable signal and focus was achieved, 1  $\mu$ l of protein solution of 4  $\mu$ M ParB, preincubated with either 1 mM CTP (Jena Bioscience) or 1 mM ATP (Jena Bioscience) was mixed with the pre-deposited solution, resulting in a final concentration of 200 nM ParB. Full mixing was achieved by pipetting up and down several times. A 6000-frame video was recorded and analyzed in the Refeyn software. As calibration, thermo scientific unstained size exclusion chromatography marker (Cat. No. 26610) was used as suggested by Refeyn.

### DLS

DLS data were collected using a DynaPro NanoStar instrument (Wyatt Technology Europe GmbH, Dernbach, GERMANY). The instrument employs a 658 nm laser and a 90° scattering angle. Samples were measured at 20 °C and 100% laser power, with automated attenuation turned on. Each experiment consisted of 8 repeats of 25 five second acquisitions. Data analysis was with manufacturer's Dynamics software package (release 7.3.18). Data were filtered with a baseline setting of 0.02, followed by averaging of the repeats. Protein concentration was 30  $\mu$ M and CTP concentration was 2.5 mM.

### SEC-Mals

SEC-Mals was performed on a Wyatt system with following components: Light scattering instrument was a Dawn Heleos 8, RI Instrument was a Optilab T-rEX and an Agilent 1260 infinity HPLC. Flow was set to 0.5 ml per minute and 100  $\mu$ l of 1.625 mg/ml ParB was injected. Separation was achieved by a Superdex 200 increase column. Fitting was performed using the ASTRA software. BSA was used for calibration of the instrument.

### Molecular cloning

All constructs were designed and cloned using a seamless cloning strategy. In brief, vectors were linearized using indicated primers (Table S1) in a PCR (Phusion Polymerase (ThermoFisher Scientific Cat. No. F530L)) reaction. Following PCR reaction, template was digested using DpnI (NEB) at 37 °C for 30 min. PCR products were visualized by agarose gel electrophoresis (agarose 0.8%, TAE, 120 V, 40 min), cut-out and purified using a QIAGEN gel extraction kit (Cat. No. 28704). Inserts were amplified by PCR using the appropriate primers (Table S1). Vector and insert were assembled by seamless cloning using the ThermoFisher Scientific /Invitrogen GeneArt™ Seamless Cloning and Assembly Enzyme Mix (A14606) and transformed into chemically competent OneShot Top10-cells (Cat. No.

C404006). Selection for successful cloning was done on LB-Ampicillin or LB-Kanamycin plates. Cells were grown overnight at 37 °C. Then, individual clones were picked and grown overnight in LB media (5 ml) containing the appropriate antibiotic (Ampicillin or Kanamycin). Plasmids were purified by a Miniprep kit (Cat. No.27104) and sequenced to verify successful cloning.

### CRedit authorship contribution statement

**Leon Babl:** Conceptualization, Investigation, Methodology, Validation, Data curation, Writing – original draft. **Giacomo Giacomelli:** Methodology, Data curation. **Beatrice Ramm:** Conceptualization, Methodology, Writing – review & editing. **Ann-Kathrin Gelmoth:** Investigation. **Marc Bramkamp:** Writing – review & editing, Supervision, Funding acquisition. **Petra Schwill:** Conceptualization, Writing – original draft, Writing – review & editing, Supervision, Funding acquisition.

---

---

### Acknowledgements

The authors would like to thank the Biophysical Core Facility of the MPI Biochemistry for support with DLS and SEC-Mals measurements and the MPI protein production facility for help with ParB purification. The authors acknowledge Tung Le for supplying *C. crescentus* and *T. thermophilus* ParB expression plasmids. L.B. acknowledges funding through the Max Planck School "Matter to life". This research was supported by the Deutsche Forschungsgemeinschaft within the Transregio Collaborative Research Center (TRR 174) Spatiotemporal Dynamics of Bacterial Cells. The authors would like to thank Kerstin Andersson and Michaela Schaper for excellent technical assistance.

### Material availability

Code used for image analysis is available at: <https://github.com/GiacomoGiacomelli/Bacterial-cells-segmentation-from-Bright-Field>.

All material is available upon request.

### Declaration of Competing Interest

The authors declare that they have no known competing financial interests or personal relationships that could have appeared to influence the work reported in this paper.

## Appendix A. Supplementary material

Supplementary data to this article can be found online at <https://doi.org/10.1016/j.jmb.2021.167401>.

Received 2 September 2021;

Accepted 7 December 2021;

Available online 10 December 2021

### Keywords:

liquid–liquid phase separation;  
partition complex;  
ParB;  
CTP

### Abbreviations:

ATP, Adenosine triphosphate; CTP, Cytidine triphosphate; LLPS, Liquid-liquid phase separation; DLS, Dynamic light scattering; SEC-MALS, Size Exclusion Chromatography-Multiple angle light scattering

## References

1. S. Autret, R. Nair, J. Errington, S. William, Genetic Analysis of the Chromosome Segregation Protein Spo0J of *Bacillus Subtilis*: Evidence for Separate Domains Involved in DNA Binding and Interactions with Soj Protein.
2. Livny, J., Yamaichi, Y., Waldor, M.K., (2007). Distribution of centromere-like *parS* sites in bacteria: Insights from comparative genomics. *J. Bacteriol.* **189** (23), 8693–8703. <https://doi.org/10.1128/JB.01239-07>.
3. Ireton, K., Gunther IV, N.W., Grossman, A.D., (1994). *spo0J* is required for normal chromosome segregation as well as the initiation of sporulation in *Bacillus subtilis*. *J. Bacteriol.* **176** (17), 5320–5329. <https://doi.org/10.1128/jb.176.17.5320-5329.1994>.
4. Abeles, A.L., Friedman, S.A., Austin, S.J., (1985). Partition of unit-copy miniplasmids to daughter cells. III. The DNA sequence and functional organization of the P1 partition region. *J. Mol. Biol.* **185** (2), 261–272. [https://doi.org/10.1016/0022-2836\(85\)90402-4](https://doi.org/10.1016/0022-2836(85)90402-4).
5. Austin, S., Abeles, A., (1983). Partition of unit-copy miniplasmids to daughter cells. II. The partition region of miniplasmid P1 encodes an essential protein and a centromere-like site at which it acts. *J. Mol. Biol.* **169** (2), 373–387. [https://doi.org/10.1016/S0022-2836\(83\)80056-4](https://doi.org/10.1016/S0022-2836(83)80056-4).
6. Austin, S., Abeles, A., (1983). Partition of unit-copy miniplasmids to daughter cells. I. P1 and F miniplasmids contain discrete, interchangeable sequences sufficient to promote equipartition. *J. Mol. Biol.* **169** (2), 353–372. [https://doi.org/10.1016/S0022-2836\(83\)80055-2](https://doi.org/10.1016/S0022-2836(83)80055-2).
7. Wang, X., Llopis, P.M., Rudner, D.Z., (2013). DNA transactions Organization and segregation of bacterial chromosomes. *Nature Rev. Genet.* **14** <https://doi.org/10.1038/nrg3375>.
8. Vecchiarelli, A.G., Mizuuchi, K., Funnell, B.E., (2012). Surfing biological surfaces: Exploiting the nucleoid for partition and transport in bacteria. *Mol. Microbiol.* <https://doi.org/10.1111/mmi.12017>. Published online.
9. Vecchiarelli, A.G., Neuman, K.C., Mizuuchi, K., (2014). A propagating ATPase gradient drives transport of surface-confined cellular cargo. *Proc. Natl. Acad. Sci. U. S. A.* <https://doi.org/10.1073/pnas.1401025111>. Published online.
10. Lim, H.C., Surovtsev, I.V., Beltran, B.G., Huang, F., Bewersdorf, J., Jacobs-Wagner, C., (2014). Evidence for a DNA-relay mechanism in ParABS-mediated chromosome segregation. *Elife.* <https://doi.org/10.7554/eLife.02758>. Published online.
11. Hu, L., Vecchiarelli, A.G., Mizuuchi, K., Neuman, K.C., Liu, J., (2017). Brownian ratchet mechanisms of ParA-mediated partitioning. *Plasmid.* <https://doi.org/10.1016/j.plasmid.2017.05.002>. Published online.
12. Surovtsev, I.V., Campos, M., Jacobs-Wagner, C., (2016). DNA-relay mechanism is sufficient to explain ParA-dependent intracellular transport and patterning of single and multiple cargos. *Proc. Natl. Acad. Sci. U. S. A.* **113** (46), E7268–E7276. <https://doi.org/10.1073/pnas.1616118113>.
13. Jalal, A.S.B., Le, T.B.K., (2020). Bacterial chromosome segregation by the ParABS system. *Open Biol.* <https://doi.org/10.1098/rsob.200097>. Published online.
14. Lynch, A.S., Wang, J.C., (1995). SopB protein-mediated silencing of genes linked to the *sopC* locus of *Escherichia coli* F plasmid. *Proc. Natl. Acad. Sci. U. S. A.* **92** (6), 1896–1900. <https://doi.org/10.1073/pnas.92.6.1896>.
15. Rodionov, O., ŁObocka, M., Yarmolinsky, M., (1999). Silencing of genes flanking the P1 plasmid centromere. *Science* (80-). <https://doi.org/10.1126/science.283.5401.546>. Published online.
16. Graham, T.G.W., Wang, X., Song, D., et al., (2014). ParB spreading requires DNA bridging. *Genes Dev.* <https://doi.org/10.1101/gad.242206.114>. Published online.
17. Broedersz, C.P., Wang, X., Meir, Y., Loparo, J.J., Rudner, D.Z., Wingreen, N.S., (2014). Condensation and localization of the partitioning protein ParB on the bacterial chromosome. *Proc. Natl. Acad. Sci. U. S. A.* <https://doi.org/10.1073/pnas.1402529111>. Published online.
18. Debaugny, R.E., Sanchez, A., Rech, J., et al., (2018). A conserved mechanism drives partition complex assembly on bacterial chromosomes and plasmids. *Mol. Syst. Biol.* <https://doi.org/10.15252/msb.20188516>. Published online.
19. Guilhas, B., Walter, J.C., Rech, J., et al., (2020). ATP-Driven Separation of Liquid Phase Condensates in Bacteria. *Mol. Cell.* <https://doi.org/10.1016/j.molcel.2020.06.034>. Published online.
20. Hyman, A.A., Weber, C.A., Jülicher, F., (2014). Liquid-liquid phase separation in biology. *Annu. Rev. Cell Dev. Biol.* **30**, 39–58. <https://doi.org/10.1146/annurev-cellbio-100913-013325>.
21. Peebles, W., Rosen, M.K., (2020). Phase Separation Can Increase Enzyme Activity by Concentration and Molecular Organization. *bioRxiv*. Published online.
22. Nott, T.J., Craggs, T.D., Baldwin, A.J., (2016). Membraneless organelles can melt nucleic acid duplexes and act as biomolecular filters. *Nature Chem.* <https://doi.org/10.1038/NCHEM.2519>. Published online.
23. Nott, T.J., Petsalaki, E., Forman-Kay, J.D., et al., (2015). Phase Transition of a Disordered Nuage Protein Generates Environmentally Responsive Membraneless Organelles. *Mol. Cell* **57**, 936–947. <https://doi.org/10.1016/j.molcel.2015.01.013>.

24. Riback, J.A., Zhu, L., Ferrolino, M.C., et al., (2020). Composition-dependent thermodynamics of intracellular phase separation. *Nature* **581** <https://doi.org/10.1038/s41586-020-2256-2>.
25. Protter, D.S.W., Parker, R., (2016). Principles and Properties of Stress Granules. *Trends Cell Biol.* **26** (9), 668–679. <https://doi.org/10.1016/j.tcb.2016.05.004>.
26. Brangwynne, C.P., Eckmann, C.R., Courson, D.S., et al., (2009). Germline P granules are liquid droplets that localize by controlled dissolution/condensation. *Science* (80-). <https://doi.org/10.1126/science.1172046>. Published online.
27. Hyman, A.A., Weber, C.A., Jülicher, F., (2014). Liquid-liquid phase separation in biology. *Annu. Rev. Cell Dev. Biol.* <https://doi.org/10.1146/annurev-cellbio-100913-013325>. Published online.
28. Kato, M., Han, T.W., Xie, S., et al., (2012). Cell-free formation of RNA granules: Low complexity sequence domains form dynamic fibers within hydrogels. *Cell* **149** (4), 753–767. <https://doi.org/10.1016/j.cell.2012.04.017>.
29. Elbaum-Garfinkle, S., Kim, Y., Szczepaniak, K., et al., (2015). The disordered P granule protein LAF-1 drives phase separation into droplets with tunable viscosity and dynamics. *Proc. Natl. Acad. Sci. U. S. A.* <https://doi.org/10.1073/pnas.1504822112>. Published online.
30. M. Feric, N. Vaidya, T.S. Harmon, et al. Coexisting liquid phases underlie nucleolar sub-compartments. [10.1016/j.cell.2016.04.047](https://doi.org/10.1016/j.cell.2016.04.047).
31. Kroschwald, S., Maharana, S., Mateju, D., et al., (2015). Promiscuous interactions and protein disaggregases determine the material state of stress-inducible RNP granules. *Elife*. **4** (AUGUST2015) <https://doi.org/10.7554/eLife.06807>.
32. Azaldegui, C.A., Vecchiarelli, A.G., Biteen, J.S., (2020). The emergence of phase separation as an organizing principle in bacteria. *Biophys. J.* <https://doi.org/10.1016/j.bpj.2020.09.023>. Published online.
33. K. Böhm, F. Meyer, A. Rhomberg, J. Kalinowski, C. Donovan, M. Bramkamp, Novel Chromosome Organization Pattern in Actinomycetales-Overlapping Replication Cycles Combined with Diploidy, (2017), [10.1128/mBio.00511-17](https://doi.org/10.1128/mBio.00511-17). Published online.
34. Donovan, C., Schwaiger, A., Krämer, R., Bramkamp, M., (2010). Subcellular localization and characterization of the ParAB system from *Corynebacterium glutamicum*. *J. Bacteriol.* **192** (13), 3441–3451. <https://doi.org/10.1128/JB.00214-10>.
35. Donovan, C., Sieger, B., Krämer, R., Bramkamp, M., (2012). A synthetic *Escherichia coli* system identifies a conserved origin tethering factor in Actinobacteria. *Mol. Microbiol.* **84** (1), 105–116. <https://doi.org/10.1111/j.1365-2958.2012.08011.x>.
36. Zimmerman, S.B., Trach, S.O., (1991). Estimation of macromolecule concentrations and excluded volume effects for the cytoplasm of *Escherichia coli*. *J. Mol. Biol.* [https://doi.org/10.1016/0022-2836\(91\)90499-V](https://doi.org/10.1016/0022-2836(91)90499-V). Published online.
37. N.M. Kanaan, C. Hamel, T. Grabinski B. Combs, Liquid-liquid phase separation induces pathogenic tau conformations in vitro. [10.1038/s41467-020-16580-3](https://doi.org/10.1038/s41467-020-16580-3).
38. G. Krainer, T.J. Welsh, J.A. Joseph, et al., Reentrant liquid condensate phase of proteins is stabilized by hydrophobic and non-ionic interactions. [10.1038/s41467-021-21181-9](https://doi.org/10.1038/s41467-021-21181-9).
39. M.D. Crabtree, J. Holland, P. Kompella, et al., Repulsive electrostatic interactions modulate dense and dilute phase properties of biomolecular condensates. [10.1101/2020.10.29.357863](https://doi.org/10.1101/2020.10.29.357863).
40. Harami, G.M., Kovács, Z.J., Pancsa, R., et al., (2020). Phase separation by ssDNA binding protein controlled via protein-protein and protein-DNA interactions. *Proc. Natl. Acad. Sci. U. S. A.* **117** (42), 26206–26217. <https://doi.org/10.1073/pnas.2000761117>.
41. Böhm, K., Giacomelli, G., Schmidt, A., et al., (2020). Chromosome organization by a conserved condensin-ParB system in the actinobacterium *Corynebacterium glutamicum*. *Nature Commun.* <https://doi.org/10.1038/s41467-020-15238-4>. Published online.
42. Langdon, E.M., Qiu, Y., Niaki, A.G., et al., (2018). mRNA structure determines specificity of a polyQ-driven phase separation. *Science* (80-). <https://doi.org/10.1126/science.aar7432>. Published online.
43. Jalal, A.S., Tran, N.T., Le, T.B., (2020). ParB spreading on DNA requires cytidine triphosphate in vitro. *Elife*. <https://doi.org/10.7554/eLife.53515>. Published online.
44. Osorio-Valeriano, M., Altegoer, F., Steinchen, W., et al., (2019). ParB-type DNA Segregation Proteins Are CTP-Dependent Molecular Switches. *Cell*. <https://doi.org/10.1016/j.cell.2019.11.015>. Published online.
45. Soh, Y.M., Davidson, I.F., Zamuner, S., et al., (2019). Self-organization of parS centromeres by the ParB CTP hydrolase. *Science* (80-). <https://doi.org/10.1126/science.aay3965>. Published online.
46. Antar, H., Soh, Y., Zamuner, S., et al., (2021). Relief of ParB autoinhibition by parS DNA catalysis and recycling of ParB by CTP hydrolysis promote bacterial centromere assembly. *Sci. Adv.* (October), 1–17. <https://doi.org/10.1126/sciadv.abj2854>.
47. M. Osorio-Valeriano, F. Altegoer, C.K. Das, et al., The CTPase activity of ParB acts as a timing mechanism to control the dynamics and function of prokaryotic DNA partition complexes. [10.1101/2021.05.05.442810](https://doi.org/10.1101/2021.05.05.442810).
48. Walter, J.C., Rech, J., Walliser, N.O., et al., (2020). Physical Modeling of a Sliding Clamp Mechanism for the Spreading of ParB at Short Genomic Distance from Bacterial Centromere Sites. *iScience* **23** (12) <https://doi.org/10.1016/j.isci.2020.101861>.
49. Jalal, A.S.B., Pastrana, C.L., Tran, N.T., et al., (2019). Structural and biochemical analyses of *Caulobacter crescentus* ParB reveal the role of its N-terminal domain in chromosome segregation. *bioRxiv*. <https://doi.org/10.1101/816959>. Published online.
50. Zwicker, D., Seyboldt, R., Weber, C.A., Hyman, A.A., Jülicher, F., (2017). Growth and division of active droplets provides a model for protocells. *Nature Phys.* <https://doi.org/10.1038/nphys3984>. Published online.
51. Zwicker, D., Baumgart, J., Redemann, S., Müller-Reichert, T., Hyman, A.A., Jülicher, F., (2018). Positioning of Particles in Active Droplets. *Phys. Rev. Lett.* <https://doi.org/10.1103/PhysRevLett.121.158102>. Published online.
52. Söding, J., Zwicker, D., Sohrabi-Jahromi, S., Boehning, M., Kirschbaum, J., (2020). Mechanisms for Active Regulation of Biomolecular Condensates. *Trends Cell Biol.* <https://doi.org/10.1016/j.tcb.2019.10.006>. Published online.
53. Zwicker, D., Hyman, A.A., Jülicher, F., (2015). Suppression of Ostwald ripening in active emulsions. *Phys. Rev. E – Stat Nonlinear, Soft Matter Phys.* <https://doi.org/10.1103/PhysRevE.92.012317>. Published online.
54. Patel, A., Malinowska, L., Saha, S., et al., (2017). Biochemistry: ATP as a biological hydrotrope. *Science*

- (80-) 356 (6339), 753–756. <https://doi.org/10.1126/science.aaf6846>.
55. Dao, T.P., Martyniak, B., Canning, A.J., et al., (2019). ALS-Linked Mutations Affect UBQLN2 Oligomerization and Phase Separation in a Position- and Amino Acid-Dependent Manner. *Structure* **27** (6), 937–951.e5. <https://doi.org/10.1016/j.str.2019.03.012>.
  56. Banani, S.F., Rice, A.M., Peeples, W.B., et al., (2016). Compositional Control of Phase-Separated Cellular Bodies. *Cell* **166** (3), 651–663. <https://doi.org/10.1016/j.cell.2016.06.010>.
  57. Choi, J.M., Holehouse, A.S., Pappu, R.V., (2020). Physical Principles Underlying the Complex Biology of Intracellular Phase Transitions. *Annu. Rev. Biophys.* **49**, 107–133. <https://doi.org/10.1146/annurev-biophys-121219-081629>.
  58. Merino-Salomón, A., Babl, L., Schwille, P., (2021). Self-organized protein patterns: The MinCDE and ParABS systems. *Curr. Opin. Cell Biol.* **72**, 106–115. <https://doi.org/10.1016/j.ceb.2021.07.001>.
  59. Le, T.B.K., Imakaev, M.V., Mirny, L.A., Laub, M.T., (2013). High-resolution mapping of the spatial organization of a bacterial chromosome. *Science* (80-) **342** (6159), 731–734. <https://doi.org/10.1126/science.1242059>.
  60. Madariaga-Marcos, J., Pastrana, C.L., Fisher, G.L.M., Dillingham, M.S., Moreno-Herrero, F., (2019). ParB dynamics and the critical role of the CTD in DNA condensation unveiled by combined force-fluorescence measurements. *Elife* **8** <https://doi.org/10.7554/ELIFE.43812>.
  61. Balaguer, F. de A., Aicart-Ramos, C., Fisher, G.L.M., et al., (2021). Ctp promotes efficient parb-dependent dna condensation by facilitating onedimensional diffusion from pars. *Elife* **10** <https://doi.org/10.7554/ELIFE.67554>.
  62. T. Quail, S. Golfier, M. Elsner, et al. Force generation by protein-DNA co-condensation. *Nature Phys.* **10.1038/s41567-021-01285-1**.
  63. J.-K. Ryu, C. Bouchoux, H.W. Liu, et al. Bridging-Induced Phase Separation Induced by Cohesin SMC Protein Complexes. vol. 7 (2021).
  64. Hyman, A.A., Weber, C.A., Ulicher, F.J., (2014). Liquid-Liquid Phase Separation in Biology. *Annu. Rev. Cell. Dev. Biol.* **30**, 39–58. <https://doi.org/10.1146/annurev-cellbio-100913-013325>.
  65. T.M. Franzmann, M. Jahnel, A. Pozniakovsky, et al., Phase separation of a yeast prion protein promotes cellular fitness. [10.1126/science.aao5654](https://doi.org/10.1126/science.aao5654).
  66. Hondele, M., Sachdev, R., Heinrich, S., et al., (2019). DEAD-box ATPases are global regulators of phase-separated organelles. *Nature* **573** (7772), 144–148. <https://doi.org/10.1038/s41586-019-1502-y>.
  67. Zarin, T., Strome, B., Nguyen Ba, A.N., Alberti, S., Forman-Kay, J.D., Moses, A.M., (2019). Proteome-wide signatures of function in highly diverged intrinsically disordered regions. *Elife* **8**, 1–26. <https://doi.org/10.7554/eLife.46883>.
  68. Dasmeh, P., Wagner, A., (2021). Natural Selection on the Phase-Separation Properties of FUS during 160 My of Mammalian Evolution. *Mol. Biol. Evol.* **38** (3), 940–951. <https://doi.org/10.1093/molbev/msaa258>.
  69. Riback, J.A., Katanski, C.D., Kear-Scott, J.L., et al., (2017). Stress-triggered phase separation is an adaptive, evolutionarily tuned response. *Cell* **168** (6), 1028–1040.e19. <https://doi.org/10.1016/j.cell.2017.02.027>.
  70. J.S. Maccreeady, J.L. Basalla, A.G. Vecchiarelli, Origin and Evolution of Carboxysome Positioning Systems in Cyanobacteria. [10.1093/molbev/msz308](https://doi.org/10.1093/molbev/msz308).
  71. Waterhouse, A.M., Procter, J.B., Martin, D.M.A., Clamp, M., Barton, G.J., (2009). Sequence analysis Jalview Version 2-a multiple sequence alignment editor and analysis workbench. *Bioinforma Appl NOTE* **25** (9), 1189–1191. <https://doi.org/10.1093/bioinformatics/btp033>.
  72. Schindelin, J., Arganda-Carreras, I., Frise, E., et al., (2012). Fiji: an open-source platform for biological-image analysis. *Nature Methods* **9** (7), 676–682. <https://doi.org/10.1038/nmeth.2019>.
  73. G. Ball, J. Demmerle, R. Kaufmann, I. Davis, I.M. Dobbie, L. Schermelleh, SIMcheck: a Toolbox for Successful Super-resolution Structured Illumination Microscopy OPEN, (2015). [10.1038/srep15915](https://doi.org/10.1038/srep15915). Published online.
  74. Ollion, J., Cochennec, J., Loll, F., Escudé, C., Boudier, T., (2013). TANGO: a generic tool for high-throughput 3D image analysis for studying nuclear organization. *Bioinformatics* **29** (14), 1840–1841. <https://doi.org/10.1093/BIOINFORMATICS/BTT276>.
  75. Ducret, A., Quardokus, E.M., Brun, Y.V., (2016). MicrobeJ, a tool for high throughput bacterial cell detection and quantitative analysis. *Nature Microbiol.* **1** (7) <https://doi.org/10.1038/NMICROBIOL.2016.77>.
  76. R: The R Project for Statistical Computing. Accessed October 28, 2021. <https://www.r-project.org/>.
  77. Ingberman, E., Nunnari, J., (1995). A continuous, regenerative coupled GTPase assay for dynamin-related proteins. *Methods Enzymol.* **2005** (404), 611–619. [https://doi.org/10.1016/S0076-6879\(05\)04053-X](https://doi.org/10.1016/S0076-6879(05)04053-X).

## Supporting Information:

### CTP-controlled liquid-liquid phase separation of ParB:

#### Highlights:

- ParB undergoes liquid-liquid phase separation *in vitro*
- parS specifically interacts with ParB condensates
- CTP stabilizes the formation of ParB condensates
- ParB liquid-liquid phase separation and control thereof is evolutionary conserved

Keywords: Liquid-liquid phase separation, partition complex, ParB, CTP

Authors: Leon Babl<sup>±</sup>, Giacomo Giacomelli<sup>§</sup>, Beatrice Ramm<sup>±</sup>, Ann-Kathrin Gelmroth<sup>±</sup>, Marc Bramkamp<sup>§</sup> and Petra Schuille<sup>±\*</sup>

Author affiliations:

<sup>±</sup>Max Planck Institute for Biochemistry, Am Klopferspitz 18, 82152 Planegg, Germany  
<sup>§</sup> Christian-Albrechts-Universität zu Kiel, Am Botanischen Garten 1-9, 24118 Kiel

Corresponding author: [schulle@biochem.mpg.de](mailto:schulle@biochem.mpg.de)

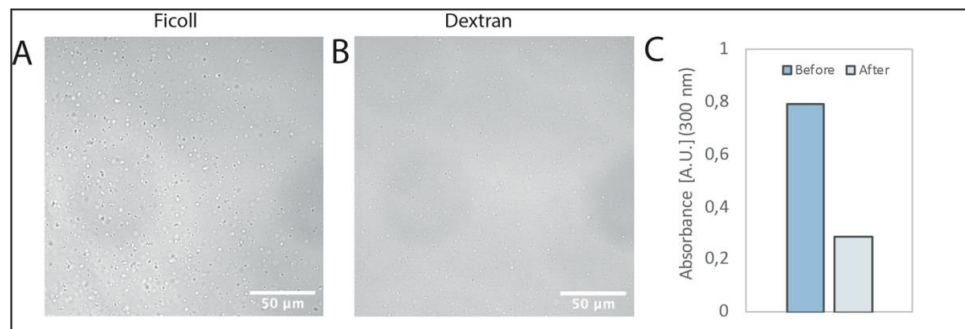


Figure S 1: ParB phase separation is not dependent on the crowder and is reversible. A) ParB phase separation observed upon introducing 30 µM ParB in 20 mM Tris pH 7.4, 125 mM NaCl and 2.5 mM MgCl<sub>2</sub> to 5% 20 kDa Dextran. B) ParB phase separation observed upon introducing 30 µM ParB in 20 mM Tris pH 7.4, 125 mM NaCl and 2.5 mM MgCl<sub>2</sub> to 5% 70 kDa Ficoll. C) Turbidity measurement before and after the addition of 0.5 M NaCl to a phase separated sample of ParB.

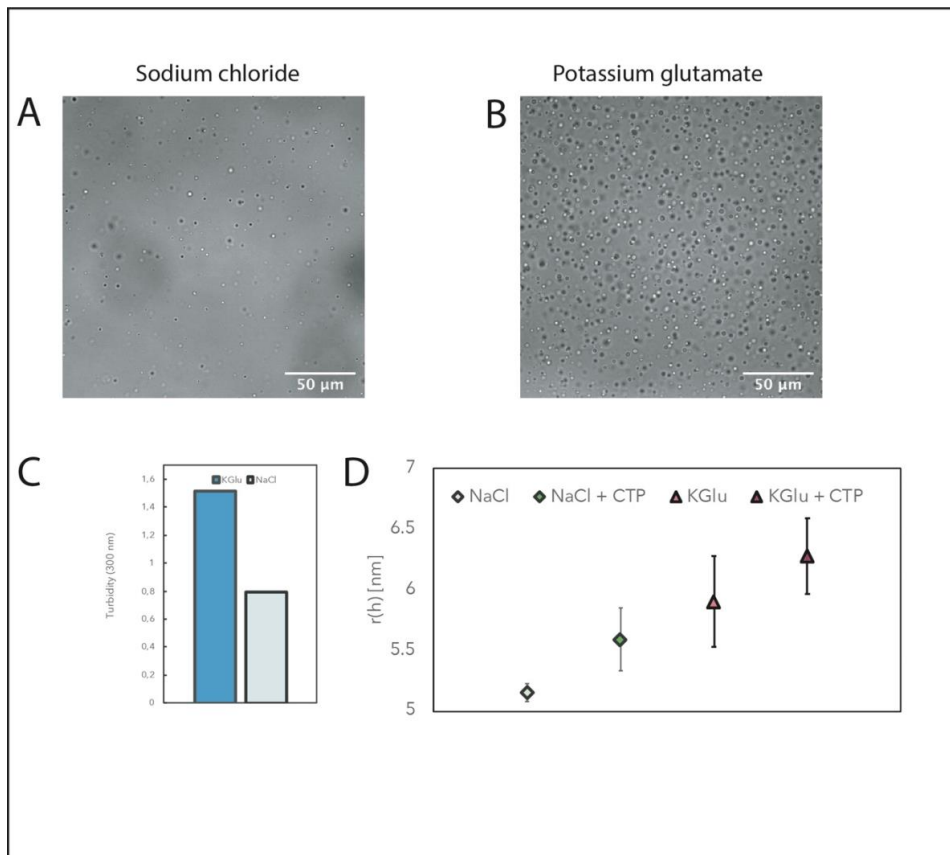


Figure S 2: Potassium glutamate stabilizes ParB phase separation. A) ParB in 140 mM NaCl and 200 mM potassium glutamate (B). C) Turbidity measurements show a clear difference between KGLu and NaCl. D) DLS measurements of ParB radius of hydration in different conditions.

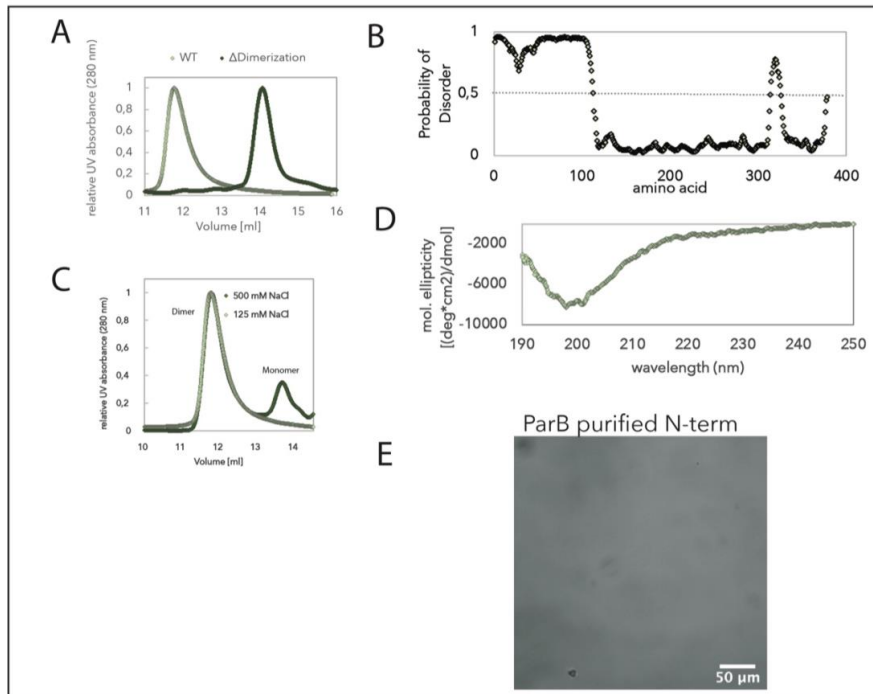


Figure S 2: Structural features of ParB liquid-liquid phase separation. A) SEC-MALS control of the delta-C-term mutant, showing complete monomerization. B) Disorder prediction using Spot-Disorder predictor of *C. glutamicum* ParB. The N-terminus is predicted to be highly disordered. C) Increase of ionic strength leads to monomerization of ParB, as observed in SEC-MALS measurements. D) CD-Spectra of purified ParB N-terminus shows a high degree of disorder. E)



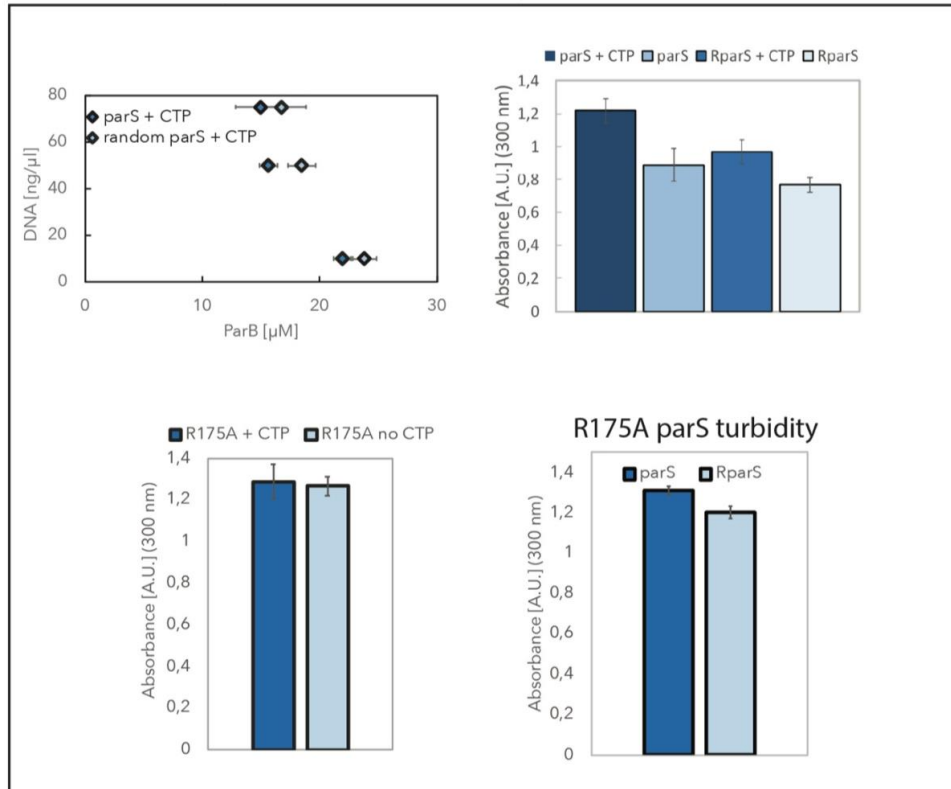


Figure S 3: ParB phase separation is differentially stabilized by CTP and parS . A) Phase diagram of ParB in presence of CTP and parS plasmid or non-parS bearing plasmid. B) Turbidity measurements in the presence of parS/random parS plasmid (50 ng/ul) with or without CTP. C) Turbidity measurement of R175A mutant with and without CTP. D) Turbidity measurement of R175A mutant with parS/random parS plasmid (50 ng/ul).

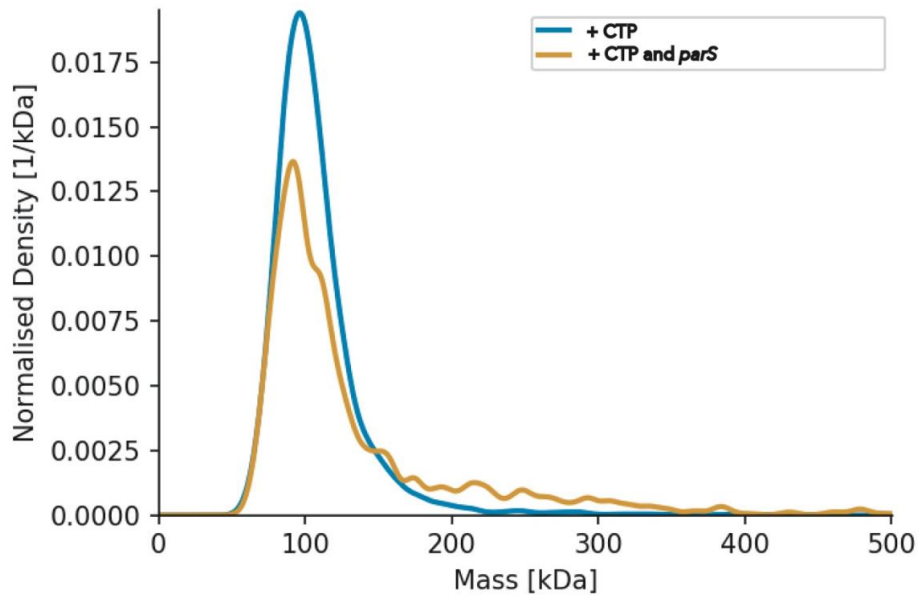


Figure S5: Massphotometry experiment showing the formation of higher order oligomers in presence of CTP and larger complexes in presence of CTP and *parS*. Conditions: 200 nM *ParB*, 25 nM *parS* and 1 mM CTP. Buffer 20 mM Tris pH 7.4, 125 mM NaCl and 5 mM MgCl<sub>2</sub>.

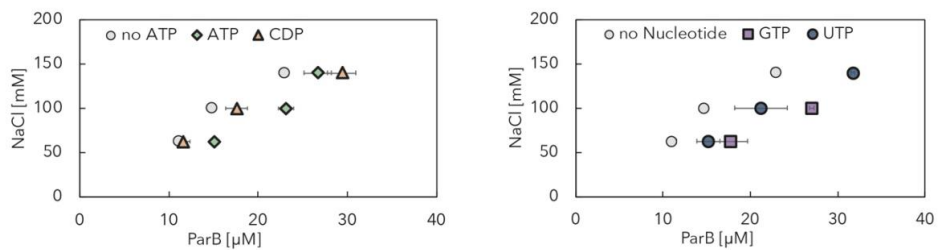


Figure S6: Phase diagrams of *C. glutamicum* *ParB* in presence of CDP, ATP or no nucleotide (left) or GTP, UTP or nucleotide (right) demonstrating a non-nucleotide specific shift to higher saturation concentrations of *ParB* by non-specific nucleotides.

## 5.3 Publication P3

### Membrane mediated phase separation of the bacterial nucleoid occlusion protein Noc

Summary:



In this study, I investigate the phase behavior of the ParB orthologue Noc. I identify similarities between Noc and ParB in the propensity to phase separate and the regulative mechanism thereof. Furthermore, I study the interaction of Noc condensates with various model membrane systems such as SLBs or GUVs [131].

Reprinted with permission from Springer Nature.

**Leon Babi**, Adrian Merino-Salomón, Nishu Kanwa and Petra Schwille, Membrane mediated phase separation of the bacterial nucleoid occlusion protein Noc, *Scientific Reports*, 2022.



# OPEN Membrane mediated phase separation of the bacterial nucleoid occlusion protein Noc

Leon Babl, Adrián Merino-Salomón, Nishu Kanwa & Petra Schwille  

Liquid–liquid phase separation is a fundamental biophysical process to organize eukaryotic and prokaryotic cytosols. While many biomolecular condensates are formed in the vicinity of, or even on lipid membranes, little is known about the interaction of protein condensates and lipid bilayers. In this study, we characterize the recently unknown phase behavior of the bacterial nucleoid occlusion protein Noc. We find that, similarly to other ParB-like proteins, CTP binding tightly regulates Noc's propensity to phase separate. As CTP-binding and hydrolysis also allows Noc to bind and spread on membranes, we furthermore establish Noc condensates as model system to investigate how lipid membranes can influence protein condensation and vice versa. Last, we show that Noc condensates can recruit FtsZ to the membrane, while this does not happen in the non-phase separated state. These findings suggest a new model of Noc mediated nucleoid occlusion, with membrane-mediated liquid–liquid phase separation as underlying principle of complex formation and regulation thereof.

## Abbreviations

GUV	Giant unilamellar vesicle
SLB	Supported lipid bilayer
LLPS	Liquid–liquid phase separation
QCM	Quartz crystal microbalance

Compartmentalization of biochemical processes is a fundamental requirement to orchestrate the wealth of reactions necessary to maintain a functional cell. Long known strategies of compartmentalization involve the formation of membrane-encapsulated substructures within the cell's interior. Prominent examples of such compartments are the eukaryotic nucleus or prokaryotic magnetosomes<sup>1</sup>. More recently, a novel strategy for cellular compartmentalization has gained significant attention: The formation of non-membrane bound organelles by protein or nucleic acid phase separation<sup>2,3</sup>.

Via a often enthalpically driven demixing of a homogenous solution into a component-dense and a component-dilute phase, biochemical reactions can be contained, accelerated and spatiotemporally controlled<sup>4–6</sup>. Highly complex cellular structures such as the nucleolus, a multilayered biomolecular condensate responsible for the production of functional rRNA, can be generated by phase separation of protein and nucleic acid components<sup>7</sup>. Recently, an increasing variety of cellular compartmentalization has been linked to liquid–liquid phase separation in eukaryotes<sup>8</sup> and also prokaryotes<sup>9</sup>.

While our understanding of the assembly and control of these remarkable cellular features is advancing, fewer studies have focused on the interactions of membrane-bound and membraneless organelles<sup>10–19</sup>. However, many of the well-characterized phase separating systems are known to form in proximity and interact with lipid membranes *in vivo*<sup>20,21</sup>. For example, the prominent membraneless organelle of the germ line, the germ granule, forms and stays in vicinity to the nucleolar membrane for its entire lifespan<sup>22</sup>. Exciting theoretical studies have started to unravel principles of phase separation on membranes and other surfaces, predicting significant differences, such as a step-wise wetting transition, to bulk phase separation<sup>23</sup>. Interestingly, the interaction of synthetic aqueous-two phase systems, such as PEG-dextran mixtures, and membrane model systems have been described in depth and have shown to be able to deform, bud and organize biological membranes<sup>24–26</sup>. Also, binding of phase separating proteins to model membrane systems through artificial tags was shown to enhance membrane tubule formation, depending on the phase separated state of the bound proteins<sup>15</sup>. Synaptic proteins have been shown to co-phase separate with membrane vesicles, which has been interpreted as the mechanism

Max Planck Institute for Biochemistry, Am Klopferspitz 18, 82152 Planegg, Germany. ✉email: schwille@biochem.mpg.de

of formation of the pre-synaptic density<sup>13</sup>. It is therefore becoming increasingly clear that many membraneless organelles interact with membrane bound compartments or the plasma membrane<sup>20</sup>.

So far, no bacterial condensates and lipid membrane interactions have been studied *in vitro*. However, recent studies have proposed that the bacterial ParB-protein family is capable of forming liquid–liquid phase separated condensates in various organisms<sup>27–29</sup>. While the largest part of the ParB-family are primarily DNA binding proteins, a subfamily is known to directly interact with lipid membranes. These so-called nucleoid occlusion proteins bind to the inner membrane leaflet and prevent the cell division machinery to form above the bacterial nucleoid<sup>30</sup>. Initially, a uniform distribution of Noc on the nucleoid was reported, but more recent studies revealed dynamic, foci-like structures of Noc on the membrane<sup>31,32</sup>. The formation of this higher-order complex and the mechanism of Z-ring inhibition above the nucleoid, however, are still poorly understood with little *in vitro* data to date.

Here we demonstrate that Noc, like other ParB proteins, undergoes a liquid–liquid phase separation depending on the environmental conditions. The phase separation is controlled by CTP-binding, and the formed droplets readily interact with and deform membranes. The formation of droplets, in reverse, is dependent on membrane characteristics, such as composition and order. Furthermore, phase separated Noc can up-concentrate FtsZ, potentially pointing to a physiological role of condensate formation in Z-ring regulation and highly similar to the *E. coli* nucleoid occlusion system<sup>33</sup>.

## Results

**Noc undergoes liquid–liquid phase separation.** It was recently shown that a variety of ParB-like proteins undergo LLPS *in vivo*<sup>27</sup> and *in vitro*<sup>28</sup>. Despite its different biological function, Noc's ability to bind and spread on membranes is closely regulated by CTP-binding and hydrolysis<sup>34</sup>. This similarity to ParB lead us to hypothesize that Noc can also undergo CTP-controlled LLPS<sup>28</sup>. In accordance with this hypothesis, *in vivo* data suggests that the formed Noc nucleoprotein complex has a higher order structure and is highly dynamic<sup>31,32</sup>.

LLPS of proteins is greatly dependent on environmental conditions, such as ionic strength, buffer composition, or temperature<sup>4,35</sup>. Potassium glutamate is highly abundant in bacterial cells and has been shown to stabilize LLPS of bacterial proteins<sup>28,36,37</sup>. We therefore exposed fluorescently labeled Noc to a buffer containing 150 mM Potassium Glutamate and observed the formation of micrometer-sized spherical droplets (Fig. 1A). Replacing Potassium Glutamate with Potassium Chloride or Sodium Chloride does not lead to phase separation. Thus, Noc phase separation, similar to ParB<sup>28</sup> and other bacterial proteins, is stabilized by Potassium Glutamate. The volume of phase separated droplets scales with protein concentration, as expected for LLPS (Fig. 1A). Noc droplets are highly dynamic, and the formation of the phase separated droplets is reversible as, upon addition of 500 mM KCl, the droplets rapidly dissolve (Fig. 1B). We also observed fusion of droplets and their relaxation into a spherical shape, indicating liquid-like behavior (Supp. Fig. 2 and Movie S1).

It was recently shown that ParB LLPS is tightly regulated by CTP-binding and that this regulation is conserved within the ParB protein family<sup>28</sup>. As Noc can also interact with CTP and its membrane binding is regulated by CTP-binding and hydrolysis, we ought to test whether CTP also stabilizes Noc LLPS<sup>34</sup>. Intriguingly, addition of CTP greatly increases the turbidity, indicating an increase in phase separated material. Also, a non-CTP-binding mutant (R89A) is unable to phase separate and shows no turbidity in absence and presence of CTP (Fig. 1C). These experiments demonstrate that CTP-binding also regulates Noc phase separation.

Taken together, we show that Noc undergoes LLPS depending on the environmental conditions, and the formation of droplets is regulated by CTP binding. These findings are remarkably similar to the properties of other ParB-protein droplets. However, the Noc subfamily has significant functional differences to most ParB-like proteins. Noc can bind to membranes to regulate the formation of the Z-ring. This is in stark contrast to the DNA-binding and nucleoid positioning functionality of many ParB-family members. We therefore sought to investigate if these biological differences manifest in the phase behavior of Noc.

**Noc condensates interact with membranes.** While Noc and ParB share a common ancestry, their biological functionality greatly differs. This difference manifests in Noc's ability to bind the bacterial chromosome to the plasma membrane to create nucleoid occlusion<sup>38</sup>. Recently, the role of CTP binding and hydrolysis in Noc membrane binding has been unraveled, and shown similar mechanisms to ParB binding and spreading on DNA<sup>34,39</sup>. These similarities lead us to conclude that Noc condensates could interact with biological membranes, making it a powerful model system to study the interaction of protein condensates with lipid membranes.

Initially, we verified the functionality of our fluorescence labeling strategy by binding Atto488-Noc to the outer membrane of giant unilamellar vesicles (GUVs), which serve as model systems to mimic the cell membrane. As recently shown, only in the presence of specific DNA sequence (dsNBS oligo) and CTP, Noc binds to the membrane<sup>34</sup>. The CTP-binding mutant, R89A, which is also deficient of LLPS, is unable to bind to the membrane in the presence of dsNBS and CTP. Interestingly, Atto488-Noc<sup>R89A</sup> could be recruited to the membrane by addition of unlabeled wildtype Noc (Fig. 2A). This finding suggests that Noc can self-interact to recruit further molecules that are deficient of membrane binding, to the membrane. Similar self-interaction is a behavior often observed for phase separating proteins. To test if phase separated Noc interacts with membranes, we added 3  $\mu$ M of Noc to a chamber containing GUVs (Fig. 2B). Upon phase separation, wetting, diffusion and fusion of condensates on GUVs was observed (Supp. Movie). This indicates that the formed condensates not only preferentially interact with membranes but remain liquid-like while binding them. To gain more insight into the formation of condensates on membranes, we performed a titration of Noc to GUVs. Interestingly, at lower concentrations of Noc, we observed the formation of film-like structures on the GUVs, whereas higher concentrations of Noc lead to the formation of round 3D-condensates (Fig. 2C). The condensate formation on the surface is specific to membranes, as we could not observe droplets or domain-like structures on Ni-NTA Agarose beads that also bound Noc on the surface (Supp. Fig. 5).

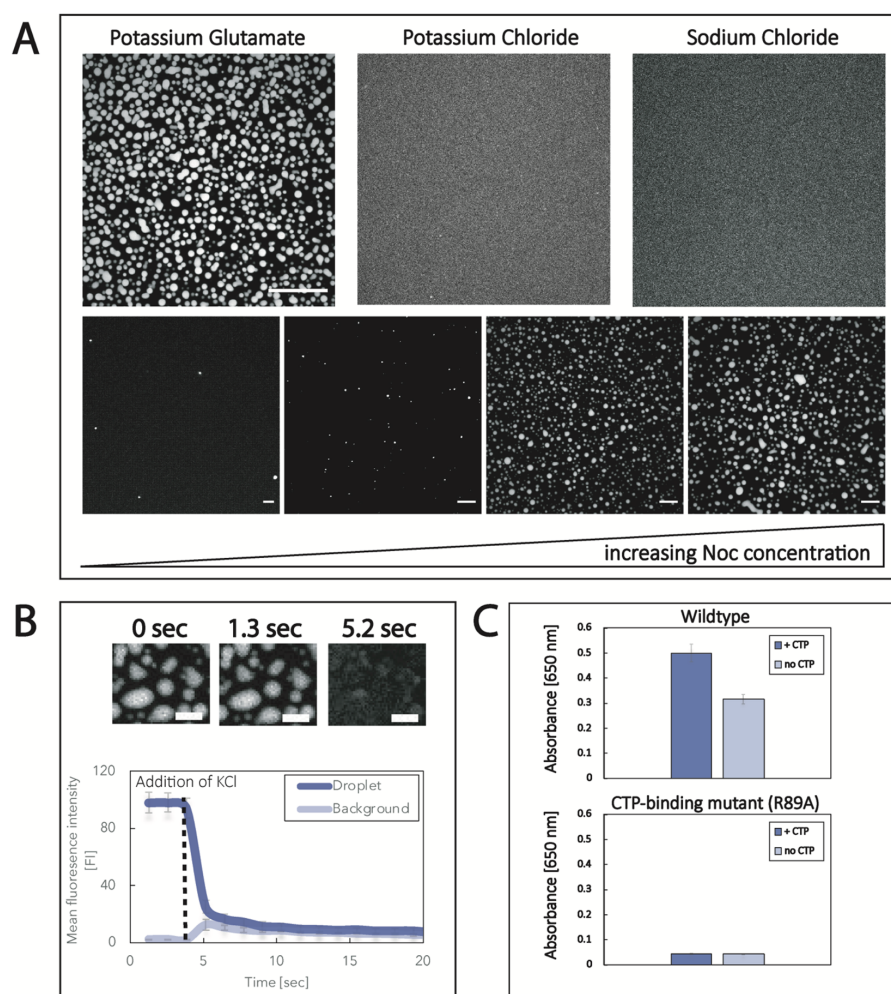


**Figure 1.** Noc undergoes liquid–liquid phase separation. **(A)** 8  $\mu\text{M}$  of Atto488-labeled Noc in different buffers (20 mM Tris pH 7.4, 150 mM KGlu, KCl or NaCl and 5 mM  $\text{MgCl}_2$ ). The scalebar is 30  $\mu\text{m}$ . Increase of concentration of Noc in KGlu-buffer leads to larger and more droplets. From left to right: 1  $\mu\text{M}$ , 2  $\mu\text{M}$ , 4  $\mu\text{M}$  and 8  $\mu\text{M}$ . The scalebar represents 20  $\mu\text{m}$ . **(B)** Dissolution of droplets after addition of 500 mM KCl. The droplets were formed in KGlu-buffer and after dissolution, 500 mM KCl were added which resulted in rapid dissolution of the Noc droplets. Protein concentration was 8  $\mu\text{M}$  and the scalebar represents 10  $\mu\text{m}$ . Error bars are the standard deviation of three different droplet and background regions of interests. **(C)** Turbidity data: 20  $\mu\text{M}$  of wildtype Noc was prepared in 20 mM Tris pH 7.4, 150 mM KGlu, 1 mM TCEP and 5 mM  $\text{MgCl}_2$  buffer and turbidity was measured with or without 1 mM CTP at 650 nm. Error bars represent the standard deviation of three replicates.

As Noc condensates are interacting with the inner, rather than the outer membrane *in vivo*<sup>40</sup>, we encapsulated Noc into water-in-oil droplets with a membrane monolayer. Interestingly, the encapsulation clearly leads to condensates wetting the inner membrane of the droplets and the formation of domain-like structures on the membrane, again demonstrating the preferential binding and phase separation of Noc on the membrane (Fig. 2D).

Taken together, these findings reveal that Noc condensates preferentially wet the surface of various membranes. Depending on the protein concentration, Noc can form film-like condensates or round 3D spheres on the membrane. When encapsulated into a membrane bound organelle, the condensates maximize the surface interaction with the membrane by wetting.

Biological membranes can vary immensely in composition, order and fluidity/flexibility<sup>41</sup>. We therefore sought to understand if membrane properties such as charge or flexibility alter Noc condensation. For this purpose, we introduced Noc to supported lipid bilayers (SLBs) as these allow more quantitative analysis of the formed droplets on the membrane.

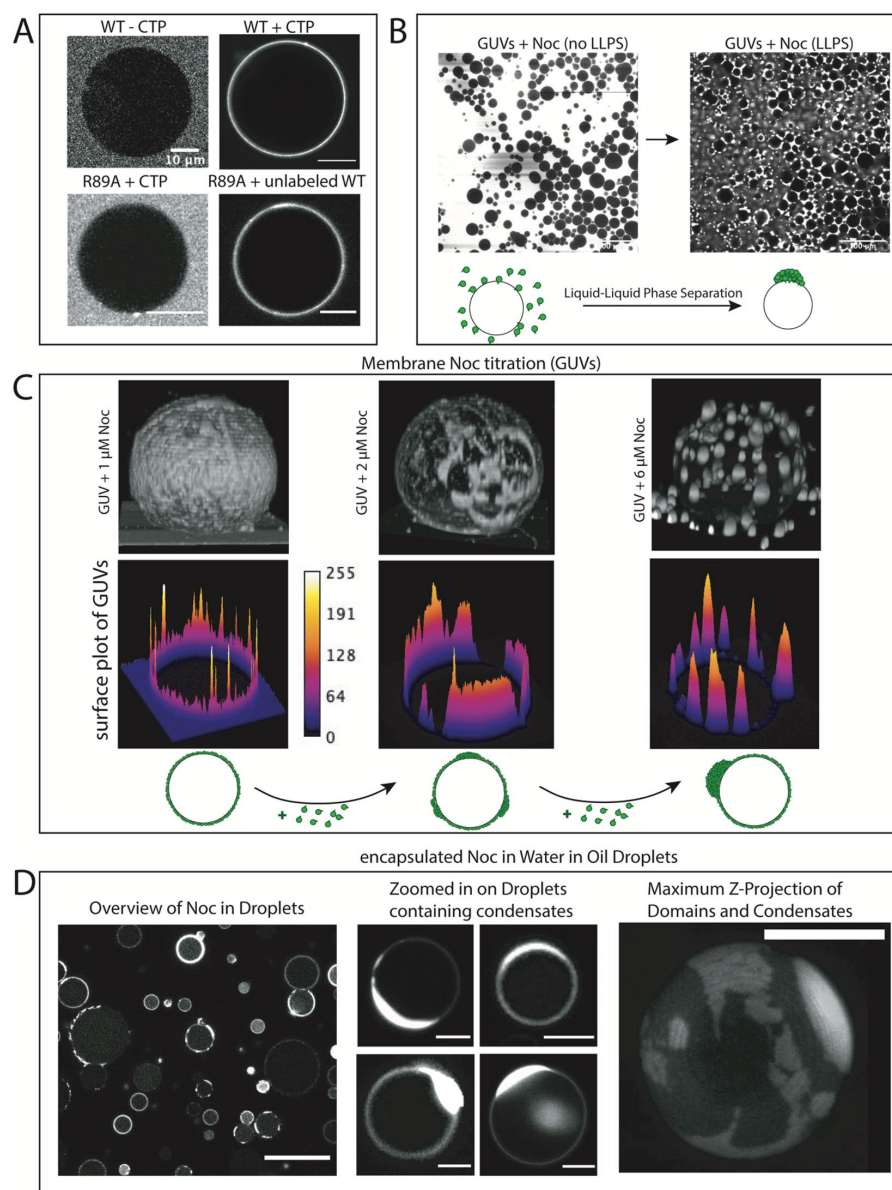


**Figure 2.** Noc condensates interact with membranes. **(A)** Noc and Noc mutants binding to GUVs (70 (POPC): 30 (POPG)). (1) 2  $\mu$ M of Atto-488 Noc in absence of CTP and dsNBS does not bind to a GUV. (2) 500 nM of Atto-488 Noc binding to a GUV (70 (POPC): 30 (POPG)) in presence of 1 mM CTP and 1.5  $\mu$ M dsNBS DNA in 20 mM Tris pH 7.4, 150 mM KGlu, 1 mM TCEP and 5 mM MgCl<sub>2</sub> buffer. (3) Atto488-Noc<sup>R89A</sup> mutant at 4  $\mu$ M in presence of 1 mM CTP and 1.5  $\mu$ M dsNBS does not bind to a GUV. (4) 3  $\mu$ M of WT Noc recruit Atto488-Noc<sup>R89A</sup> to the membrane. **(B)** Addition of 3  $\mu$ M Atto-488 Noc to a sample containing GUVs (70 (POPC): 30 (POPG)). Buffer composition is 20 mM Tris pH 7.4, 150 mM KGlu, 1 mM TCEP, 1 mM CTP, 2.5  $\mu$ M dsNBS and 5 mM MgCl<sub>2</sub>. The scale bar represents 100  $\mu$ m. **(C)** Titration of Noc in samples containing GUVs (70 (POPC): 30 (POPG)) in presence of 1 mM CTP and 2.5  $\mu$ M dsNBS. From left to right: 1  $\mu$ M, 2  $\mu$ M and 6  $\mu$ M Atto488-Noc. Images are reconstituted using ImageJ 3D Viewer plugin. **(D)** Encapsulation of Noc in water-in-oil droplets. An apparent concentration 80  $\mu$ M of Atto488-Noc was encapsulated in the water-in-oil droplets. However, the final concentration in the droplets is significantly lower, as Noc is partially lost during droplet encapsulation. Images on the left show an overview of several droplets. The middle image shows zoomed-in droplets with Noc condensates wetting the inside membrane. The image on the right shows a maximum Z-projection of an individual droplet containing a condensate and film-like structures. Scalebars represent 10  $\mu$ m.

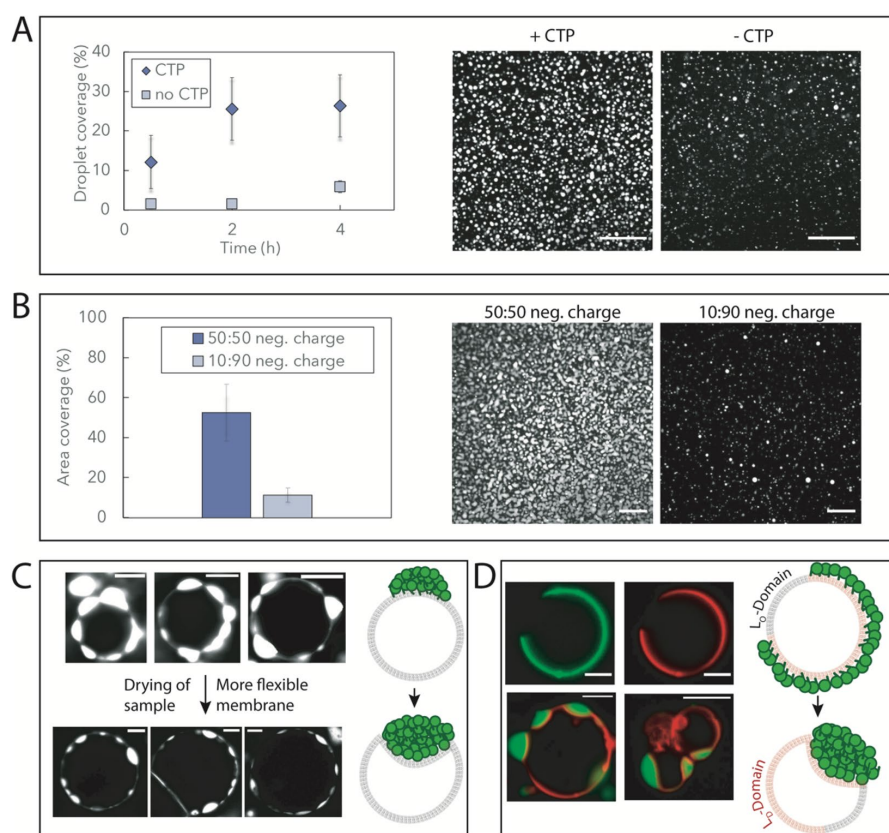


**Figure 3.** Noc condensates are influenced by membranes and can deform flexible membrane bilayers. **(A)** Droplet formation of Atto488-Noc on supported lipid bilayers (70:30 DOPC:DOPG) in presence and absence of CTP. The amount of phase separated material on the SLBs was monitored for 4 h. The area covered by droplets was calculated by thresholding the images and calculating the area fraction of the droplets. The images represent the amount of SLB coverage after 2 h and the scalebar is 50 μm. The protein concentration is 8 μM and the buffer is 20 mM Tris pH 7.4, 150 mM KGlu, 1 mM TCEP, 1 mM CTP, 2.5 μM dsNBS and 5 mM MgCl<sub>2</sub>. Error bars represent the standard deviation of three replicates. **(B)** Droplet formation of Atto488-Noc on supported lipid bilayers with different amounts of charged lipids (DOPG). The area covered by droplets was calculated by thresholding the images and calculating the area fraction of the droplets. The images represent the amount of SLB coverage after 2 h and the scalebar is 50 μm. The protein concentration is 16 μM and the buffer is 20 mM Tris pH 7.4, 150 mM KGlu, 1 mM TCEP, 1 mM CTP, 2.5 μM dsNBS and 5 mM MgCl<sub>2</sub>. Error bars represent the standard deviation of three replicates. **(C)** Noc condensates on GUVs (70:30 POPC:POPG) before and after drying the sample for 2 h. To allow evaporation of buffer, the oil layer above the buffer was removed. The protein concentration is 8 μM. The buffer is 20 mM Tris pH 7.4, 150 mM KGlu, 1 mM TCEP, 1 mM CTP, 2.5 μM dsNBS and 5 mM MgCl<sub>2</sub>. Scalebar 10 μm. **(D)** Noc condensates on phase-separated GUVs. The protein concentration is 2 μM (upper panel) and 12 μM (lower panel). The buffer is 20 mM Tris pH 7.4, 150 mM KGlu, 1 mM TCEP, 1 mM CTP, 2.5 μM dsNBS and 5 mM MgCl<sub>2</sub>. Scalebar 5 μm.

As Noc droplets also form in the absence of membrane binding (Fig. 1A), we compared a membrane bound to non-membrane bound state by adding CTP to the sample. We observed a significantly increased membrane coverage by phase separated droplets in the presence of CTP (Fig. 3A). While CTP generally stabilizes Noc phase separation, also in absence of a membrane, the measured difference between phase separated material in presence or absence CTP on SLBs is even higher than expected from the turbidity data (Fig. 1C) in bulk. It is therefore likely that membrane binding stabilizes the formation of Noc condensates.

Similarly, protein condensates are highly susceptible to changes in the direct electrostatic environment<sup>35</sup>. To test whether membranes can truly stabilize Noc LLPS, we prepared SLBs with different percentages of negatively charged lipids. Intriguingly, increasing the negative charge from 10 to 50% lead to a significant increase in phase separated material on the membrane (Fig. 3B). These findings provide evidence that membranes can alter the formation of condensates by affecting the immediate electrostatic environment.



This opens the question if vice versa, protein condensates can influence lipid membranes. For example, it has been demonstrated that protein condensates can cause GUV tubulation when artificially bound to the membrane, and synthetic aqueous two phase systems have been shown to cause membrane bending<sup>15,42</sup>. We therefore slowly dried GUV containing samples to cause an osmolar mismatch with the surrounding buffer. This mismatch creates more flexible membranes as water leaves the GUVs, lowering the bending rigidity of the membrane and making it more flaccid in nature. While Noc condensates on non-flexible membranes are clearly pointing outwards, upon drying the membrane becomes flexible and the condensates point into the GUVs (Fig. 3C).

To mimic more complex membrane compositions often found in vivo<sup>41,43</sup>, we performed similar experiments with membrane-phase separated GUVs to account for the presence of membrane rafts in the cells. Based on the lipid composition, GUVs partition into liquid-ordered ( $L_o$ ) and liquid-disordered ( $L_D$ ) domains. Interestingly, Noc was found to colocalize with the  $L_D$ -domains (red-colored), which are known to be more flexible. Upon increasing Noc concentration, Noc condensates were also only observed on the  $L_D$ -domains of the GUVs and clearly deformed the phase separated GUVs at high protein concentrations (Fig. 3D). This preferential binding to  $L_D$  domains potentially results from the higher fluidity of  $L_D$  domains as compared to the more rigid  $L_o$  domains, accumulating more protein and facilitating the phase transition at the  $L_D$  domains.

Thus, Noc condensation on membranes is influenced by the protein affinity towards the membrane, as well as the membrane's physical properties. Together with the film-like structures (Fig. 2) depending on Noc concentration, these findings point towards a surface mediated condensation for the assembly of Noc droplets on membranes. Once formed, Noc condensates can deform membranes similar to recent findings of tubule formation by protein phase separation on GUVs<sup>15</sup>.

**Noc condensates can recruit FtsZ to lipid membranes.** Last, we investigate the potential role of Noc condensates in *B. subtilis* nucleoid occlusion. The *E. coli* nucleoid occlusion factor SlmA has been shown to form liquid-like condensates which absorb FtsZ and hinder its polymerization<sup>33</sup>. The conservation of liquid condensate formation between SlmA and Noc is particularly intriguing, as the two proteins are not known to share similarities in mechanism and protein structure. While SlmA has been demonstrated to bind to FtsZ and alter its polymerization dynamics, Noc is thought to not or very weakly interact with FtsZ.

In accordance with previous findings<sup>40</sup>, we could not observe a relevant direct binding using labeled FtsZ and titrating Noc in microscale thermophoresis experiments. Using quartz crystal microbalance (QCM) experiments, we quantitatively compared membrane coverage in presence and absence of FtsZ and could not detect significant additional protein attachment in presence of *B. subtilis* FtsZ and Noc, compared to a control only containing Noc (Supp. Fig. 3). Also, FtsZ GTPase activity is not altered by titrating in Noc, in presence and absence of dsNBS DNA (Supp. Fig. 4). These findings demonstrate that Noc and FtsZ do most likely not or only weakly interact, and Noc does not recruit FtsZ to lipid bilayers in the non-phase separated state. However, it is known that biomolecular condensates can utilize weak (high  $\mu\text{M}$  to low mM  $K_D$ ) affinities to significantly up-concentrate molecules<sup>44</sup>. We therefore tested if Noc condensates can concentrate FtsZ, similar to the *E. coli* orthologue SlmA. Upon phase separation of Noc, strong partitioning of labeled FtsZ was observed (Fig. 4B). Similarly, non-membrane bound FtsZ was strongly partitioned into Noc droplets on GUVs (Fig. 4C). This is most likely a result of the high local Noc concentration, offering a plethora of interactions to FtsZ and therefore potentiating any weak interaction. In vivo, however, FtsZ is bound to the membrane by FtsA and SepF<sup>45–47</sup>. We therefore constructed a membrane-bound version of FtsZ (FtsZ-mScarlet-MTS) and measured its partitioning into Noc droplets on SLBs. Expectedly, the membrane-bound FtsZ, FtsZ-mScarlet-MTS, was also strongly up-concentrated within the membrane-bound Noc droplets (Fig. 4D). Interestingly, Noc droplets can also up-concentrate *E. coli* FtsZ, suggesting that the Noc-FtsZ interaction is located at the conserved regions of FtsZ (Supp. Fig. 6).

To summarize, we show that Noc in a non-phase separated state does not recruit or enrich FtsZ on the membrane, however upon phase separation it recruits FtsZ to the membrane. These findings are potentially pointing towards a regulative role of Noc LLPS in nucleoid occlusion, intriguingly in high similarity to the *E. coli* system<sup>33</sup>.

## Discussion

Self-organization of ParB-like proteins is an increasingly studied topic. A variety of members from this protein family have been shown to undergo liquid–liquid phase separation in vitro and in vivo<sup>27,28,48</sup>. We demonstrate that a functionally unrelated ParB-like protein, Noc, also undergoes LLPS. Intriguingly, the mechanism of regulation of phase separation appears to be conserved among the ParB-family members. Noc condensates physically interact with biological membranes, resulting in condensate and membrane deformations. Likewise, membrane composition and order can influence condensation. Lastly, we show that Noc condensates up-concentrate FtsZ in bulk and on membranes, pointing towards a regulatory mechanism of Noc condensation in Z-ring assembly.

The formation of liquid-like condensates is supposed to be a crucial mechanism in cellular compartmentalization<sup>8</sup>. While we know that protein evolution can impact on sequence, structure and function, it is not yet clear if similar mechanisms are in place for the phase properties of proteins. In eukaryotes, it has been hypothesized that an individual protein family, the DEAD-box helicases, regulates a large fraction of the biomolecular condensates found in vivo<sup>49</sup>. However, this protein family only has few prokaryotic members. We therefore recently suggested that the prokaryotic ParB protein family could serve a similar role in bacteria, as several of these proteins, or proteins with similar functionality, have been shown to undergo liquid–liquid phase separation<sup>28,50,51</sup>. To scrutinize this hypothesis, we purified the functionally unrelated ParB-like protein, Noc, and showed that this protein also undergoes LLPS. Intriguingly, Noc phase separation is also regulated by CTP, as previously shown for ParB. These similarities of phase properties and regulation thereof are an excellent example of the potential evolutionary conservation of LLPS within protein families.

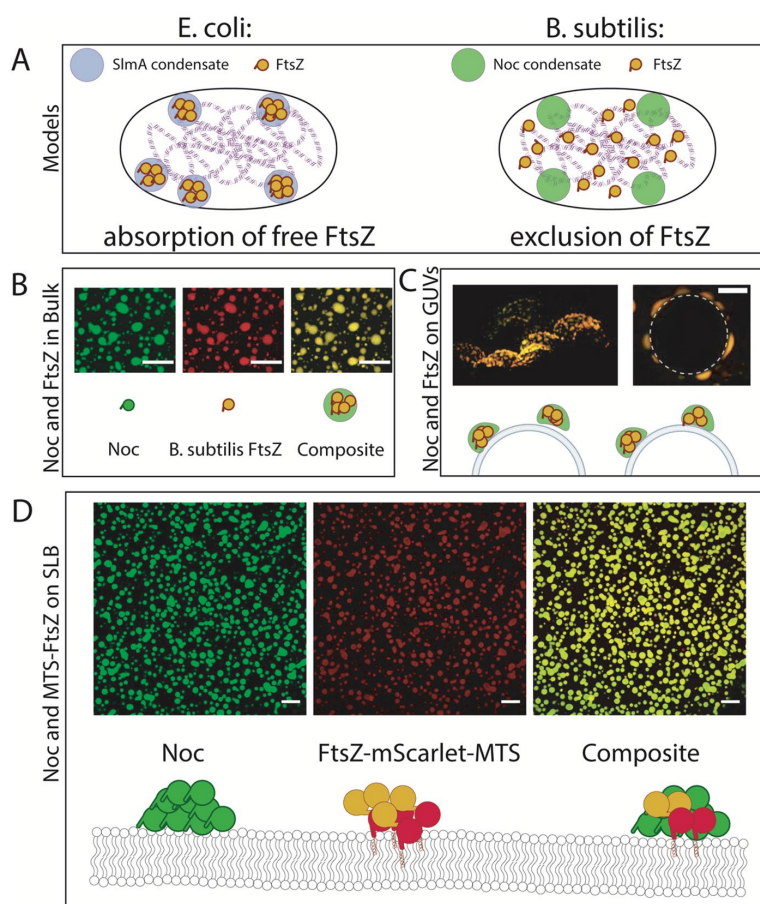


**Figure 4.** Noc condensates non-specifically up-concentrate FtsZ on the membrane and in bulk. **(A)** Current models of Nucleoid occlusion in *E. coli* (left) and *B. subtilis* (right). **(B)** Partitioning of *B. subtilis* FtsZ into Noc droplets in bulk. Left: 8  $\mu\text{M}$  Noc, 10  $\mu\text{M}$  *B. subtilis* FtsZ<sup>Alexa647</sup>. Buffer conditions: 50 mM Mes pH 6.5, 50 mM KCl, 10 mM MgCl<sub>2</sub>, 1 mM EDTA and 2 mM GTP. The scalebar represents 10  $\mu\text{m}$ . **(C)** Partitioning of *B. subtilis* FtsZ into Noc droplets on GUVs. 4  $\mu\text{M}$  Noc, 1  $\mu\text{M}$  FtsZ in 20 mM Tris pH 7.4, 150 mM KGLu, 5 mM MgCl<sub>2</sub>, 1 mM CTP and 2.5  $\mu\text{M}$  dsNBS. The GUVs consist of 70:30 POPC:POPG. Scalebar 10  $\mu\text{m}$ . **(D)** Partitioning of *B. subtilis* FtsZ-mScarlet-MTS on SLBs. Noc concentration is 5  $\mu\text{M}$  and 600 nM FtsZ-mScarlet-MTS. Buffer conditions: 50 mM Mes pH 6.5, 50 mM KCl, 10 mM MgCl<sub>2</sub>, 1 mM EDTA, 5 mM GTP, 1 mM CTP and 2.5  $\mu\text{M}$  dsNBS. The SLB consists of 70:30 DOPC:DOPG lipids. Scalebar 50  $\mu\text{m}$ .

However, a striking difference between Noc and ParB is Noc's N-terminal membrane binding helix. Through regulation by CTP hydrolysis and DNA binding, Noc can bind and spread on membranes<sup>34</sup>. This mechanism of binding and spreading is highly similar to ParB binding and spreading on DNA. These similarities led us to the conclusion that Noc condensates could interact with, and potentially be regulated by, lipid membranes. While recent advances related more biomolecular condensates with membrane binding, only few studies systematically investigate the influence of membranes on condensates, and vice versa<sup>12,15,20</sup>. Intriguingly, we found that membrane binding, membrane composition and membrane order can regulate the formation of condensates. These findings point towards a coupling of membrane- and protein phase separation, which likely plays a fundamental role in the organization of biological condensates in vivo. Also, forces generated by protein condensates acting on membranes have attracted attention and could be of broad interest, for example as recently shown for endocytosis<sup>32,33</sup>. The formation of film- or domain-like structures on GUVs and in water-in-oil droplets by Noc is highly similar to recent reports of phase separating proteins on membrane surfaces, where domain-like architectures were observed<sup>15,17</sup>. These findings indicate a wetting-like transition of Noc on the membrane, as recently shown for a DNA-binding protein<sup>54</sup> and studied theoretically<sup>23</sup>.

Taken together, we demonstrate that Noc readily forms condensates on a variety of model membranes, governed by liquid-liquid phase separation. We show that membrane properties such as charge or fluidity

alter the condensate formation. In accordance with recent reports of artificial coacervates bending and wetting membranes, we observe that Noc condensates generate forces on membranes, deforming and wetting a variety of model membranes. Therefore, Noc droplets represent a new and exciting class of biomolecular condensates, which not only interact with membrane-bound compartments but are also “out-of-equilibrium” through constant CTP-hydrolysis. We hope that the described findings will catalyze novel theoretical and experimental studies, advancing our understanding of out-of-equilibrium protein condensation on biological surfaces.

## Methods and materials

**Protein purification.** *Noc and Noc mutants.* Noc and its R89A mutant were purified as previously described<sup>34</sup>. In brief, protein was expressed in *E. coli* Rosetta (DE3) cells in LB medium at 37 °C supplemented with carbenicillin. Protein expression was induced at OD of ~0.6 after cooling the culture to 4 °C with 1 mM IPTG. Expression was continued for 3–4 h at 28 °C. Cells were spun down and lysed by sonication. The cell debris was removed through centrifugation at 28,000 g for 30 min at 4 °C. The lysate was then loaded into a 5-mL HisTrap column (GE Healthcare) that had been equilibrated with buffer A [100 mM Tris–HCl pH 8.0, 250 mM NaCl, 10 mM imidazole, and 5% (v/v) glycerol]. Protein was eluted from the column using an increasing gradient of imidazole (10–500 mM) in the same buffer. Noc-containing fractions were pooled together and diluted to a conductivity of 16 mS/cm before being loaded onto a 5-mL Heparin HP column (GE Healthcare) that had been equilibrated with 100 mM Tris–HCl pH 8.0, 25 mM NaCl, and 5% (v/v) glycerol. Protein was eluted from the Heparin column using an increasing gradient of NaCl (25 mM to 1 M) in the same buffer. Noc was further purified using a Superdex-75 gel filtration column (GE Healthcare). The gel filtration column was pre-equilibrated with buffer containing 10 mM Tris–HCl pH 8.0, 250 mM NaCl and 5 mM MgCl<sub>2</sub>. Eluted protein fractions were analyzed for purity by SDS-PAGE. Mutants were purified with the same protocol, for the KCK-tag variant for fluorescent labeling, TCEP (1 mM) was added prior to labeling and for storage.

*B. subtilis FtsZ.* The protein was purified as described elsewhere<sup>55,56</sup>. In brief, the protein was expressed in *E. coli* C41 (DE3) cells at 37 °C in LB medium to an OD<sub>600</sub> of 0.6. Expression of the protein was induced with 1 mM IPTG and the cells grown for another 4 h at 37 °C. Cells were harvested by centrifugation and washed with 50 mM Tris pH 8.8, 100 mM NaCl, 1 mM EDTA. Cells were lysed by three rounds of sonication in 50 mM Tris pH 8.8, 100 mM NaCl, 1 mM EDTA and lysate was cleared by spinning at 160,000g for 45 min at 4 °C. All subsequent steps were carried out at 4 °C. Protein was precipitated by slowly adding 0.43 equivalents of saturated Ammonium sulfate solution and incubation on ice for 20 min. Precipitates were separated by centrifugation at 10,000 g at 4 °C for 10 min. The supernatant was kept, and another 0.16 equivalents of Ammonium sulfate were slowly added. After another 20 min incubation on ice, the protein was spun down. The pellet was resuspended in 50 ml of 50 mM Tris pH 8.5, 50 mM KCl, 1 mM EDTA, 1% sucrose and loaded onto a GE HealthCare MonoQ 10/100 column. The protein was eluted by applying a gradient with 50 mM Tris pH 8.5, 500 mM KCl, 1 mM EDTA, 1% sucrose to the column. Protein was then dialyzed into 50 mM HEPES pH 7.5, 50 mM KCl, 2.5 mM MgCl<sub>2</sub>, 1 mM EGTA and 10% sucrose, frozen in liquid nitrogen and stored at –80 °C.

*E. coli FtsZ.* *E. coli* FtsZ purification: FtsZ was purified by following the calcium precipitation method previously described<sup>37</sup>. Briefly, FtsZ was expressed in C21 cells in LB medium at 37 °C. Protein expression was induced with IPTG for 3 h followed by centrifugation and lysis of the cells by sonication. Cell debris was removed by centrifugation at 50,000 g using an MLA 80 rotor at 4 °C for 1 h. FtsZ was polymerized by adding 1 mM GTP and 20 mM CaCl<sub>2</sub> to a buffer containing 50 mM PIPES 5 mM MgCl<sub>2</sub>, 1 mM EDTA<sub>KOH</sub> pH 6.5 followed by incubation for 15 min at 30 °C using a water bath. FtsZ Polymers were spun down at 16,000 g in ML-80 for 15 min at 4 °C and subsequently resuspended in buffer without GTP and CaCl<sub>2</sub>, disassembling the polymers into the FtsZ monomeric state. 1 mM GTP and 20 mM CaCl<sub>2</sub> was added again to promote FtsZ polymerization a second time. FtsZ was incubated at 30 °C for 15 min and FtsZ polymers were spun down and resuspended afterwards as described above. Resuspended FtsZ was centrifuged at 16,000 g for 15 min at 4 °C. The remaining supernatant was loaded onto a Hi-TRAP Q-Sepharose column and the protein was eluted from the column by using a gradient of KCl (25 mM–1 M). Fractions of FtsZ were pooled and frozen at –80 °C. FtsZ concentration and purity were measured by absorbance at 280 nm and SDS-PAGE respectively.

**Protein labeling.** *Noc Atto488 maleimide.* Atto488 maleimide was bought from SigmaAldrich (Cat. Nr. 28,562) KCK-tagged Noc was purified as described and cysteines reduced by addition of 1 mM TCEP. Labeling was achieved by following the manufacturer’s instruction. Labeling efficiency was determined to be ~20%.

*B. subtilis Alexa-Fluor 647 NHS Ester.* Protein was dialyzed into 20 mM HEPES pH 8.0, 1 mM EDTA, 50 mM KCl and 5 mM MgCl<sub>2</sub>. Protein concentration was adjusted to 250 μM and 350 μg Alexa-Fluor 647 NHS-Ester dissolved in DMSO were added. The sample was incubated at room temperature (22 °C) for 45 min. Free dye was separated by a gravity flow column (equilibrated in 50 mM Tris pH 7.9 50 mM KCl 10% Glycerol, 2.5 mM MgCl<sub>2</sub> and 1 mM EGTA). Fractions containing FtsZ were pooled and flash frozen in liquid nitrogen.

*E. coli NHS-647.* *E. coli* FtsZ was covalently labelled in the amine groups with Alexa 488 NHS ester as previously described<sup>58,59</sup>. FtsZ was labeled at its polymerized state by mixing FtsZ in presence of 1 mM GTP and 10 mM of CaCl<sub>2</sub> with a 1:4 molar excess of Alexa 488 dye for 15 min at 30 °C followed by ultracentrifugation for 15 min at 19,000 g to remove inactive protein. Labelled FtsZ polymers were resuspended in cold buffer to favor depolymerization and incubated for 20 min at 4 °C. Free dye was separated by a HiTrap Desalting column (GE

Healthcare). The degree of labeling of different fractions was estimated by absorbance and the protein was flash frozen at  $-80\text{ }^{\circ}\text{C}$  in 50 mM Tris-HCl, 150 mM KCl, 5 mM  $\text{MgCl}_2$ , and 10% Glycerol pH 7.5.

**Molecular cloning.** All constructs were designed and cloned using a seamless cloning strategy. In brief, vectors were linearized using indicated primers (Table S1) in a PCR (Phusion Polymerase (ThermoFisher Scientific Cat. No. F530L)). Following PCR, template was digested using DpnI (NEB) at  $37\text{ }^{\circ}\text{C}$  for 30 min. PCR products were visualized by agarose gel electrophoresis (agarose 0.8%, TAE, 120 V, 40 min), cut-out and purified using a QIAGEN gel extraction kit (Cat. No. 28704). Inserts were amplified by PCR using the appropriate primers (Table S1). Vector and insert were assembled by seamless cloning using the ThermoFisher Scientific/Invitrogen GeneArt™ Seamless Cloning and Assembly Enzyme Mix (A14606) and transformed into chemically competent OneShot Top10-cells (Cat. No. C404006). Selection for successful cloning was done on LB-Ampicillin or LB-Kanamycin plates. Cells were grown overnight at  $37\text{ }^{\circ}\text{C}$ . Then, individual clones were picked and grown overnight in LB media (5 ml) containing the appropriate antibiotic (Ampicillin or Kanamycin). Plasmids were purified by a Miniprep kit (Cat. No.27104) and sequenced to verify successful cloning.

**GUV preparation.** *Double emulsion (homogeneous GUVs).* Lipid vesicles were produced by the double emulsion method<sup>60</sup> with slight modifications. Briefly, 1-palmitoyl-2-oleoyl-glycero-3-phosphocholine (POPC) and 1-palmitoyl-2-oleoyl-sn-glycero-3-phospho-(1'-rac-glycerol) (POPG) (Avanti Polar Lipids, Alabaster, AL, USA) were mixed and dissolved in chloroform at different molecular ratios (70:30) with a final concentration of 25 g/L. For fluorescence visualization of the vesicle membrane, 0.005% of 1,2-dioleoyl-sn-glycero-3-phosphoethanolamine (DOPE) labelled with ATTO 655 (ATTO-Tech GmbH, Siegen, Germany) was included to the lipid mixture. 100  $\mu\text{L}$  of the lipid mixture was dried under  $\text{N}_2$  and re-dissolved in 25  $\mu\text{L}$  of decane (TCI Deutschland GmbH, Eschborn, Germany). 1 mL of mineral oil (Carl Roth GmbH, Karlsruhe, Germany) was supplemented to the mixture and thoroughly vortexed for  $\sim 1$  min. 50  $\mu\text{L}$  of this lipid-in-oil mixture was carefully added on top of 100  $\mu\text{L}$  of reaction buffer in a 96-Well Flat-Bottom Microplate (SensioPlate, Greiner Bio-One GmbH, Kremsmuenster, Austria) previously passivated with 5 g/l of casein for  $\sim 30$  min. This mixture was incubated for  $\sim 20$ –30 min to favor the formation of a lipidic monolayer. At the same time, the inner solution containing 30 mg/mL Ficoll and 10 mg/mL BSA suspended in reaction buffer was prepared. Subsequently, 2.5  $\mu\text{L}$  of inner solution was added to a 100  $\mu\text{L}$  of lipid-in-oil in a 1.5 mL Eppendorf tube and water-in-oil emulsion was formed by tipping the tube thoroughly. 80  $\mu\text{L}$  of this emulsion was then carefully dripped on top of the previously formed monolayer and subsequently centrifuged for 10 min at 1000 g to obtain lipid vesicles. After centrifugation, the 96 well-plate allowed the direct visualization of lipid vesicles on the confocal microscope.

*Electroformation (phase-separated GUVs).* Phase separated Giant Unilamellar Vesicles (GUVs) utilized throughout this work were prepared by electroformation in PTFE chambers with Pt electrodes, as previously described elsewhere with minor modifications<sup>61</sup>. The lipid composition chosen was DOPC:DOPG:DSPC:Cholesterol (40:20:20:20) doped with 0.1 mol% Atto655-DOPE to introduce phase separation and negative charge. Briefly, 6  $\mu\text{L}$  of the lipid mixture (2 mg  $\text{mL}^{-1}$  in chloroform) was spread onto two Pt wires to make a thin film and dried in a desiccator for 30 min. The PTFE chamber was filled with 350  $\mu\text{L}$  of an aqueous solution of sucrose with approximate 340  $\text{mOsm kg}^{-1}$  osmolarity (iso-osmolar compared to the imaging buffer). While keeping the PTFE chambers at  $60\text{ }^{\circ}\text{C}$ , an AC electric field of 2 V (RMS) was applied at a frequency of 10 Hz for 1 h, followed by 2 Hz for 0.5 h. The chambers were allowed to cool down to room temperature before performing any experiments.

**Water-in-oil droplets.** A mixture of lipids for a final volume of 500  $\mu\text{L}$  (70:30 DOPC:DOPG; 0.01% ATTO655-DOPE) was prepared at a concentration of 1.5 mg/ml and dried under nitrogen. 10  $\mu\text{L}$  of Decane was added and the solution was vortexed until a turbid solution was achieved. 500  $\mu\text{L}$  of mineral oil was added and aliquoted in  $5 \times 100\text{ } \mu\text{L}$ . 1  $\mu\text{L}$  of inner solution containing 20 mM Tris pH 7.4 150 mM KGLu, 5 mM  $\text{MgCl}_2$ , 1 mM CTP, 1 mM TCEP and 1.5  $\mu\text{M}$  dsNBS plus the appropriate Noc-Atto488 concentration was added. Droplet formation was achieved by thoroughly vortexing the sample. Imaging was done in 96-Well Flat-Bottom Microplate (SensioPlate, Greiner Bio-One GmbH, Kremsmuenster, Austria) previously passivated with 5 g/l of casein for  $\sim 30$  min.

**Supported lipid bilayer (SLB) preparation.** SLBs were formed via vesicle fusion. Coverslips were rinsed with ethanol and distilled water, and surface-etched with oxygen plasma (30 s at 0.3 mbar, Zepto, Diener Electronics). Lipids dissolved in chloroform were mixed in glass vials, and after evaporation of the solvent under a gentle  $\text{N}_2$  stream, the lipids were re-suspended in SLB formation buffer (25 mM tris, 150 mM KCl, 5 mM  $\text{MgCl}_2$ , pH 7.5) to 4  $\mu\text{g}/\mu\text{L}$ , and vortex until the lipid films are completely resuspended, forming a cloudy solution containing Multilamellar Vesicles (MLVs) of various sizes. The obtained large multilamellar vesicle suspensions were then sonicated until solutions were clear. These small unilamellar vesicle solutions were either stored at  $-20\text{ }^{\circ}\text{C}$  and re-sonicated before use or used immediately. The sonicated small unilamellar vesicle solutions diluted to ca. 0.5  $\mu\text{g}/\mu\text{L}$  in SLB formation buffer were added into liquid chambers pre-warmed to  $37\text{ }^{\circ}\text{C}$ , filling the chamber. After 5 min incubation at  $37\text{ }^{\circ}\text{C}$ , liquid chambers now containing SLBs were washed with  $10 \times 200\text{ } \mu\text{L}$  SLB washing buffer (25 mM Tris pH 7.5, 150 mM KCl).

**QCM-D.** Prior to each measurement, silicon dioxide ( $\text{SiO}_2$ )-coated quartz crystal sensors (Biolin Scientific, Gothenburg, Sweden) were treated with a 3:1 mixture of sulfuric acid and hydrogen peroxide (piranha-solution). Subsequently, sensors were rinsed with ultrapure water, dried under a stream of nitrogen, and mounted in the

flow modules of the Qsense Analyzer (Biolin Scientific, Gothenburg, Sweden). After baseline stabilization, supported lipid bilayer formation (SLB) was induced through constant injection (flow rate: 0.15 mL/min) of a 1 mg/mL mixture of small unilamellar vesicles (DOPC/DOPC, 70:30 mol %) in buffer (25 mM Tris- HCl pH 7.5, 150 mM KCl, 5 mM MgCl<sub>2</sub>), spiked with 5 mM CaCl<sub>2</sub>. The formed bilayer was washed with buffer until no frequency change was observed. Then, 150 µl of sample was flown over the sensor at 0.1 ml/min and the change in frequency monitored at overtone F9.

**Turbidity.** 80 µl of sample were prepared by mixing protein with the buffer containing crowding agents and molecules of interest in 384 Greiner Black Flat Plates. After 10 min of incubation, turbidity was measured using a TECAN plate reader at room temperature at 650 nm.

**Microscopy.** All images were taken on a Zeiss LSM780 confocal laser scanning microscope using a Zeiss C-Apochromat × 40/1.20 water-immersion objective (Carl Zeiss). Longer time series were acquired using the built-in autofocus system. Noc Atto 488 was excited using a 488 nm argon laser and FtsZ-Alexa 647 using a 633 nm He-Ne laser. Images were typically recorded with a pinhole size of 2.6–4 Airy units for the channels 512 × 512-pixel resolution and a pixel dwell time of 1.27 µs. Line-averaging was set to 2. Images were analysed in ImageJ<sup>62</sup>.

Received: 11 July 2022; Accepted: 18 October 2022

Published online: 26 October 2022

## References

1. Toro-Nahuelpan, M. *et al.* MamY is a membrane-bound protein that aligns magnetosomes and the motility axis of helical magnetotactic bacteria. *Nat. Microbiol.* **4**, 1978–1989 (2019).
2. Hyman, A. A., Weber, C. A. & Jülicher, F. Liquid-liquid phase separation in biology. *Annu. Rev. Cell Dev. Biol.* **30**, 39–58 (2014).
3. Shin, Y. & Brangwynne, C. P. Liquid phase condensation in cell physiology and disease. *Science* <https://doi.org/10.1126/science.aaf4382> (2017).
4. Nott, T. J. *et al.* Phase transition of a disordered nuage protein generates environmentally responsive membraneless organelles. *Mol. Cell* **57**, 936–947 (2015).
5. Peebles, W. & Rosen, M. K. Mechanistic dissection of increased enzymatic rate in a phase-separated compartment. *Nat. Chem. Biol.* **17**, 693–702 (2021).
6. Protter, D. S. W. & Parker, R. Principles and properties of stress granules. *Trends Cell Biol.* **26**, 668–679 (2016).
7. Feric, M. *et al.* Coexisting liquid phases underlie nucleolar subcompartments. *Cell* **165**, 1686–1697 (2016).
8. Hyman, A. A., Weber, C. A. & Jülicher, F. Liquid-liquid phase separation in biology. *Annu. Rev. Cell Dev. Biol.* <https://doi.org/10.1146/annurev-cellbio-100913-013325> (2014).
9. Azaldegui, C. A., Vecchiarelli, A. G. & Biteen, J. S. The emergence of phase separation as an organizing principle in bacteria. *Biophys. J.* <https://doi.org/10.1016/j.bpj.2020.09.023> (2020).
10. Zeng, M. *et al.* Phase transition in postsynaptic densities underlies formation of synaptic complexes and synaptic plasticity. *Cell* **166**, 1163–1175.e12 (2016).
11. Milovanovic, D., Wu, Y., Bian, X. & De Camilli, P. A liquid phase of synapsin and lipid vesicles. *Science* **361**, 604–607 (2018).
12. Kusumaatmaja, H., May, A. I. & Knorr, R. L. Intracellular wetting mediates contacts between liquid compartments and membrane-bound organelles. *J. Cell Biol.* **220**, 1–10 (2021).
13. Wu, X. *et al.* RIM and RIM-BP form presynaptic active-zone-like condensates via phase separation. *Mol. Cell* **73**, 971–984 (2019).
14. Wu, X. *et al.* Vesicle tethering on the surface of phase-separated active zone condensates. *Mol. Cell* **81**, 13–24 (2021).
15. Yuan, F. *et al.* Membrane bending by protein phase separation. *Proc. Natl. Acad. Sci. U. S. A.* **118**, e2017435118 (2021).
16. Li, P. *et al.* Phase transitions in the assembly of multivalent signalling proteins. *Nature* **483**, 336–340 (2012).
17. Case, L. B., Ditlev, J. A. & Rosen, M. K. Regulation of transmembrane signaling by phase separation. *Annu. Rev. Biophys.* **48**, 465–494 (2019).
18. Zhao, Y. G. & Zhang, H. Phase separation in membrane biology: The interplay between membrane-bound organelles and membraneless condensates. *Dev. Cell* **55**, 30–44 (2020).
19. Nesterov, S. V., Ilyinsky, N. S. & Uversky, V. N. Liquid-liquid phase separation as a common organizing principle of intracellular space and biomembranes providing dynamic adaptive responses. *Biochim. Biophys. Acta Mol. Cell Res.* **1868**, 119102 (2021).
20. Botterbusch, S. & Baumgart, T. Interactions between phase-separated liquids and membrane surfaces. *Appl. Sci.* **11**, 1–16 (2021).
21. Snead, W. T. & Gladfelter, A. S. The control centers of biomolecular phase separation: How membrane surfaces, PTMs, and active processes regulate condensation. *Mol. Cell* **76**, 295–305 (2019).
22. Voronina, E., Seydoux, G., Sassone-Corsi, P. & Nagamori, I. RNA granules in germ cells. *Cold Spring Harb. Perspect. Biol.* **3**, (2011).
23. Zhao, X., Bartolucci, G., Honigsmann, A., Jülicher, F. & Weber, C. A. Thermodynamics of wetting, prewetting and surface phase transitions with surface binding. *New J. Phys.* **23**, 123003 (2021).
24. Helfrich, M. R., Mangeney-Slavin, L. K., Long, M. S., Djoko, K. Y. & Keating, C. D. Aqueous phase separation in giant vesicles. *J. Am. Chem. Soc.* **124**, 13374–13375 (2002).
25. Long, M. S., Jones, C. D., Helfrich, M. R., Mangeney-Slavin, L. K. & Keating, C. D. Dynamic microcompartmentation in synthetic cells. *Proc. Natl. Acad. Sci. U. S. A.* **102**, 5920–5925 (2005).
26. Long, M. S., Cans, A. S. & Keating, C. D. Budding and asymmetric protein microcompartmentation in giant vesicles containing two aqueous phases. *J. Am. Chem. Soc.* **130**, 756–762 (2008).
27. Guilhas, B. *et al.* ATP-driven separation of liquid phase condensates in bacteria. *Mol. Cell* <https://doi.org/10.1016/j.molcel.2020.06.034> (2020).
28. Babl, L. *et al.* CTP-controlled liquid-liquid phase separation of ParB. *J. Mol. Biol.* **434**, 167401 (2022).
29. Merino-Salomón, A., Babl, L. & Schwille, P. Self-organized protein patterns: The MinCDE and ParABS systems. *Curr. Opin. Cell Biol.* **72**, 106–115 (2021).
30. Wu, L. J. & Errington, J. Coordination of cell division and chromosome segregation by a nucleoid occlusion protein in *Bacillus subtilis*. *Cell* **117**, 915–925 (2004).
31. Wu, L. J. *et al.* Noc protein binds to specific DNA sequences to coordinate cell division with chromosome segregation. *EMBO J.* **28**, 1940–1952 (2009).

32. Adams, D. W., Wu, L. J. & Errington, J. Nucleoid occlusion protein Noc recruits DNA to the bacterial cell membrane. *EMBO J.* **34**, 491–501 (2015).
33. Monterroso, B. *et al.* Bacterial FtsZ protein forms phase-separated condensates with its nucleoid-associated inhibitor SlmA. *EMBO Rep.* **20**, 1–13 (2019).
34. Jalal, A. S. B. *et al.* CTP regulates membrane-binding activity of the nucleoid occlusion protein Noc. *Mol. Cell* **81**, 3623–3636 (2021).
35. Crabtree, M. D. *et al.* Repulsive electrostatic interactions modulate dense and dilute phase properties of biomolecular condensates. *bioRxiv* 2020–10 (2021).
36. Harami, G. M. *et al.* Phase separation by ssDNA binding protein controlled via protein-protein and protein-DNA interactions. *Proc. Natl. Acad. Sci. U. S. A.* **117**, 26206–26217 (2020).
37. Kozlov, A. G. *et al.* How Glutamate promotes liquid-liquid phase separation and DNA binding cooperativity of *E. coli* SSB protein. *J. Mol. Biol.* **434**(9). <https://doi.org/10.1016/j.jmb.2022.167562>. (2022).
38. Jalal, A. S. B. *et al.* Diversification of DNA-binding specificity by permissive and specificity-switching mutations in the ParB/Noc protein family. *Cell Rep.* **32**, 107928 (2020).
39. Jalal, A. S. *et al.* A ctp-dependent gating mechanism enables parB spreading on dna. *Elife* **10**, 1–29 (2021).
40. Adams, D. W., Wu, L. J. & Errington, J. Nucleoid occlusion protein Noc recruits DNA to the bacterial cell membrane. *EMBO J.* **34**, 491–501 (2015).
41. Gohrbandt, M. *et al.* Low membrane fluidity triggers lipid phase separation and protein segregation in living bacteria. *EMBO J.* **41**, 1–21 (2022).
42. Li, Y., Kusumaatmaja, H., Lipowsky, R. & Dimova, R. Wetting-induced budding of vesicles in contact with several aqueous phases. *J. Phys. Chem. B* **116**, 1819–1823 (2012).
43. Bramkamp, M. Fluidity is the way to life: Lipid phase separation in bacterial membranes. *EMBO J.* <https://doi.org/10.15252/embj.2022110737> (2022).
44. Banani, S. F. *et al.* Compositional control of phase-separated cellular bodies. *Cell* **166**, 651–663 (2016).
45. Duman, R. *et al.* Structural and genetic analyses reveal the protein SepF as a new membrane anchor for the Z ring. *Proc. Natl. Acad. Sci. U. S. A.* **110**, E4601–E4610 (2013).
46. Jensen, S. O., Thompson, L. S. & Harry, E. J. Cell division in *Bacillus subtilis*: FtsZ and FtsA association is Z-ring independent, and FtsA is required for efficient midcell Z-ring assembly. *J. Bacteriol.* **187**, 6536–6544 (2005).
47. Pichoff, S. & Lutkenhaus, J. Tethering the Z ring to the membrane through a conserved membrane targeting sequence in FtsA. *Mol. Microbiol.* **55**, 1722–1734 (2005).
48. MacCready, J. S., Basalla, J. L., Vecchiarelli, A. G. & Echave, J. Origin and evolution of carboxysome positioning systems in cyanobacteria. *Mol. Biol. Evol.* **37**, 1434–1451 (2020).
49. Hondele, M. *et al.* DEAD-box ATPases are global regulators of phase-separated organelles. *Nature* **573**, 144–148 (2019).
50. MacCready, J. S., Basalla, J. L., Vecchiarelli, A. G. & Echave, J. Origin and evolution of carboxysome positioning systems in cyanobacteria. *Mol. Biol. Evol.* **37**, 1434–1451 (2020).
51. Merino-Salomón, A., Babl, L. & Schwille, P. Self-organized protein patterns: The MinCDE and ParABS systems. *Curr. Opin. Cell Biol.* **72**, 106–115 (2021).
52. Day, K. J. *et al.* Liquid-like protein interactions catalyse assembly of endocytic vesicles. *Nat. Cell Biol.* **23**, 366–376 (2021).
53. Bergeron-Sandoval, L. P. *et al.* Endocytic proteins with prion-like domains form viscoelastic condensates that enable membrane remodeling. *Proc. Natl. Acad. Sci. U. S. A.* **118**, e2113789118 (2021).
54. Morin, J. A. *et al.* Sequence-dependent surface condensation of a pioneer transcription factor on DNA. *Nat. Phys.* **18**, 271–276 (2022).
55. Buske, P. J. & Levin, P. A. A flexible C-terminal linker is required for proper FtsZ assembly in vitro and cytokinetic ring formation in vivo. *Mol. Microbiol.* **89**, 249–263 (2013).
56. Buske, P. J. & Levin, P. A. Extreme C terminus of bacterial cytoskeletal protein FtsZ plays fundamental role in assembly independent of modulatory proteins. *J. Biol. Chem.* **287**, 10945–10957 (2012).
57. Rivas, G. *et al.* Magnesium-induced linear self-association of the FtsZ bacterial cell division protein monomer. The primary steps for FtsZ assembly. *J. Biol. Chem.* **275**, 11740–11749 (2000).
58. González, J. M. *et al.* Essential cell division protein FtsZ assembles into one monomer-thick ribbons under conditions resembling the crowded intracellular environment. *J. Biol. Chem.* **278**, 37664–37671 (2003).
59. Reija, B. *et al.* Development of a homogeneous fluorescence anisotropy assay to monitor and measure FtsZ assembly in solution. *Anal. Biochem.* **418**, 89–96 (2011).
60. Pautot, S., Frisken, B. J. & Weitz, D. A. Engineering asymmetric vesicles. *Proc. Natl. Acad. Sci. U. S. A.* **100**, 10718–10721 (2003).
61. García-Sáez, A. J., Carrer, D. C. & Schwille, P. Fluorescence correlation spectroscopy for the study of membrane dynamics and organization in giant unilamellar vesicles. In *BT-Liposomes: Methods and Protocols, Volume 2: Biological Membrane Models* (ed. Weissig, V.) 493–508 (Humana Press, 2010).
62. Schindelin, J. *et al.* Fiji: An open-source platform for biological-image analysis. *Nat. Methods* **9**(7), 676–682 (2012).

## Acknowledgements

The authors thank Kerstin Andersson, Katharina Nakel and Michaela Schaper for excellent technical assistance, as well as the Biophysical Core Facility of the MPI Biochemistry for support with thermophoresis measurements. We furthermore acknowledge Tung Le and Adam Jalal at the John Innes Centre for supplying Noc expression plasmids and discussions, and Jeffrey Errington and Ling Juan Wu at Newcastle University for helpful discussions. LB is a member of the Max Planck School “Matter to Life” supported by the German Federal Ministry of Education and Research (BMBF) in collaboration with the Max Planck Society. This research was supported by the Deutsche Forschungsgemeinschaft within the Transregio Collaborative Research Center (TRR 174) Spatiotemporal Dynamics of Bacterial Cells. A. M.-S. is part of IMPRS-LS.

## Author contributions

L.B. Conceptualization, Investigation, Methodology, Validation, Data Curation, Writing—Original Draft. A.M. Methodology, Data Curation. N.K. Methodology. P.S. Conceptualization, Writing—Original Draft, Writing—Review & Editing, Supervision, Funding acquisition.

## Funding

Open Access funding enabled and organized by Projekt DEAL.

## Competing interests

The authors declare no competing interests.

### Additional information

**Supplementary Information** The online version contains supplementary material available at <https://doi.org/10.1038/s41598-022-22680-5>.

**Correspondence** and requests for materials should be addressed to P.S.

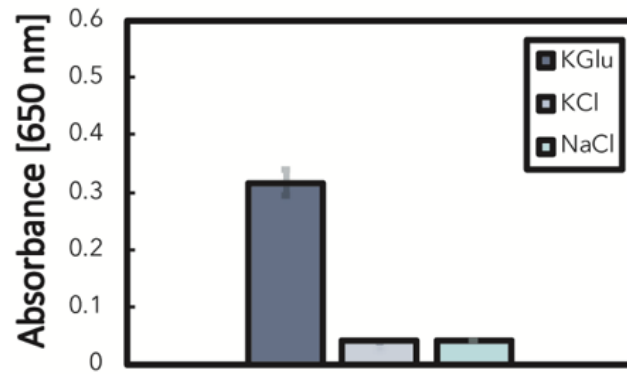
**Reprints and permissions information** is available at [www.nature.com/reprints](http://www.nature.com/reprints).

**Publisher's note** Springer Nature remains neutral with regard to jurisdictional claims in published maps and institutional affiliations.

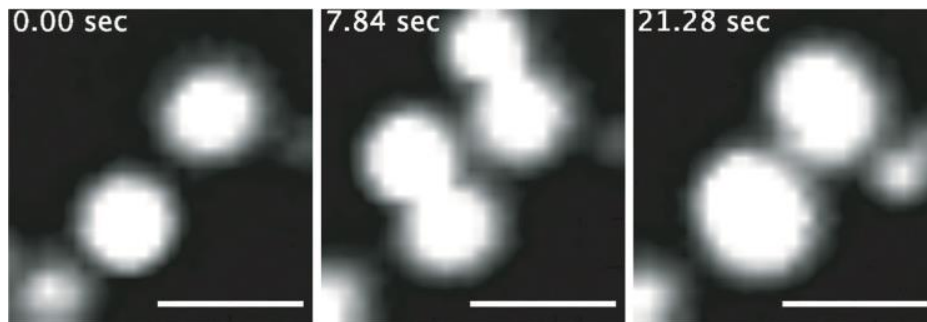


**Open Access** This article is licensed under a Creative Commons Attribution 4.0 International License, which permits use, sharing, adaptation, distribution and reproduction in any medium or format, as long as you give appropriate credit to the original author(s) and the source, provide a link to the Creative Commons licence, and indicate if changes were made. The images or other third party material in this article are included in the article's Creative Commons licence, unless indicated otherwise in a credit line to the material. If material is not included in the article's Creative Commons licence and your intended use is not permitted by statutory regulation or exceeds the permitted use, you will need to obtain permission directly from the copyright holder. To view a copy of this licence, visit <http://creativecommons.org/licenses/by/4.0/>.

© The Author(s) 2022

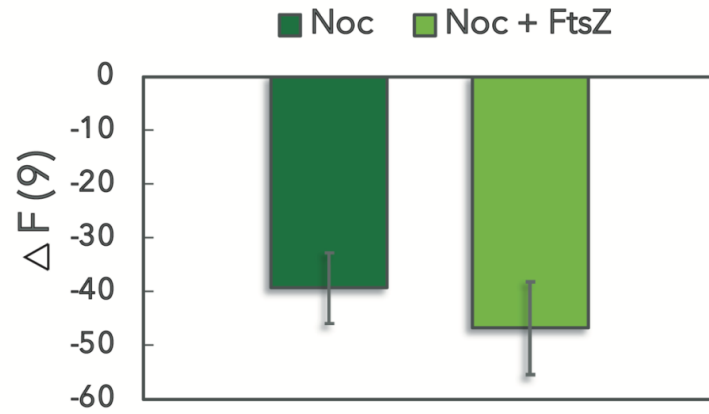


Suppl. Figure 1: Turbidity of Noc in different salts. 20  $\mu$ M wildtype Noc was introduced into 20 mM Tris pH 7.4 with either 150 mM KClu, KCl or NaCl with 5 mM  $MgCl_2$  and turbidity was measured at 650 nm. Error bars represent the standard deviation of three replicates.

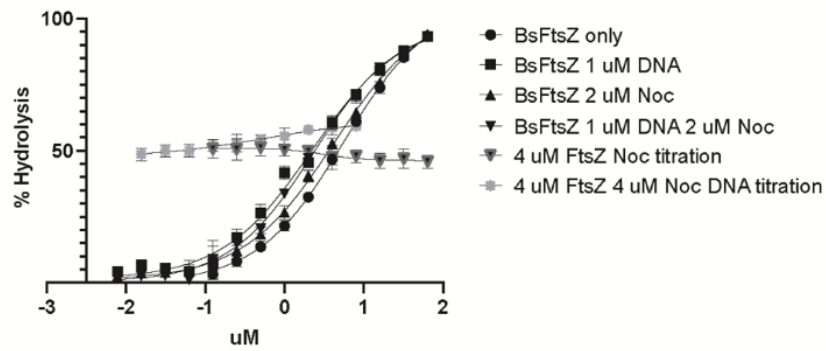


Suppl. Figure 2: Fusion of Noc droplets. The scalebar represents 5  $\mu$ m.

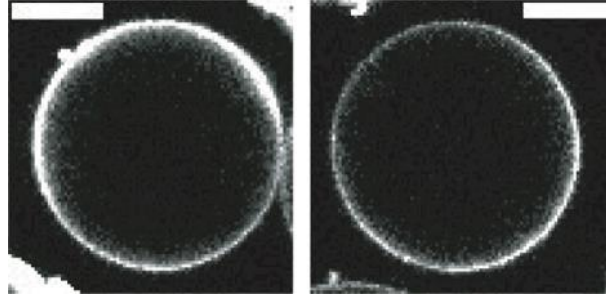




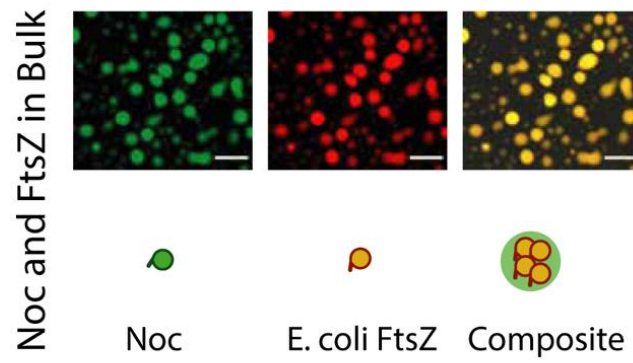
Suppl. Figure 3: Comparison of QCM frequency shift between Noc and Noc + FtsZ binding to a supported lipid bilayer. Protein concentrations were 5  $\mu\text{M}$  Noc and 6  $\mu\text{M}$  FtsZ. The buffer contained 50 mM Tris pH 7.4, 150 mM KCl, 5 mM MgCl<sub>2</sub>, 5  $\mu\text{M}$  dsNBS, 1 mM CTP and 1 mM GTP. Error bars represent the standard deviation of three replicates. The difference between Noc and Noc + FtsZ is not statistically significant (two-tailed t-test).



Suppl. Figure 4: GTPase activity of *B. subtilis* FtsZ in presence of Noc, dsNBS and Noc + dsNBS. No significant difference in hydrolysis rate is observed for all tested scenarios. Either Noc was titrated into the solution and FtsZ concentration was kept constant, or FtsZ was titrated, and Noc/DNA concentration was maintained constant.



Suppl. Figure 5: Ni-NTA Agarose beads with Noc ( $3 \mu\text{M}$ ) bound to the surface do not show condensates on the beads.



Suppl. Figure 6: Partitioning of *E. coli* FtsZ into Noc droplets in bulk  $8 \mu\text{M}$  Noc,  $5 \mu\text{M}$  *E. coli* FtsZAlexa647  $20 \text{ mM}$  Tris pH 7.4,  $150 \text{ mM}$  KGlu,  $5 \text{ mM}$  MgCl<sub>2</sub> and  $2 \text{ mM}$  GTP. Scalebar  $10 \mu\text{m}$ .

# Discussion and perspectives

Herein, I want to revisit the main findings of this thesis. First, I established the liquid-liquid phase separation of *C. glutamicum* ParB by *in vitro* reconstitution of the bacterial partition complex. This allowed me to identify the regulative mechanisms governing ParBs nucleation and partition complex size by DNA and CTP-binding. I then went on to understand if the phase behavior of ParB is an evolutionary conserved mechanism. To this end, I purified and characterized two other ParB homologues from different bacteria, namely *C. crescentus* and *T. thermophilus*, their potential phase behavior.

Intriguingly, both tested proteins showed similar liquid-liquid phase separation. Also, both proteins phase separated more readily in the presence of CTP, pointing towards an evolutionary conservation, not only of the principle phase behavior, but also its regulative mechanism. While this evolutionary conservation is intriguing, the actual differences between *C. glutamicum*, *C. crescentus* and *T. thermophilus* ParBs are rather small. They fulfil similar functions within the cell and share relatively high sequence similarities.

The ParB protein family however, offers an orthologue which allowed me to put the conservation of the phase behavior to test. The nucleoid occlusion protein Noc is primarily a membrane binding protein, which targets the bacterial nucleoid to the plasma membrane to prevent premature cell division. Therefore, this protein is functionally unrelated to other ParB protein family members, which are mostly responsible for genome or plasmid segregation. I could therefore put the hypothesis from P2 in P3 to a rigorous test.

In P2, I found that ParB can undergo a liquid-liquid phase separation *in vitro* as previously speculated by *in silico* analysis and *in vivo* imaging. I found that DNA in general, and the physiological binding site of ParB, parS, more specifically enhance ParB's propensity to phase separate *in vitro*. Together with a collaboration partner, we confirmed this finding *in vivo* using super resolution microscopy. While parS binding can dictate the nucleation site of ParB phase separation, the cell cannot control the amount of phase separated material. I therefore looked for a more precise regulative mechanism of ParB

phase separation.

The recently discovered CTPase activity of ParB is a likely candidate, as it is thought to control partition complex size and ParB diffusion on DNA [118, 119, 120]. Indeed, CTP-binding readily stabilized ParB's phase separation, lowering the saturation concentration necessary for droplet formation. A mutation of the CTP-binding site, abolishing CTPase activity, leads to a loss of this regulative mechanism. Also, ATP, as previously described for eukaryotic phase separating proteins, destabilizes the phase separation [132]. Using mass photometry and DLS measurements, I found that CTP binding leads to the formation of higher order ParB oligomers, which likely stabilizes the phase separation. Similar processes of dilute phase oligomerization have since been described for varying other phase separating proteins [133, 134, 135, 136].

Evolutionary conservation of membraneless organelle regulation and properties is an exciting, but not well understood topic. Bacteria, in contrast to eukaryotes, offer a plethora of phylogenetic differences among the many species. As the ParB protein family is part of most bacterial genomes, I was able to test the conservation of the characterized phase behavior in close and distant relatives of *C. glutamicum* ParB. For this purpose, I purified the previously characterized *T. thermophilus* and *C. crescentus* ParBs. These proteins are thought to fulfill similar tasks to *C. glutamicum* ParB and share relatively high sequence similarity. Upon exposure to molecular crowding, both proteins formed liquid-like droplets. While the saturation concentrations differed between the homologues, their response to changes in the ionic strength of the surrounding environment was highly similar. Also, I found that CTP, like for *C. glutamicum* ParB, stabilized the liquid-liquid phase separation of the *C. crescentus* and *T. thermophilus* ParB protein. These experiments demonstrate that the propensity to phase separate and the regulation thereof are conserved within parts of the ParB protein family.

In P3, I put the hypothesis of evolutionary conservation to a more rigorous test by characterizing the phase behavior of the ParB orthologue Noc. While these proteins still share sequence similarities, their biological function and specific sequence features differ dramatically. While ParB proteins interact with DNA to segregate the bacterial genome or plasmids, Noc has a N-terminal sequence feature allowing it to bind the bacterial nucleoid to the membrane [124]. Also, Noc is not responsible for genome or plasmid segregation, but a regulative factor of bacterial cell division. Therefore, there are significant sequence and functional differences between Noc and ParB.

Upon purification, Noc showed exciting liquid-liquid phase behavior, readily forming liquid-like droplets upon changes in the buffer environment. Also, addition of CTP enhanced Noc's droplet formation in great similarity to ParB. While these similarities are striking, I also identified differences in the fundamental phase behavior. Mutations

in the CTP binding pocket of Noc leads to a complete loss of its ability to phase separate, while ParB CTPase mutants are still able to undergo liquid-liquid phase separation. The N-terminal membrane binding helix in Noc's sequence, and its CTP dependent membrane binding activity allowed me to characterize the impact of lipid membranes on the formed biomolecular condensates and vice versa. The local environment of the membrane influences Noc's phase separation, as more droplets formed on highly negatively charged supported lipid bilayers (SLBs) compared to less charged SLBs. By titrating Noc onto giant unilamellar vesicles, a wetting-like transition was observable, indicated by film- or domain-like structures at lower Noc concentrations to clear 3D condensates at higher concentrations. Interestingly, these 3D condensates were able to deform deflated membranes.

Lastly, I put Noc's propensity to phase separate into a potential biological context. Similar to the *E. coli* nucleoid occlusion system SlmA, which also phase separates in presence of bacterial cell division machinery. Intriguingly, I found that Noc interacts with FtsZ, one of the main components of the bacterial cell division, only in the phase separated state, potentially indicating an important *in vivo* role of Noc LLPS.

In P1, we compared the similarities and differences of two prominent bacterial protein systems, the MinCDE and ParABS system, and their ability to self-organize. We identified similarities in the molecular architecture of both protein systems and their organization on macromolecules such as the lipid bilayer and the bacterial nucleoid.

Taken together, I established ParB and Noc as liquid-liquid phase separating proteins. As suggested by P2, the propensity to phase separate and the regulation thereof are highly conserved between homologues and orthologues. However, I also identified differences in the phase behavior. Both proteins interact with macromolecular structures: ParB binds the bacterial nucleoid or plasmids to help faithful segregation of genetic material. Noc, in contrast, is a membrane binding protein. These differences also manifest in the phase behavior: Noc LLPS is stabilized by the presence of a lipid bilayer and ParB's saturation concentration is lowered in the presence of plasmids containing parS. While the macromolecules stabilizing the phase separation differ, the concept of surface condensation by Noc and ParB is likely conserved.

More importantly, the main regulative mechanism of ParB protein LLPS identified in this thesis is CTP binding and hydrolysis. For all tested homologues and orthologues, the presence of CTP lowered the saturation concentration and therefore stabilized the liquid-liquid phase separation. Likely, this is due to a conformational change upon CTP binding which allows the formation of higher order oligomers as shown in P2. Overall, the work presented in this cumulative thesis has contributed to the elucidation of the phase separation of ParB proteins. More specifically: I provide explicit *in vitro* evidence for ParB phase separation and revealed the molecular components contributing to the regulation of

the liquid-liquid phase separation, namely the strong change of saturation concentration via the canonical CTP-binding and the simultaneous presence of low-affinity interactions. Based on our results and the reported *in vivo* formation of higher order structures, I furthermore established the recently unknown phase behaviour of the *B. subtilis* ParB orthologue Noc.

# Bibliography

- [1] A. Oparin, *The origin of life*. New York: Macmillan, 1938.
- [2] A. Rietveld and K. Simons, “The differential miscibility of lipids as the basis for the formation of functional membrane rafts,” *Biochimica et Biophysica Acta - Reviews on Biomembranes*, vol. 1376, no. 3, pp. 467–479, 1998.
- [3] S. K. and I. E., “Functional rafts in cell membranes.,” *Nature*, vol. 387, no. 6633, pp. 569–572, 1997.
- [4] B. M. Adhikari, A. Prasad, and M. Dhamala, “Time-delay-induced phase-transition to synchrony in coupled bursting neurons,” *Chaos: An Interdisciplinary Journal of Nonlinear Science*, vol. 21, p. 23116, may 2011.
- [5] J. M. Yeomans, *Statistical mechanics of phase transitions*. Clarendon Press, 1992.
- [6] M. ALDANA, H. LARRALDE, and B. VÁZQUEZ, “On the emergence of collective order in swarming systems: a recent debate,” *International Journal of Modern Physics B*, vol. 23, pp. 3661–3685, jul 2009.
- [7] M. Beekman, D. J. T. Sumpter, and F. L. W. Ratnieks, “Phase transition between disordered and ordered foraging in Pharaoh’s ants,” *Proceedings of the National Academy of Sciences*, vol. 98, pp. 9703–9706, aug 2001.
- [8] A. A. Hyman, C. A. Weber, and F. Jülicher, “Liquid-liquid phase separation in biology,” *Annual review of cell and developmental biology*, vol. 30, pp. 39–58, oct 2014.
- [9] C. P. Brangwynne, C. R. Eckmann, D. S. Courson, A. Rybarska, C. Hoege, J. Gharakhani, F. Jülicher, and A. A. Hyman, “Germline P granules are liquid droplets that localize by controlled dissolution/condensation,” *Science*, 2009.
- [10] E. F. Heffern, H. Huelskamp, S. Bahar, and R. F. Inglis, “Phase transitions in biology: From bird flocks to population dynamics,” *Proceedings of the Royal Society B: Biological Sciences*, vol. 288, no. 1961, 2021.
- [11] K. Fossheim and A. Sudbø, *Superconductivity: physics and applications*. John Wiley Sons, 2004.
- [12] T. Vicsek, A. Czirók, E. Ben-Jacob, I. Cohen, and O. Shochet, “Novel type of phase transition in a system of self-driven particles,” *Physical review letters*, vol. 75, no. 6, p. 1226, 1995.

- [13] S. J. Singer and G. L. Nicolson, "The fluid mosaic model of the structure of cell membranes," *Science*, vol. 175, no. 4023, pp. 720–731, 1972.
- [14] A. Stier and E. Sackmann, "Spin labels as enzyme substrates Heterogeneous lipid distribution in liver microsomal membranes," *Biochimica et Biophysica Acta (BBA) - Biomembranes*, vol. 311, no. 3, pp. 400–408, 1973.
- [15] M. J. Karnovsky, A. M. Kleinfeld, R. L. Hoover, and R. D. Klausner, "The concept of lipid domains in membranes.," *Journal of Cell Biology*, vol. 94, pp. 1–6, jul 1982.
- [16] T. N. Estep, D. B. Mountcastle, Y. Barenholz, R. L. Biltonen, and T. E. Thompson, "Thermal behavior of synthetic sphingomyelin-cholesterol dispersions," *Biochemistry*, vol. 18, pp. 2112–2117, may 1979.
- [17] F. Goodsaid-Zalduondo, D. A. Rintoul, J. C. Carlson, and W. Hansel, "Luteolysis-induced changes in phase composition and fluidity of bovine luteal cell membranes.," *Proceedings of the National Academy of Sciences*, vol. 79, pp. 4332–4336, jul 1982.
- [18] E. Sezgin, I. Levental, S. Mayor, and C. Eggeling, "The mystery of membrane organization: Composition, regulation and roles of lipid rafts," *Nature Reviews Molecular Cell Biology*, vol. 18, no. 6, pp. 361–374, 2017.
- [19] T. Baumgart, A. T. Hammond, P. Sengupta, S. T. Hess, D. A. Holowka, B. A. Baird, and W. W. Webb, "Large-scale fluid/fluid phase separation of proteins and lipids in giant plasma membrane vesicles," *Proceedings of the National Academy of Sciences*, vol. 104, pp. 3165–3170, feb 2007.
- [20] L. J. Pike, "Lipid rafts: bringing order to chaos," *Journal of Lipid Research*, vol. 44, pp. 655–667, apr 2003.
- [21] S. K. Pierce, "Lipid rafts and B-cell activation," *Nature Reviews Immunology*, vol. 2, no. 2, pp. 96–105, 2002.
- [22] D. Holowka, J. A. Gosse, A. T. Hammond, X. Han, P. Sengupta, N. L. Smith, A. Wagenknecht-Wiesner, M. Wu, R. M. Young, and B. Baird, "Lipid segregation and IgE receptor signaling: a decade of progress," *Biochimica et Biophysica Acta (BBA)-Molecular Cell Research*, vol. 1746, no. 3, pp. 252–259, 2005.
- [23] P. S. Kabouridis, "Lipid rafts in T cell receptor signalling," *Molecular membrane biology*, vol. 23, no. 1, pp. 49–57, 2006.
- [24] R. G. Parton and A. A. Richards, "Lipid rafts and caveolae as portals for endocytosis: new insights and common mechanisms," *Traffic*, vol. 4, no. 11, pp. 724–738, 2003.
- [25] C. Salaün, D. J. James, and L. H. Chamberlain, "Lipid rafts and the regulation of exocytosis," *Traffic*, vol. 5, no. 4, pp. 255–264, 2004.
- [26] S. Mañes and A. Viola, "Lipid rafts in lymphocyte activation and migration," *Molecular membrane biology*, vol. 23, no. 1, pp. 59–69, 2006.
- [27] S. Mañes, G. del Real, and C. Martínez-a, "Pathogens: raft hijackers," *Nature Reviews Immunology*, vol. 3, no. 7, pp. 557–568, 2003.
- [28] F. Lafont and F. G. Van Der Goot, "Bacterial invasion via lipid rafts," *Cellular microbiology*, vol. 7, no. 5, pp. 613–620, 2005.



- [29] N. Chazal and D. Gerlier, “Virus Entry, Assembly, Budding, and Membrane Rafts,” *Microbiology and Molecular Biology Reviews*, vol. 67, pp. 226–237, jun 2003.
- [30] P. Liu, Y. Ying, Y.-G. Ko, and R. G. W. Anderson, “Localization of Platelet-derived Growth Factor-stimulated Phosphorylation Cascade to Caveolae (),” *Journal of Biological Chemistry*, vol. 271, no. 17, pp. 10299–10303, 1996.
- [31] T. J. Nott, E. Petsalaki, J. D. Forman-Kay, A. J. Baldwin, P. Farber, D. Jarvis, E. Fussner, A. Plochowitz, T. D. Craggs, D. P. Bazett-Jones, and T. Pawson, “Phase Transition of a Disordered Nuage Protein Generates Environmentally Responsive Membraneless Organelles,” *Molecular Cell*, vol. 57, pp. 936–947, 2015.
- [32] M. Hofweber and D. Dormann, “Friend or foe—Post-translational modifications as regulators of phase separation and RNP granule dynamics,” *Journal of Biological Chemistry*, vol. 294, no. 18, pp. 7137–7150, 2019.
- [33] P. J. Flory, “Thermodynamics of high polymer solutions,” *The Journal of chemical physics*, vol. 10, no. 1, pp. 51–61, 1942.
- [34] M. L. Huggins, “Solutions of Long Chain Compounds,” *Journal of Chemical Physics*, vol. 9, p. 440, 1941.
- [35] D. Qian, T. J. Welsh, N. A. Erkamp, S. Qamar, J. Nixon-Abell, G. Krainer, P. St. George-Hyslop, T. C. Michaels, and T. P. Knowles, “Tie-Line Analysis Reveals Interactions Driving Heteromolecular Condensate Formation,” *Physical Review X*, vol. 12, p. 41038, dec 2022.
- [36] L. Jawerth, E. Fischer-Friedrich, S. S. S. Saha, J. Wang, T. Franzmann, X. Zhang, J. Sachweh, M. Ruer, M. Ijavi, S. S. S. Saha, J. Mahamid, A. A. Hyman, and F. Jülicher, “Protein condensates as aging Maxwell fluids,” *Science*, vol. 370, pp. 1317–1323, dec 2020.
- [37] S. Alberti and A. A. Hyman, “Biomolecular condensates at the nexus of cellular stress, protein aggregation disease and ageing,” *Nature reviews Molecular cell biology*, vol. 22, no. 3, pp. 196–213, 2021.
- [38] S. Alberti and D. Dormann, “Liquid-Liquid Phase Separation in Disease.,” *Annual review of genetics*, vol. 53, pp. 171–194, dec 2019.
- [39] B. Portz, B. L. Lee, and J. Shorter, “FUS and TDP-43 Phases in Health and Disease,” *Trends in Biochemical Sciences*, vol. 46, no. 7, pp. 550–563, 2021.
- [40] I. A. Klein, A. Boija, L. K. Afeyan, S. W. Hawken, M. Fan, A. Dall’Agnese, O. Oksuz, J. E. Henninger, K. Shrinivas, and B. R. Sabari, “Partitioning of cancer therapeutics in nuclear condensates,” *Science*, vol. 368, no. 6497, pp. 1386–1392, 2020.
- [41] D. M. Mitrea, M. Mittasch, B. F. Gomes, I. A. Klein, and M. A. Murcko, “Modulating biomolecular condensates: a novel approach to drug discovery,” *Nature Reviews Drug Discovery*, pp. 1–22, 2022.
- [42] J. Wang, J.-M. Choi, A. S. Holehouse, H. O. Lee, X. Zhang, M. Jahnel, S. Maharana, R. Lemaitre, A. Pozniakovsky, D. Drechsel, I. Poser, R. V. Pappu, S. Alberti, and

- A. A. Hyman, “A Molecular Grammar Governing the Driving Forces for Phase Separation of Prion-like RNA Binding Proteins,” *Cell*, vol. 174, no. 3, pp. 688–699.e16, 2018.
- [43] S. F. Banani, A. M. Rice, W. B. Peeples, Y. Lin, S. Jain, R. Parker, and M. K. Rosen, “Compositional Control of Phase-Separated Cellular Bodies,” *Cell*, vol. 166, pp. 651–663, jul 2016.
- [44] W. Borchers, A. Bremer, M. B. Borgia, and T. Mittag, “How do intrinsically disordered protein regions encode a driving force for liquid–liquid phase separation?,” *Current Opinion in Structural Biology*, vol. 67, pp. 41–50, 2021.
- [45] J. M. Choi, A. S. Holehouse, and R. V. Pappu, “Physical Principles Underlying the Complex Biology of Intracellular Phase Transitions,” *Annual Review of Biophysics*, vol. 49, pp. 107–133, may 2020.
- [46] E. W. Martin, A. S. Holehouse, I. Peran, M. Farag, J. J. Incicco, A. Bremer, C. R. Grace, A. Soranno, R. V. Pappu, and T. Mittag, “Valence and patterning of aromatic residues determine the phase behavior of prion-like domains.,” *Science (New York, N.Y.)*, vol. 367, pp. 694–699, feb 2020.
- [47] W. Basile, M. Salvatore, C. Bassot, and A. Elofsson, “Why do eukaryotic proteins contain more intrinsically disordered regions?,” *PLoS computational biology*, vol. 15, p. e1007186, jul 2019.
- [48] F. Erdel and K. Rippe, “Formation of Chromatin Subcompartments by Phase Separation,” *Biophysical Journal*, vol. 114, no. 10, pp. 2262–2270, 2018.
- [49] J.-K. Ryu, C. Bouchoux, H. W. Liu, E. Kim, M. Minamino, R. de Groot, A. J. Katan, A. Bonato, D. Marenduzzo, D. Michieletto, F. Uhlmann, and C. Dekker, “Bridging-induced phase separation induced by cohesin SMC protein complexes.,” *Science advances*, vol. 7, feb 2021.
- [50] P. D. Boyer, “The ATP Synthase—a splendid molecular machine,” *Annual Review of Biochemistry*, vol. 66, pp. 717–749, jun 1997.
- [51] P. W. Voorhees, “The theory of Ostwald ripening,” *Journal of Statistical Physics*, vol. 38, pp. 231–252, 1985.
- [52] D. Zwicker, A. A. Hyman, and F. Jülicher, “Suppression of Ostwald ripening in active emulsions,” *Physical Review E - Statistical, Nonlinear, and Soft Matter Physics*, 2015.
- [53] D. Zwicker, R. Seyboldt, C. A. Weber, A. A. Hyman, and F. Jülicher, “Growth and division of active droplets provides a model for protocells,” *Nature Physics*, 2017.
- [54] J. Söding, D. Zwicker, S. Sohrabi-Jahromi, M. Boehning, and J. Kirschbaum, “Mechanisms for Active Regulation of Biomolecular Condensates,” *Trends in Cell Biology*, vol. 30, no. 1, pp. 4–14, 2020.
- [55] J. Kirschbaum and D. Zwicker, “Controlling biomolecular condensates via chemical reactions,” *Journal of the Royal Society Interface*, vol. 18, no. 179, 2021.
- [56] S. Saha, C. A. Weber, M. Nusch, O. Adame-Arana, C. Hoegel, M. Y. Hein, E. Osborne-Nishimura, J. Mahamid, M. Jahnel, L. Jawerth, A. Pozniakovski, C. R.

- Eckmann, F. Jülicher, and A. A. Hyman, “Polar Positioning of Phase-Separated Liquid Compartments in Cells Regulated by an mRNA Competition Mechanism,” *Cell*, vol. 166, no. 6, pp. 1572–1584.e16, 2016.
- [57] H. Schmidt, A. Putnam, D. Rasoloson, and G. Seydoux, “Protein-based condensation mechanisms drive the assembly of RNA-rich P granules,” *eLife*, vol. 10, pp. 1–25, 2021.
- [58] W. Peeples and M. K. Rosen, “Mechanistic dissection of increased enzymatic rate in a phase-separated compartment,” *Nature Chemical Biology*, vol. 17, no. 6, pp. 693–702, 2021.
- [59] M. Hondele, S. Heinrich, P. de Los Rios, and K. Weis, “Membraneless organelles: Phasing out of equilibrium,” *Emerging Topics in Life Sciences*, vol. 4, no. 3, pp. 343–354, 2020.
- [60] W. T. Snead and A. S. Gladfelter, “The Control Centers of Biomolecular Phase Separation: How Membrane Surfaces, PTMs, and Active Processes Regulate Condensation,” *Molecular Cell*, vol. 76, no. 2, pp. 295–305, 2019.
- [61] X. Zhao, G. Bartolucci, A. Honigmann, F. Jülicher, and C. A. Weber, “Thermodynamics of wetting, prewetting and surface phase transitions with surface binding,” *New Journal of Physics*, vol. 23, no. 12, p. 123003, 2021.
- [62] B. Gouveia, Y. Kim, J. W. Shaevitz, S. Petry, H. A. Stone, and C. P. Brangwynne, “Capillary forces generated by biomolecular condensates,” *Nature*, vol. 609, no. 7926, pp. 255–264, 2022.
- [63] J. A. Morin, S. Wittmann, S. Choubey, A. Klosin, S. Golfier, A. A. Hyman, F. Jülicher, and S. W. Grill, “Sequence-dependent surface condensation of a pioneer transcription factor on DNA,” *Nature Physics*, vol. 18, no. 3, pp. 271–276, 2022.
- [64] S. Mondal and T. Baumgart, “Membrane reshaping by protein condensates,” *Biochimica et Biophysica Acta (BBA) - Biomembranes*, vol. 1865, no. 3, p. 184121, 2023.
- [65] T. Wiegand and A. A. Hyman, “Drops and fibers - how biomolecular condensates and cytoskeletal filaments influence each other.,” *Emerging Topics in Life Sciences*, vol. 4, pp. 247–261, dec 2020.
- [66] M. Rouches, S. L. Veatch, and B. B. Machta, “Surface densities prewet a near-critical membrane,” *Proceedings of the National Academy of Sciences of the United States of America*, vol. 118, no. 40, pp. 1–12, 2021.
- [67] R. Renger, J. A. Morin, R. Lemaitre, M. Ruer-gruss, and F. Jülicher, “Co-condensation of proteins with single- and,” *PNAS*, 2022.
- [68] O. Beutel, R. Maraschini, K. Pombo-Garcia, C. Martin-Lemaitre, A. Honigmann, K. Pombo-García, C. Martin-Lemaitre, and A. Honigmann, “Phase separation of zonula occludens proteins drives formation of tight junctions,” *Cell*, vol. 179, no. 4, pp. 923–936, 2019.

- [69] M. Zeng, Y. Shang, Y. Araki, T. Guo, R. L. Huganir, and M. Zhang, “Phase Transition in Postsynaptic Densities Underlies Formation of Synaptic Complexes and Synaptic Plasticity,” *Cell*, vol. 166, no. 5, pp. 1163–1175, 2016.
- [70] L. B. Case, J. A. Ditlev, and M. K. Rosen, “Regulation of Transmembrane Signaling by Phase Separation,” *Annual Review of Biophysics*, vol. 48, pp. 465–494, 2019.
- [71] M. S. Long, A. S. Cans, and C. D. Keating, “Budding and asymmetric protein microcompartmentation in giant vesicles containing two aqueous phases,” *Journal of the American Chemical Society*, vol. 130, no. 2, pp. 756–762, 2008.
- [72] M. Andes-Koback and C. D. Keating, “Complete budding and asymmetric division of primitive model cells to produce daughter vesicles with different interior and membrane compositions,” *Journal of the American Chemical Society*, vol. 133, no. 24, pp. 9545–9555, 2011.
- [73] R. Lipowsky, “Response of Membranes and Vesicles to Capillary Forces Arising from Aqueous Two-Phase Systems and Water-in-Water Droplets,” *Journal of Physical Chemistry B*, vol. 122, no. 13, pp. 3572–3586, 2018.
- [74] S. Botterbusch and T. Baumgart, “Interactions between phase-separated liquids and membrane surfaces,” *Applied Sciences (Switzerland)*, vol. 11, no. 3, pp. 1–16, 2021.
- [75] F. Yuan, H. Alimohamadi, B. Bakka, A. N. Trementozzi, K. J. Day, N. L. Fawzi, P. Rangamani, and J. C. Stachowiak, “Membrane bending by protein phase separation,” *Proceedings of the National Academy of Sciences of the United States of America*, vol. 118, mar 2021.
- [76] J. Agudo-Canalejo, S. W. Schultz, H. Chino, S. M. Migliano, C. Saito, I. Koyama-Honda, H. Stenmark, A. Brech, A. I. May, N. Mizushima, and R. L. Knorr, “Wetting regulates autophagy of phase-separated compartments and the cytosol,” *Nature*, vol. 591, pp. 142–146, mar 2021.
- [77] H. Kusumaatmaja, A. I. May, M. Feeney, J. F. McKenna, N. Mizushima, L. Frigerio, and R. L. Knorr, “Wetting of phase-separated droplets on plant vacuole membranes leads to a competition between tonoplast budding and nanotube formation,” *Proceedings of the National Academy of Sciences*, vol. 118, p. e2024109118, sep 2021.
- [78] A. Mangiarotti, M. Siri, Z. Zhao, L. Malacrida, and R. Dimova, “Biomolecular condensates modulate membrane lipid packing and hydration,” *bioRxiv*, p. 2023.01.04.522768, jan 2023.
- [79] T. Lu, S. Liese, L. Schoenmakers, C. A. Weber, H. Suzuki, W. T. S. Huck, and E. Spruijt, “Endocytosis of Coacervates into Liposomes,” *Journal of the American Chemical Society*, vol. 144, pp. 13451–13455, aug 2022.
- [80] M. Kozak and M. Kaksonen, “Condensation of Ede1 promotes the initiation of endocytosis,” *eLife*, vol. 11, pp. 1–25, 2022.
- [81] D. S. Protter and R. Parker, “Principles and Properties of Stress Granules,” 2016.
- [82] S. Boeynaems, S. Alberti, N. L. Fawzi, T. Mittag, M. Polymenidou, F. Rousseau,

- J. Schymkowitz, J. Shorter, B. Wolozin, L. Van Den Bosch, P. Tompa, and M. Fuxreiter, “Protein Phase Separation: A New Phase in Cell Biology.,” *Trends in cell biology*, vol. 28, pp. 420–435, jun 2018.
- [83] A. Klosin, F. Oltsch, T. Harmon, A. Honigmann, F. Jülicher, A. A. Hyman, and C. Zechner, “Phase separation provides a mechanism to reduce noise in cells,” *Science*, 2020.
- [84] T. Pederson, “The nucleolus.,” *Cold Spring Harbor perspectives in biology*, vol. 3, mar 2011.
- [85] M. Feric, N. Vaidya, T. S. Harmon, D. M. Mitrea, L. Zhu, T. M. Richardson, R. W. Kriwacki, R. V. Pappu, and C. P. Brangwynne, “Coexisting Liquid Phases Underlie Nucleolar Subcompartments,” *Cell*, vol. 165, no. 7, pp. 1686–1697, 2016.
- [86] I. Raška, P. J. Shaw, and D. Cmarko, “New Insights into Nucleolar Architecture and Activity,” in *A Survey of Cell Biology* (K. W. B. T. I. R. o. C. Jeon, ed.), vol. 255, pp. 177–235, Academic Press, 2006.
- [87] D. L. J. Lafontaine, J. A. Riback, R. Bascetin, and C. P. Brangwynne, “The nucleolus as a multiphase liquid condensate,” *Nature Reviews Molecular Cell Biology*, vol. 22, no. 3, pp. 165–182, 2021.
- [88] C. P. Brangwynne, T. J. Mitchison, and A. A. Hyman, “Active liquid-like behavior of nucleoli determines their size and shape in *Xenopus laevis* oocytes.,” *Proceedings of the National Academy of Sciences of the United States of America*, vol. 108, pp. 4334–4339, mar 2011.
- [89] S. C. Weber and C. P. Brangwynne, “Inverse size scaling of the nucleolus by a concentration-dependent phase transition.,” *Current biology : CB*, vol. 25, pp. 641–646, mar 2015.
- [90] S. R. Wenthe and M. P. Rout, “The nuclear pore complex and nuclear transport,” *Cold Spring Harbor perspectives in biology*, vol. 2, no. 10, p. a000562, 2010.
- [91] M. Raices and M. A. D’Angelo, “Nuclear pore complexes and regulation of gene expression.,” *Current opinion in cell biology*, vol. 46, pp. 26–32, jun 2017.
- [92] K. Ribbeck and D. Görlich, “The permeability barrier of nuclear pore complexes appears to operate via hydrophobic exclusion,” *The EMBO journal*, vol. 21, no. 11, pp. 2664–2671, 2002.
- [93] S. Frey, R. P. Richter, and D. Gorlich, “FG-rich repeats of nuclear pore proteins form a three-dimensional meshwork with hydrogel-like properties,” *Science*, vol. 314, no. 5800, pp. 815–817, 2006.
- [94] S. Frey and D. Görlich, “A saturated FG-repeat hydrogel can reproduce the permeability properties of nuclear pore complexes,” *Cell*, vol. 130, no. 3, pp. 512–523, 2007.
- [95] B. L. Carroll and J. Liu, “Structural conservation and adaptation of the bacterial flagella motor,” *Biomolecules*, vol. 10, no. 11, pp. 1–24, 2020.
- [96] M. Hondele, R. Sachdev, S. Heinrich, J. Wang, P. Vallotton, B. M. Fontoura, and

- K. Weis, “DEAD-box ATPases are global regulators of phase-separated organelles,” *Nature*, vol. 573, no. 7772, pp. 144–148, 2019.
- [97] P. Dasmeh and A. Wagner, “Natural Selection on the Phase-Separation Properties of FUS during 160 My of Mammalian Evolution,” *Molecular Biology and Evolution*, vol. 38, no. 3, pp. 940–951, 2021.
- [98] C. Jegers, T. M. Franzmann, J. Hübner, J. Schneider, C. Landerer, S. Wittmann, A. Toth-Petroczy, R. Sprangers, A. A. Hyman, and S. Alberti, “A conserved and tunable mechanism for the temperature-controlled condensation of the translation factor Ded1p,” *bioRxiv*, p. 2022.10.11.511767, 2022.
- [99] J. A. Riback, C. D. Katanski, J. L. Kear-Scott, E. V. Pilipenko, A. E. Rojek, T. R. Sosnick, and D. A. Drummond, “Stress-Triggered Phase Separation Is an Adaptive, Evolutionarily Tuned Response,” *Cell*, vol. 168, no. 6, pp. 1028–1040.e19, 2017.
- [100] T. M. Franzmann, M. Jahnel, A. Pozniakovsky, J. Mahamid, A. S. Holehouse, E. Nüske, D. Richter, W. Baumeister, S. W. Grill, R. V. Pappu, A. A. Hyman, and S. Alberti, “Phase separation of a yeast prion protein promotes cellular fitness,” *Science*, vol. 359, no. 6371, 2018.
- [101] T. Zarin, B. Strome, A. N. Nguyen Ba, S. Alberti, J. D. Forman-Kay, and A. M. Moses, “Proteome-wide signatures of function in highly diverged intrinsically disordered regions,” *eLife*, vol. 8, p. e46883, 2019.
- [102] C. Greening and T. Lithgow, “Formation and function of bacterial organelles,” *Nature Reviews Microbiology*, vol. 18, no. 12, pp. 677–689, 2020.
- [103] D. Faivre and D. Schüler, “Magnetotactic Bacteria and Magnetosomes,” *Chemical Reviews*, vol. 108, pp. 4875–4898, nov 2008.
- [104] T. O. Yeates, C. A. Kerfeld, S. Heinhorst, G. C. Cannon, and J. M. Shively, “Protein-based organelles in bacteria: carboxysomes and related microcompartments,” *Nature Reviews Microbiology*, vol. 6, no. 9, pp. 681–691, 2008.
- [105] C. A. Azaldegui, A. G. Vecchiarelli, and J. S. Biteen, “The emergence of phase separation as an organizing principle in bacteria,” *Biophysical Journal*, vol. 120, no. 7, pp. 1123–1138, 2021.
- [106] J. S. MacCready, J. L. Basalla, and A. G. Vecchiarelli, “Origin and evolution of carboxysome positioning systems in cyanobacteria,” *Molecular biology and evolution*, vol. 37, no. 5, pp. 1434–1451, 2020.
- [107] S. Saurabh, T. N. Chong, C. Bayas, P. D. Dahlberg, H. N. Cartwright, W. E. Moerner, and L. Shapiro, “ATP-responsive biomolecular condensates tune bacterial kinase signaling,” *Science Advances*, vol. 8, no. 7, p. eabm6570, 2022.
- [108] A.-M. Ladouceur, B. S. Parmar, S. Biedzinski, J. Wall, S. G. Tope, D. Cohn, A. Kim, N. Soubry, R. Reyes-Lamothe, and S. C. Weber, “Clusters of bacterial RNA polymerase are biomolecular condensates that assemble through liquid–liquid phase separation,” *Proceedings of the National Academy of Sciences*, vol. 117, no. 31, pp. 18540–

- 18549, 2020.
- [109] B. Guilhas, J. C. Walter, J. Rech, G. David, N. O. Walliser, J. Palmeri, C. Mathieu-Demaziere, A. Parmeggiani, J. Y. Bouet, A. Le Gall, and M. Nollmann, “ATP-Driven Separation of Liquid Phase Condensates in Bacteria,” *Molecular Cell*, 2020.
  - [110] A. S. B. Jalal, N. T. Tran, C. E. Stevenson, E. W. Chan, R. Lo, X. Tan, A. Noy, D. M. Lawson, and T. B. K. Le, “Diversification of DNA-Binding Specificity by Permissive and Specificity-Switching Mutations in the ParB/Noc Protein Family.,” *Cell reports*, vol. 32, p. 107928, jul 2020.
  - [111] K. Böhm, G. Giacomelli, A. Schmidt, A. Imhof, R. Koszul, M. Marbouty, and M. Bramkamp, “Chromosome organization by a conserved condensin-ParB system in the actinobacterium *Corynebacterium glutamicum*,” *Nature Communications*, vol. 11, 2020.
  - [112] A. G. Vecchiarelli, K. Mizuuchi, and B. E. Funnell, “Surfing biological surfaces: Exploiting the nucleoid for partition and transport in bacteria,” 2012.
  - [113] A. G. Vecchiarelli, K. C. Neuman, and K. Mizuuchi, “A propagating ATPase gradient drives transport of surface-confined cellular cargo,” *Proceedings of the National Academy of Sciences of the United States of America*, 2014.
  - [114] H. C. Lim, I. V. Surovtsev, B. G. Beltran, F. Huang, J. Bewersdorf, and C. Jacobs-Wagner, “Evidence for a DNA-relay mechanism in ParABS-mediated chromosome segregation,” *eLife*, 2014.
  - [115] A. Merino-Salomón, L. Babl, and P. Schwille, “Self-organized protein patterns: The MinCDE and ParABS systems,” *Current Opinion in Cell Biology*, vol. 72, pp. 106–115, oct 2021.
  - [116] C. P. Broedersz, X. Wang, Y. Meir, J. J. Loparo, D. Z. Rudner, and N. S. Wingreen, “Condensation and localization of the partitioning protein ParB on the bacterial chromosome,” *Proceedings of the National Academy of Sciences of the United States of America*, 2014.
  - [117] J.-C. Walter, J. Rech, N.-O. Walliser, J. Dornigac, F. Geniet, J. Palmeri, A. Parmeggiani, and J.-Y. Bouet, “Physical Modeling of a Sliding Clamp Mechanism for the Spreading of ParB at Short Genomic Distance from Bacterial Centromere Sites,” *iScience*, vol. 23, no. 12, p. 101861, 2020.
  - [118] M. Osorio-Valeriano, F. Altegoer, W. Steinchen, S. Urban, Y. Liu, G. Bange, and M. Thanbichler, “ParB-type DNA Segregation Proteins Are CTP-Dependent Molecular Switches,” *Cell*, 2019.
  - [119] M. Osorio-Valeriano, F. Altegoer, C. K. Das, W. Steinchen, G. Panis, L. Connolley, G. Giacomelli, H. Feddersen, L. Corrales-Guerrero, and P. I. Giammarinaro, “The CTPase activity of ParB determines the size and dynamics of prokaryotic DNA partition complexes,” *Molecular cell*, vol. 81, no. 19, pp. 3992–4007, 2021.
  - [120] Y. M. Soh, I. F. Davidson, S. Zamuner, J. Basquin, F. P. Bock, M. Taschner, J. W.

- Veening, P. de Los Rios, J. M. Peters, and S. Gruber, “Self-organization of parS centromeres by the ParB CTP hydrolase,” *Science*, 2019.
- [121] H. Antar, Y.-M. Soh, S. Zamuner, F. P. Bock, A. Anchimiuk, P. D. L. Rios, and S. Gruber, “Relief of ParB autoinhibition by parS DNA catalysis and recycling of ParB by CTP hydrolysis promote bacterial centromere assembly,” *Science advances*, vol. 7, no. 41, p. eabj2854, 2021.
- [122] T. G. Bernhardt and P. A. J. De Boer, “SlmA, a nucleoid-associated, FtsZ binding protein required for blocking septal ring assembly over chromosomes in *E. coli*,” *Molecular cell*, vol. 18, no. 5, pp. 555–564, 2005.
- [123] L. J. Wu and J. Errington, “Coordination of cell division and chromosome segregation by a nucleoid occlusion protein in *Bacillus subtilis*,” *Cell*, vol. 117, no. 7, pp. 915–925, 2004.
- [124] D. W. Adams, L. J. Wu, and J. Errington, “Nucleoid occlusion protein Noc recruits DNA to the bacterial cell membrane,” *The EMBO journal*, vol. 34, no. 4, pp. 491–501, 2015.
- [125] H. Cho, H. R. McManus, S. L. Dove, and T. G. Bernhardt, “Nucleoid occlusion factor SlmA is a DNA-activated FtsZ polymerization antagonist,” *Proceedings of the National Academy of Sciences*, vol. 108, no. 9, pp. 3773–3778, 2011.
- [126] B. Monterroso, S. Zorrilla, M. Sobrinos-Sanguino, M. A. Robles-Ramos, M. López-Álvarez, W. Margolin, C. D. Keating, and G. Rivas, “Bacterial FtsZ protein forms phase-separated condensates with its nucleoid-associated inhibitor SlmA,” *EMBO reports*, vol. 20, no. 1, p. e45946, 2019.
- [127] Y. Yu, J. Zhou, F. J. Gueiros-Filho, D. B. Kearns, and S. C. Jacobson, “Noc corrals migration of FtsZ protofilaments during cytokinesis in *Bacillus subtilis*,” *Mbio*, vol. 12, no. 1, pp. e02964–20, 2021.
- [128] S. Peng, W. Li, Y. Yao, W. Xing, P. Li, and C. Chen, “Phase separation at the nanoscale quantified by dcFCCS,” *Proceedings of the National Academy of Sciences*, vol. 117, no. 44, pp. 27124–27131, 2020.
- [129] M.-T. Wei, S. Elbaum-Garfinkle, A. S. Holehouse, C. C.-H. Chen, M. Feric, C. B. Arnold, R. D. Priestley, R. V. Pappu, and C. P. Brangwynne, “Phase behaviour of disordered proteins underlying low density and high permeability of liquid organelles,” *Nature chemistry*, vol. 9, no. 11, pp. 1118–1125, 2017.
- [130] L. Babl, G. Giacomelli, B. Ramm, A.-K. Gelmroth, M. Bramkamp, and P. Schwille, “CTP-controlled liquid–liquid phase separation of ParB,” *Journal of Molecular Biology*, vol. 434, no. 2, p. 167401, 2022.
- [131] L. Babl, A. Merino-Salomón, N. Kanwa, and P. Schwille, “Membrane mediated phase separation of the bacterial nucleoid occlusion protein Noc,” *Scientific Reports*, vol. 12, no. 1, p. 17949, 2022.
- [132] A. Patel, L. Malinowska, S. Saha, J. Wang, S. Alberti, Y. Krishnan, and A. A.



- Hyman, “ATP as a biological hydrotrope,” *Science*, vol. 356, pp. 753–756, may 2017.
- [133] M. C. Ferrolino, D. M. Mitrea, J. R. Michael, and R. W. Kriwacki, “Compositional adaptability in NPM1-SURF6 scaffolding networks enabled by dynamic switching of phase separation mechanisms,” *Nature communications*, vol. 9, no. 1, p. 5064, 2018.
- [134] P. Yang, C. Mathieu, R.-M. Kolaitis, P. Zhang, J. Messing, U. Yurtsever, Z. Yang, J. Wu, Y. Li, and Q. Pan, “G3BP1 is a tunable switch that triggers phase separation to assemble stress granules,” *Cell*, vol. 181, no. 2, pp. 325–345, 2020.
- [135] D. W. Sanders, N. Kedersha, D. S. W. Lee, A. R. Strom, V. Drake, J. A. Riback, D. Bracha, J. M. Eeftens, A. Iwanicki, and A. Wang, “Competing protein-RNA interaction networks control multiphase intracellular organization,” *Cell*, vol. 181, no. 2, pp. 306–324, 2020.
- [136] J. Guillén-Boixet, A. Kopach, A. S. Holehouse, S. Wittmann, M. Jahnel, R. Schlüßler, K. Kim, I. R. E. A. Trussina, J. Wang, and D. Mateju, “RNA-induced conformational switching and clustering of G3BP drive stress granule assembly by condensation,” *Cell*, vol. 181, no. 2, pp. 346–361, 2020.



# List of abbreviations

**ADP** Adenosine Diphosphate.

**ATP** Adenosine Triphosphate.

**CTP** Cytidine triphosphate.

**DNA** Deoxyribonucleic acid.

**DOPC** dipalmitoylphosphatidylcholine.

**DOPG** 1,2-Dioleoyl-sn-glycero-3-phosphoglycerol.

**FCS** Fluorescence correlation spectroscopy.

**FRAP** Fluorescence Recovery After Photobleaching.

**GFP** Green Fluorescent Protein.

**GTP** Guanosine triphosphate.

**GUV** Giant unilamellar vesicles.

**IPTG** isopropyl  $\beta$ -D-1-thiogalactopyranoside.

**LLPS** Liquid-liquid phase separation.

**LUV** Large unilamellar vesicles.

**mts** Membrane Targeting Sequence.

**NO** Nucleoid Occlusion.

**PEG** Polyethylene glycol.

**QCM-D** Quartz Crystal Microbalance with Dissipation monitoring.

**SLB** Supported lipid bilayers.

**SUV** Small unilamellar vesicles.



# Acknowledgements

It is tough to summarize the last few years in a paragraph or two, but I'll try my very best. I owe the people that surrounded me during these (sometimes difficult) times everything and not a single page of this dissertation would have been possible without all of them.

First, I want to thank *Prof. Petra Schwille*, for her supervision, her open-mindedness and constant positive engagement. Thank you for the freedom to shape this thesis the way I envisioned it, for letting me try tons of things and then helping me to focus on the important bits and pieces! Also, thank you for being a great role model of how to maintain a healthy curiosity over many years of being a scientist. I am also pretty sure you are one of the very few PhD supervisors that can take their students on an alpine style multi-pitch climb! You helped me to grow to become an independent researcher and I will be forever grateful for this gift!

Next, I want to thank *Prof. Job Boekhoven* for taking over the role of my official supervisor at TUM! Also, thank you very much for your hugely valuable input in the TAC committee and evaluation meetings. Obviously, the Schwillies as a whole are making a fantastic lab environment to work and thrive in, so first of all thank you for all the coffee breaks, lunches and nice chats! In particular, I want to thank Beatrice Ramm for helping me getting started in the lab! Also, huge thanks to Shunshi Kohyama for proofreading of this thesis and being a great go-to lab mate for questions. A huge thank you to Adrian for being an awesome lab mate, with whom I could always share a rant or laugh! I want to thank my co-authors and collaborators, namely Michele Stasi who allowed me to play a little bit of chemist and the Bramkamp group for helping me out with great in vivo data. Also, thanks to Shunshi and Bela for letting me be a very minor part in the cool synMinE project! I'd also like to thank the technicians in the lab: Michaela, the cloning queen, Katharina the assay machine and Kerstin, the protein producer number one! Sigrid, thank you for keeping the membrane lab up-and-running and helping me with vesicle preparations. Thank you Frank and Helge for all the administrative support!

Well, I did not spend all of my time in the lab, and I was lucky enough to be surrounded by a bunch of fantastic people! I want to thank the whole Landsi198 community for the laughs, the long evenings and good company over the last three years, cheers to that! Special thanks to you Sebi, enduring my occasional bad moods and cooking many tasty tomato sauces! Thank you Thomas for taking me on all these amazing adventures: Iceland, climbing, skiing and fixing my van. I appreciate every second we spend in the great outdoors!

Last and most importantly, I want to thank the ones that were there day and night. Thank you Lena, thank you Mum, thank you Dad and thank you Vinci. There is no possible way I could express the feeling of overwhelming gratitude I have. Your support means the world to me and I'd be nowhere without you. Thank you Lena for being on my side (9 years already, pretty damn crazy) all the time, your smile and laughter makes me forget the occasional tough times! I can only imagine what the next years will bring, but I am sure it will good times and big adventures. To my family: it is very difficult to express the gratitude I feel. You gave me a home, a constant feeling of shelter, warmth and love. Thank you so much.